DESIGN AND SYNTHESIS OF NEW RECEPTORS FOR MOLECULAR RECOGNITION OF ENVIRONMENTAL POLLUTING CATIONS

Thesis

Submitted in partial fulfilment of the requirements for the degree of

DOCTOR OF PHILOSOPHY

by

Momidi Bharath Kumar

DEPARTMENT OF CHEMISTRY

NATIONAL INSTITUTE OF TECHNOLOGY KARNATAKA

SURATHKAL, MANGALORE–575025

OCTOBER, 2020

CERTIFICATE

This is to *certify* that the Research Thesis entitled "**Design and synthesis of new receptors for molecular recognition of environmental polluting cations**" submitted by **Mr. Momidi Bharath Kumar (Register Number: 145014CY14P01)** as the record of the research work carried out by him is *accepted as the Research Thesis submission* in partial fulfilment of the requirements for the award of degree of Doctor of Philosophy.

<div align="right">

Research Guide

Name: Dr. Darshak R. Trivedi

(Signature with Date and Seal)

</div>

Chairman – DRPC

(Signature with Date and Seal)

ACKNOWLEDGEMENT

Mere words are not enough to express my gratitude to my family, father Late. Mr. Chandra Sekhar Momidi, mother Mrs. Vijayalakshmi Momidi, wife Mrs. Srilakshmi Momidi, Brother Mr. Bhargava Narayana Momidi and my lovely daughter Moksha Narayani for their constant support, encouragement and prayers. Finally, I thank the God almighty for strengthening me during hardships to successfully complete this endeavor.

M. Bharath Kumar

ABSTRACT

The colorimetric chemosensors for the recognition of heavy metal ions is an exciting area in the field of supramolecular chemistry as it has various applications in chemistry, biology and environment. In view of the stereochemical and rich redox reactivity, the transition metal ions such as Cu^{2+}, Zn^{2+}, Mn^{2+} and Fe^{3+} play an essential role in many biological processes and involves in active participation in small molecule binding and transport. Further, the heavy metal ions such as Hg^{2+}, Cd^{2+}, Pb^{2+}, arsenic are highly toxic due to their clinical and environmental reasons.

Considering the facts from the literature, four new series of Schiff base molecules based on different structural backbone *Viz*., benzothiazole, thiocarbohydrazide, thiophene-2-carboxyaldehyde and quinoline has been designed, synthesized and characterized as chemosensors for the colorimetric detection of heavy metal ions (Cu^{2+}, Hg^{2+} and Cd^{2+}). The chemical structure of the all synthesized chemosensors is confirmed by different standard spectroscopic techniques like, FT-IR, ^{1}H-NMR, ^{13}C-NMR, HR-MS and LC-mass (ESI-MS). The 3D structure of selected chemosensors was elucidated using Single Crystal X-Ray diffraction (SCXRD) studies.

The qualitative and quantitative analysis of heavy metal ions with the designed chemosensors has been carried out using UV-Vis spectroscopic studies and the binding constant (k) for the chemosensor-metal ion complex has been calculated using Benesi–Hildebrand equation and Bindfit method. Further, the detection and quantification limits have been estimated using signal to noise ration formula given by the ICH guidelines (Q2R1) from the UV-Vis titration data. Furthermore, the binding mechanism has been proposed based on UV-Vis titration and the same has been confirmed by FT-IR, ^{1}H-NMR and LC-mass. Finally, the experimental results were compared with the theoretical density functional theory (DFT) studies for some series of molecules. From the experimental and theoretical DFT results, it can be concluded that, the simple organic molecules could act as very good colorimetric chemosensor for the detection of heavy metal ions such as Hg^{2+} and Cd^{2+} ions.

Keywords: Colorimetric chemosensor, UV-Vis titration, B-H plot, Binding constant, Heavy metal ions.

NOMENCLATURE

ABBREVIATIONS

CSD	:	Cambridge Structural Database
CCDC	:	Cambridge Crystallographic Data Centre
FT–IR	:	Fourier Transform Infrared
NMR	:	Nuclear Magnetic Resonance
SC–XRD	:	Single Crystal X-ray Diffraction
UV–Vis	:	Ultraviolet-Visible
DFT	:	Density Functional Theory
DMSO-d_6	:	Dimethyl Sulfoxide-deuterated
CDCl$_3$	:	Chloroform-deuterated
MP	:	Melting point
WHO	:	World health organization
USP	:	United states pharmacopeia
ICH	:	International council for harmonisation
US–EPA	:	United states environmental protection agency
AAS	:	Atomic absorption spectroscopy
ICP-MS	:	Inductively coupled plasma mass spectrometry
ICP–OES	:	Inductively coupled plasma optical emission spectrometry
LC–MS	:	Liquid chromatography–mass spectrometry
ESI	:	Electro spray ionization
DL	:	Detection limit
QL	:	Quantification limit
DMF	:	Dimethylformamide
EtOH	:	Ethanol
equiv.	:	Equivalence
Fig.	:	Figure
HPLC	:	High-performance liquid chromatography
ACN	:	Acetonitrile

AcOH	:	Acetic acid
ICT	:	Intramolecular charge transfer
HOMO	:	Highest occupied molecular orbitals
LUMO	:	Lowest unoccupied molecular orbitals
TMS	:	Tetramethylsilane
TLC	:	Thin-layer chromatography
RT	:	Room temperature
ORTEP	:	Oak ridge thermal ellipsoidal plot

SYMBOLS AND UNITS

α	:	Alpha
cm	:	Centimeter
nm	:	Nanometer
°	:	Degree
Å	:	Angstrom
°C	:	Degree Celsius
∠	:	Angle
g	:	Gram
mg	:	Milligram
μg	:	Microgram
Hz	:	Hertz
$^{-1}$	:	Inverse
λ	:	Lamda
L	:	Liter
mL	:	Milliliter
μL	:	Microlitter
M	:	Molar/Mole
mM	:	Millimol
μM	:	Micromol
ppm	:	Parts per million
ppb	:	Parts per billion
MHz	:	Megahertz
μ	:	Mu
Σ	:	Sigma
π	:	Pai
θ	:	Theta
V	:	Volume
kJ	:	Kilojoule
N	:	Normal/Normality
min	:	Minute
H/h	:	Hour

Table of Contents

1.0   INTRODUCTION

This chapter comprises a brief introduction to supramolecular chemistry including cations and cations binding chemistry. Besides, the history of cations and its importance, challenges in their detection have been discussed in depth. Also, this chapter includes a detailed literature survey on the reported cation receptors, scope and objectives of the present research work.

1.1.   SUPRAMOLECULAR CHEMISTRY

Supramolecular chemistry has been defined by Jean- Marie Lehn as "the intermolecular bond, covering the structures and functions of the entities formed by the association of two or more chemical species", who shared the Nobel Prize for this work in the year 1987. Broadly, supramolecular chemistry can be expressed as 'chemistry beyond the molecule'. Perhaps it can also be defined as 'the chemistry of non-covalent bond' and 'non-molecular chemistry'. The supramolecular chemistry was defined in terms of the non-covalent interaction between a 'host' and a 'guest' molecule (steed et al. 2009). The traditional chemistry focuses on the covalent bond; whereas supramolecular chemistry concentrates on the weaker and reversible non-covalent interaction between the molecules. Thus the supramolecular division focuses on the chemical systems made up of a discrete number of assembled molecular subunits or components. This can be illustrated using the Fig. 1.1.
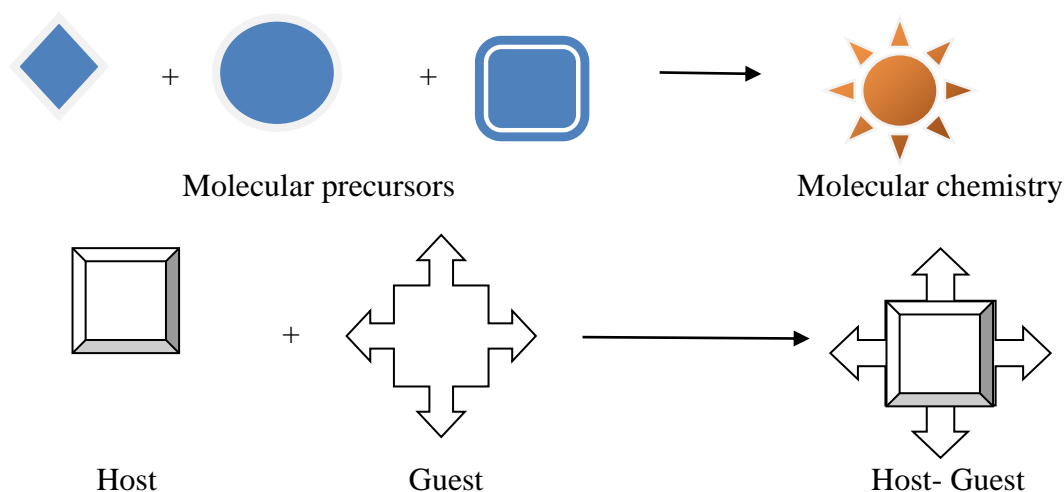
Fig. 1.1: The representation of Host-Guest Chemistry

1.2 ENVIRONMENTALLY AND BIOLOGICALLY IMPORTANT CATIONS

The metal cations like copper, cobalt and zinc presented in the environment are essential for human health. Even though, these cations are biologically important for human life, on the other hand there exceed in limit will be hazardous to health and hence it can be considered as pollutants. Also, heavy metal cations such as lead, cadmium and mercury etc., presented in the environment could be extremely harmful to human health. The detailed discussion of aforementioned ions is given below.

1.2.1. Copper (Cu)

In humans, copper is essential for overall good health. However, on over exposed, it can cause the adverse effect on human health. Exposure to copper can occur by breathing air, drinking water, eating food, and by skin contact with soil or water. Over exposure of copper can cause vomiting, diarrhea, stomach cramps, and nausea. Large intake can cause liver or kidney damage, or even death in cases of extreme exposure. People with Wilson's disease have a genetic defect that results in the accumulation of copper in tissues, including liver and kidney. The excess copper in these people can cause damage to the kidney, liver, and brain; hemolytic anemia; and other effects. Acute exposure via inhalation of copper dusts or fumes can cause a condition called "metal fume fever", characterized by chills, fever, dry throat and aching muscles. The maximum dietary tolerable level of Copper is 1.5 mg/L^{-1}.

1.2.2. Cobalt (Co)

Cobalt is a natural element found throughout the environment. As cobalt is widely dispersed in the environment, humans may have exposed to it by breathing air, drinking water and eating food that contain cobalt. Cobalt has both beneficial and as well as adverse effects on human health. It is beneficial for humans because it is part of vitamin B$_{12}$. Cobalt compounds are also used to manufacture color glass, ceramics, and paints. It is used in preparation of pigments like cobalt blue and cobalt green. For common livestock species, the maximum dietary tolerable level of cobalt is 10mg L^{-1} and if consumed in large doses it could be harmful, cause heart effects, thyroid damage, vomiting, high blood pressure, and slower respiration. Cobalt dust may cause asthma-like disease with symptoms ranging from cough, shortness of breath and

dyspnea to decreased pulmonary function, nodular fibrosis, permanent disability and death.

1.2.3. Zinc (Zn)

Zinc is the second most abundant transition-metal ion in the human body and its highest concentration occurs in brain, plays crucial roles in many biological processes acting as the structural and catalytic cofactors as neural signal transmitters or modulators, regulators of gene in neurological disorders, such as Parkinson's disease, Alzheimer's disease, amyotrophic lateral sclerosis, and epileptic seizures. Zinc is most important metal widely used in electroplating industries. The maximum dietary tolerable level of zinc is 5 mg/L^{-1}

1.2.4. Lead (Pb)

Lead is the most abundant and toxic substance. It is often encountered in the environment due to its use in batteries, gasoline and pigments, etc. Lead pollution is a persisting problem and a long –lasting threat to human health and the environment, as the 300 million tons of lead mined to date are still circulating mostly in soil and ground water. Even very low concentration of lead exposure can cause neurological, reproductive, cardiovascular, and developmental disorders, which introduce particularly serious problems in children including slowed motor responses decreased IQs, and hypertension. The maximum dietary tolerable level of lead is 0.05 mg/L^{-1}

1.2.5. Cadmium (Cd)

Cadmium is also an extremely toxic and carcinogenic metal. A major exposure source is smoking and through food, but inhalation of cadmium-containing dust is most dangerous path. Cadmium can be found in electroplated steel, pigments in plastics, electric batteries and so on. A high exposure level of cadmium is associated with increased risks of cardiovascular diseases. Cancer mortality and damage to liver and kidney. The maximum dietary tolerable level is 0.01 mg/L^{-1}.

1.2.6. Mercury (Hg)

Mercury is well known as one of the most toxic metals and is widespread in air. Water, and soil gets polluted by many sources such as mining, solid waste incineration and combustion of fossil fuels. It is to be frightened that, mercury-containing chemicals have been linked with a number of human health problems, including Minamata, myocardial infarction, and some kinds of autism, damage of

brain, kidneys, damage of sensory parts of the central nervous system, immune system and endocrine system. The maximum dietary tolerable level is 0.001 mg/L^{-1}.

1.2.7. Chromium (Cr)

Chromium is widely used industrial chemicals. The toxicities associated with this metal ion are well known. However, less information is available concerning the mechanisms of toxicity. The results of *in-vitro and in-vivo* studies demonstrate that induce an oxidative stress that results in oxidative deterioration of biological macromolecules. However, different mechanisms are involved in the production of the oxidative stress by chromium. The maximum dietary tolerable level of chromium is 0.05 mg/L^{-1}

1.3 CATION RECEPTOR CHEMISTRY

In general cation receptors are the molecules which can recognize or sense the cations (i.e. positively charged species). In spite of the fact that instrumental strategies, for example, cation screen tests are accessible for the discovery of cation, it expends additional time and requires skilled efforts to work. The colorimetric technique for identification is widely accepted because of the minimal effort, instantaneous detection and simple/safe to handle and quick-tempered when compared with instrumental techniques. Along these lines, outlining novel synthetic receptors for the colorimetric discovery of cations gained significant consideration and subsequently, from couple of decades the colorimetric cation receptor science has been examined widely (Garcia-Garrido et al. 2007; Steed 2009; Kubik 2009; Caltagirone and Gale 2009; Gale and Gunnlaugsson 2010; Lau et al. 2011; Gale 2011; Dydio et al. 2011; Moragues et al. 2011; Ngo et al. 2012; Yin et al. 2013; Gale et al. 2014). However, several number of the comprehensive studies follows host-guest and non-covalent binding method to design different receptors.

1.3.1. Host- guest chemistry

In the host guest chemistry, the word chemosensor is more closely related with a molecular event. Sensor is a system that on stimulation by any form of energy undergoes change in its own state and thus one or more of its physiognomies. This change is used to investigate the stimulant both qualitatively and quantitatively. The

optical and photo-physical changes in a molecule are originate more valuable in this regard. These receptor molecules display selective response to specific ions or neutral species to be used as chromosensors. A suitable definition of a chemical sensor from the Cambridge definition is "*chemical sensors are miniaturized devices that can deliver real time and on-line information on the presence of specific compounds or ions in even composite samples*". Chemical sensors employ specific transduction procedures to yield analyte information. The most widely used methods employed in chemical sensors are optical absorption, luminescence, redox potential etc., but sensors based on other spectroscopies as well as on optical parameters, such as refractive index and reflectivity, have also been developed.

It is imperative to explain the binding in the process of non-covalent binding. Generally, binding is the process where a molecular 'guest' binds to additional molecule 'host' to form a supramolecular or a 'host-guest' complex (Fig. 1.2). Usually, the host is a large molecule or an enzyme or a synthetic cyclic molecule which owns a central hole or cavity. The guest may be monatomic cation, or small synthetic anions. Specifically, the host is defined as the molecular entity owning 'convergent' binding sites such as Lewis basic donor atoms. The guest possesses 'divergent' binding sites such as Lewis acid metal cations.
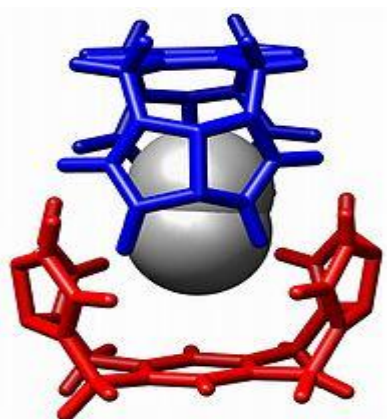

Fig 1.2. Host- guest chemistry

According to Donald Cram the host-guest association can be defined as "*Complexes are composed of two or more units or ions held together in distinctive structural relationships by electrostatic forces other than those of full covalent bonds*", molecular complexes are generally held together by metal-to-ligand binding,

by van der Waals attractive forces, by solvent reorganizing, and by partially made and broken covalent bonds (transition states). High structural organization is usually produced only through multiple binding sites. A highly structured molecular complex is composed of at least one host and one guest component. A host–guest relationship involves a balancing stereo electronic arrangement of binding sites in host and guest. The host component is defined as an organic molecule or ions whose binding sites converge in the complex and the guest component as any molecule or ion whose binding sites diverge in the complex."

1.3.2. Design of chemosensor

Outline of the chemosensors comprise of three components as shown in (Fig. 1.3) a chemical receptor capable of identifying the guest of attention usually with high selectivity; a transducer or signaling component which alters that binding event into a quantifiable physical change and finally a method of calculating this change and converting it to useful information.
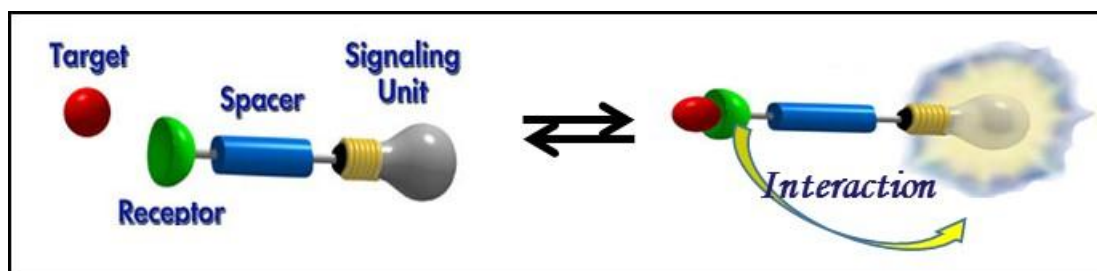
Fig 1.3. Schematic diagram showing binding of a guest by a host, producing a complex with changed optical properties.

There are three distinctive approaches which have been utilized by various groups in following the synthetic receptors, which vary in the way the first two units are arranged with respect to each other.

1. Binding site-signaling approach (Fig 1.4a)

2. Displacement approach (Fig 1.4b)

3. Chemodosimeter approach (Fig 1.4c)

These differ in the way the first two units are arranged with respect to each other. In the "binding site-signaling subunit" method the two parts are connected through a covalent bond. The contact of the analyte with the binding site makes changes in the electronic properties of the signaling subunit subsequent in sensing of the target ion.

The displacement approach is based in the formation of molecular assemblies of binding site-signaling subunit, which on organization of a definite ion with the binding site results in the release of the signaling subunit into the solution with a simultaneous change in their optical properties. In the Chemodosimeter method an exact ion-induced chemical reaction occurs which consequences in an optical signal. Out of these three methodologies the first one has been widely exploited, depending on the kind of signals produced on the binding event, se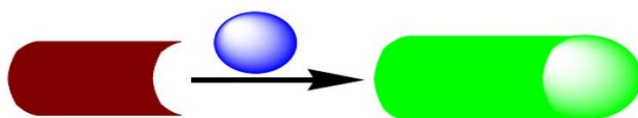nsors may be put into two types, electronic sensors or optical sensors. The previous produce signals in the form of changes in the electro chemical properties whereas the later bring the changes in optical properties.
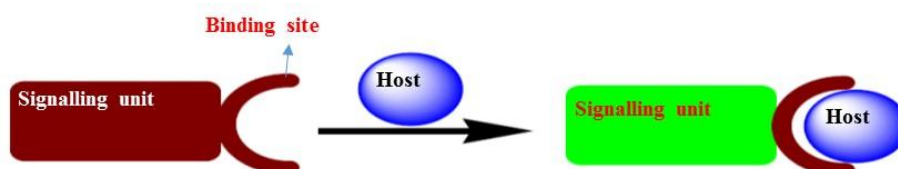
Fig 1.4a. Schematic diagram showing Binding site-signaling approach
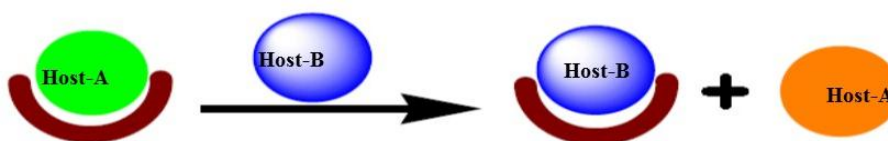
Fig 1.4b. Schematic diagram showing Displacement approach

Fig 1.4c. Schematic diagram showing Chemodosimeter approach

1.4 BRIEF LITERATURE REVIEW FOR CATION RECEPTORS

The development of chemosensors for selective cation is one of the most attracting research area in the field of supramolecular and biological chemistry. As, cations plays an imperative role in biological, chemical, environmental and industrial processes, their detection is vital for human life. For example, Co^{2+} is a key component in Vitamin-B_{12} and Zn^{2+} has a specific role to play in activity as series of biological enzymes. Further, these metal cations are considered as environmental pollutants and harmful to human health, it would be wise and cutting edge in many

terms to make use of transition metals as they are versatile nature. In the following section, some literature on chemosensors for the detections of these cations.

Ranyuk et al. (2009) synthesised a 1, 8-diaminoanthraquinone based signalling unit (R 1.1) for the selective detection of lead cation. Therefore, sensing molecule efficiently sense the Pb^{2+} ions in aqueous solutions and is effective even at neutral pH. Further, the molecule has been adopted for different metal cations just by changing the number and nature of side arms.
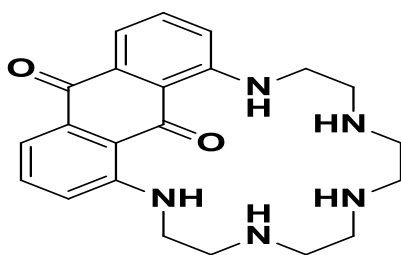
R 1.1

Further, Zhao et al. (2010) reported the rhodamine based derivative (R 1.2) carrying 7-hydroxyl quinoline group as active sen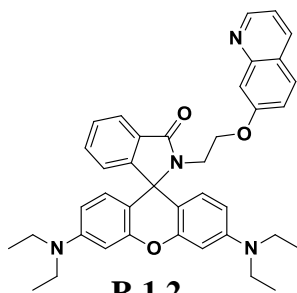sor. The molecules displayed good UV absorption and fluorescence emission in aqueous solution with highly selective and sensitive towards Hg^{2+}.

R 1.2

Martinez et al. (2010) designed and synthesised bis (pyrenyl) azadiene- based molecule (**R 1.3**) which was colorimetrically and flourometrically sensitive to Cu^{2+} and Hg^{2+}. The molecule changed the colour and enhanced the fluorescence on formation of complex with the metal ions in acetonitrile solution. The detection level was found to be in the order 10^{-6} M. Further, Goswami et al. (2010) designed and synthesised 1, 8-diaminonapthalene based analogue (**R 1.4**) which showed significant red shift only upon the addition of Cu^{2+} ions. The molecules also exhibited effective ratio metric response towards Cu^{2+} ions over other transition metals ions. The mechanism for the colour change involves ICT. The visual sensitivity of the molecule

was remarkable as it showed dual colour change from colourless (receptor molecule) to purple followed by blue as Cu^{2+} ion concentration increased.
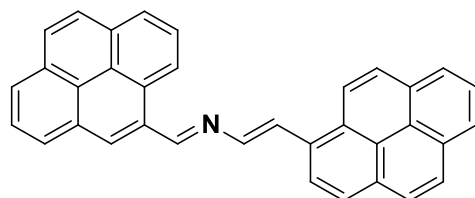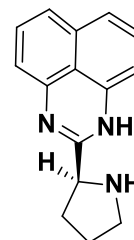
R 1.3   **R 1.4**

Cheng et al. (2011) synthesised azobenzene derivatives which can sense the Hg^{2+} ions. Chemosensor was highly selective towards Hg^{2+}. The colour changed from light yellow to dark red up on addition of Hg^{2+} ions were observed. The mechanism for selective binding was intramolecular charge transfer (ICT).
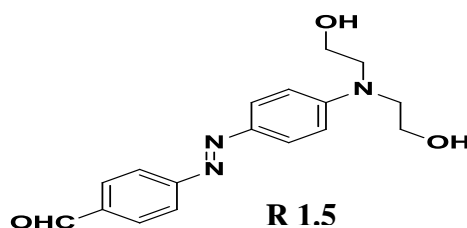
R 1.5

Nagarjun et al. (2011) developed novel aldazine- based colorimetric receptor (**R 1.6**) for Cu^{2+}. The receptor showed high selectivity and sensitivity towards Cu^{2+}. In the presence of Cu^{2+} absorption band of receptor at 425nm red shifted to 545nm. The colour of solution changes from pale yellow to purple colour.
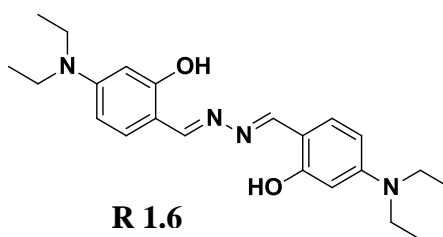
R 1.6

Kumari et al. (2012) developed simple salophen molecule (**R 1.7**) which is highly sensitive and selective towards of Hg^{2+}. Hg^{2+} ions coordinate to the receptor through NONO (Nitrogen-oxygen) binding site forming 1:1 complex. In this case "Turn-on" behavior based on solvent polarity was observed. The detection limit of receptor was found to be with Mercury is 1µg L^{-1}. Further, Tang et al. (2013)

9

synthesised thiosemicarbazide based Schiff base receptor (**R 1.8**) as a highly selective probe for Cu^{2+} detection in aqueous medium. The receptor exhibited high sensitivity with a low detection limit of 2.0 µM levels.

R 1.7

R 1.8
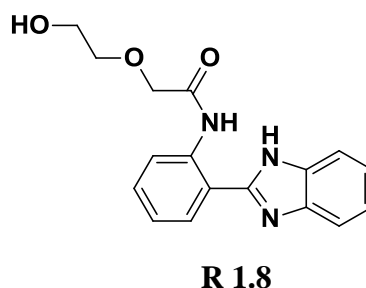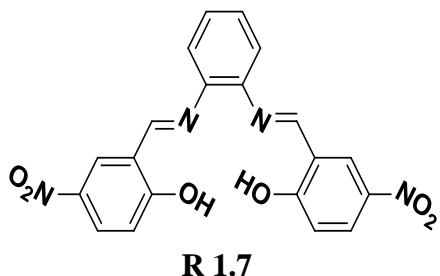
Kim et al. (2013) designed NBD-based sensors bearing a dipicolyl amine derivative (**R 1.9**), which selectively detects Hg^{2+} ions through color changes from yellow to colorless. In addition, it exhibited high selectivity for Hg^{2+} ion by ON-OFF fluorescence quenching behavior.

R 1.9
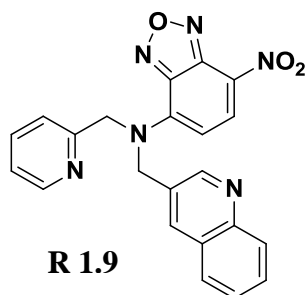
Pinherio et al. (2014) synthesized pyrene based receptor (**R 1.10**) which shows colorimetric detection for Hg^{2+} metal ion at low concentration. Later, Wei et al. (2014) developed double naphthalene Schiff base receptor (**R 1.11**) for selective detection of Hg^{2+}. Receptor displayed a color change from colorless to blue in the presence of Hg^{2+} under the 365 nm UV lamp.

R 1.10

R 1.11
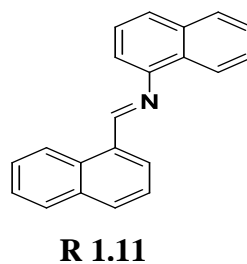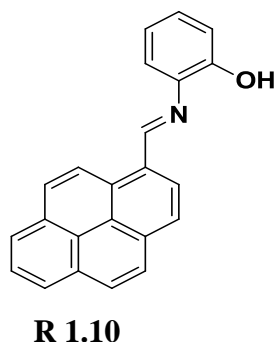
Kamlakar et al. (2014) developed a novel donor-acceptor receptor (**R 1.12**) for selective detection of Pb^{2+} and Fe^{3+} ions. The addition of Pb^{2+} to receptor shows remarkable enhancement in the absorption band at 209 nm intensity indicting the excellent selectivity and sensitivity of the receptor towards Pb^{2+}.
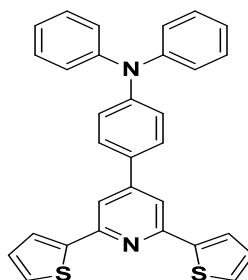
R 1.12

Lavanya et al. (2014) developed simple quinoline – Carbaldehyde receptor (**R 1.13**) for selective detection of Cu^{2+} and Hg^{2+}. The uniqueness of this probe is that it forms stable complexes with Cu^{2+} and Hg^{2+} ions. The 1:1 ratio stoichiometric complexation with Cu^{2+} ions showed a color change from yellow to colorless while with Hg^{2+} ions, it showed a 2:1 stoichiometric complexation and the color change from yellow to pink.
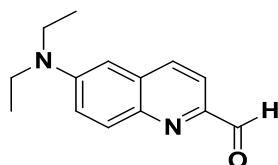
R 1.13

Chen et al. (2014) designed and synthesised Schiff base derivative (**R 1.14**) which is based on pyridine -2,6- carboxaldehyde and 2- amino ethanol which was colorimetrically sensitive towards Fe^{2+}. The compound displays a colour change from colourless to black in presence of Fe^{2+}.
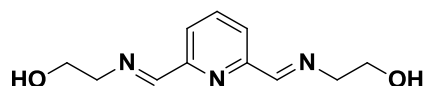
R 1.14

Tai-bao et al. (2015) designed and synthesised double naphthalene Schiff base derivative (**R 1.15**), which was flourmetrically sensitive towards Hg^{2+}. The compound displays a colour change from colourless to blue in presence of Hg^{2+} under the 365

UV lamp. The detection limit was found to be the order 5.595×10^{-8} M in DMSO medium. Also, Wang et al. (2015) synthesised pyrene-based turn-on-off fluorescent sensor (**R 1.16**) for Cu^{2+} in living cells.
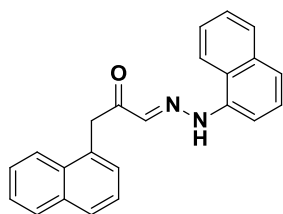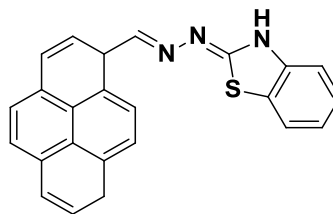
R 1.15   **R 1.16**

Choi et al. (2015) designed and synthesised a new sensor (**R 1.17**) based on diethylaminosalicylaldehyde and imidazole derivatives which was flourmetrically sensitive towards Hg^{2+}. The compound displays a color change from colorless to yellow colour which might be attributed to the ligand to metal charge transfer (LMCT) process.
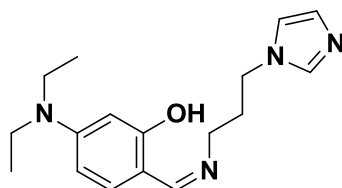
R 1.17

Kundu et.al. (2015) designed and synthesized Schiff base derivative (**R 1.18**), based on aryl ether amine which is colorimetrically selectively binds Fe^{3+} and Hg^{2+}. The compound displays color change from colorless to yellow color with Fe^{3+} and Hg^{2+}.
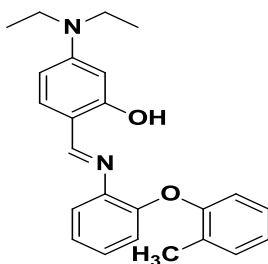
R 1.18

Li et.al. (2015) designed and synthesized Schiff base derivative (**R 1.19**) based on A triphenylamine and isoprene off-on flourmetrically and colorimetrically probes for Cu^{2+} ion. The detection limit of Cu^{2+} ion was calculated as 1.56×10^{-6} M.

R 1.19
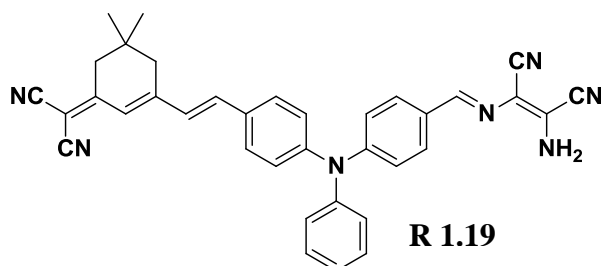
Yogesh et.al (2015) designed and synthesized highly selective fluorometric sensor (**R 1.20**) for the detection of Cu^{2+} and Hg^{2+} by using a benzothiazole based receptor in semi-aqueous medium and molecular docking.

R 1.20
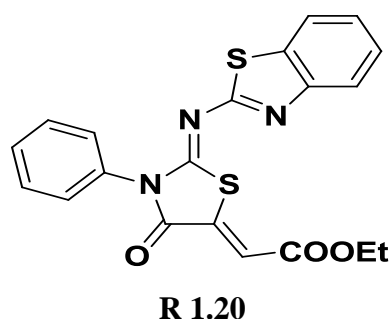
Umesh et.al (2015) designed, synthesized and developed fluorescent based receptor (**R 1.21**) for the highly selective and sensitive detection of Cu^{2+} and Zn^{2+} in semi-aqueous system. The fluorescence of receptor was enhanced and quenched respectively with the addition of Zn^{2+} and Cu^{2+} ions. Later, Nilesh et.al (2015) designed and synthesized Benzothiozole derivative (**R 1.22**) linked "off-on" multi-responsive and a high sensitivity and selectivity for Zn^{2+} through a turn-on fluorescence response the detection limit down to 0.40 μM.
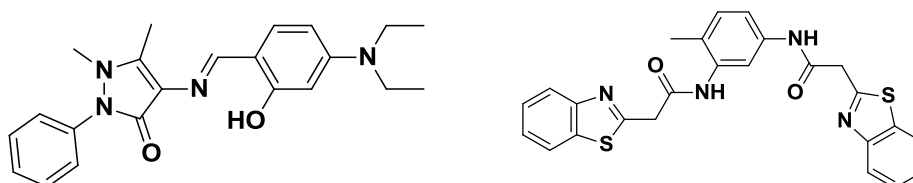
Sivamani et.al (2017) developed aldoxime based biphenyl-azo derivative (**R 1.23**) for detection of Hg^{2+} and F^-. Gargi et.al (2017) synthesized amino- benzothiazole based receptor (**R 1.24**) for the selective detection of Hg^{2+} ions. Later, She et.al (2017) designed congeneric fluorescent sensor (**R 1.25**) that utilize Rhodamine–B for detection of Hg^{2+} ions.
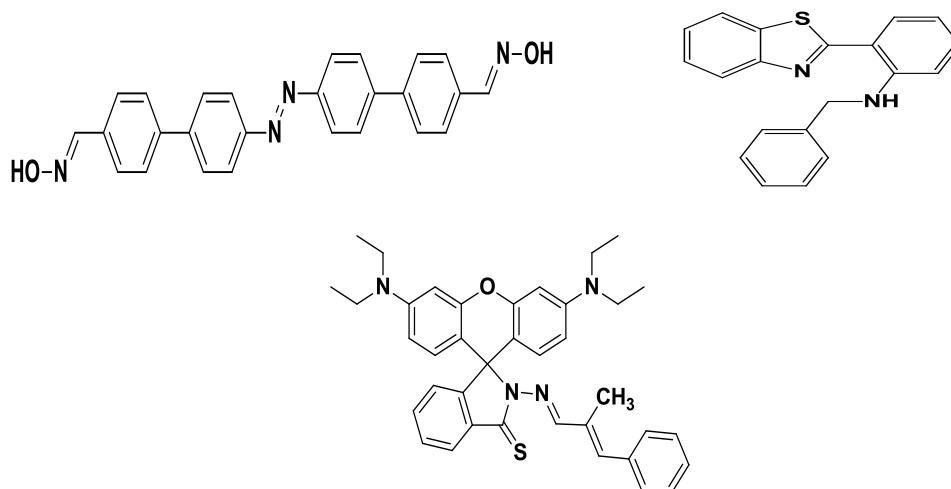
Tekuri et.al (2017) designed and synthesized a new heterocyclic thiophene 2-carboxylic acid hydrazide based chemosensor (**R 1.26**) for selective detection of Cd^{2+} and Cu^{2+}
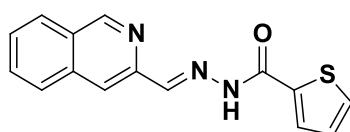
Yin et al. synthesized a derivative of carbazole chemosensor (fluorescence) for the detection of Cu^{2+} (Yin et al. 2018). The receptor showed the colorimetric and fluorometric response for the Cu^{2+} ions in the acetonitrile solution. The sensor displayed a 1:1 stoichiometric complex with Cu^{2+} ions, and the calculated DL was 2.74×10^{-8} M from the fluorescence method.
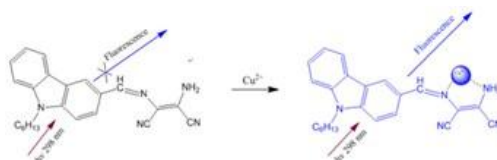
R 1.27

Kalyani Rout et al. have been a synthesis of new guanidine based bis Schiff base chemosensor for colorimetric detection of Hg(II) and fluorescent detection of Zn(II) ions **(Rout et al. 2019)**. The sensor displayed a naked eye response from yellow to red for Hg^{2+}. The detection limit for Hg^{2+} and Zn^{2+} is found to be 9.89×10^{-7} M and 1.23×10^{-6} M, respectively. Further, the chemosensor has applications in real sample

14

analysis in environmental and biological samples and building molecular logical devices.
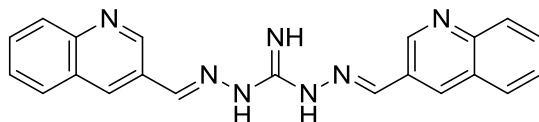
R 1.28

Thangaraj Anand and Suban K Sahoo have synthesized a new sensor **N1.** In the 1:1 of $CH_3OH:H_2O$ (v/v) medium, it exhibited selectivity and sensitivity for Hg^{2+} and Cu^{2+} ions by a distinct colorimetric change from pale yellow to pink color. It showed 1:1 stoichiometry with Cu^{2+}/Hg^{2+} ions. The N1 displayed detection limit of 4.70×10^{-7} M and 1.23×10^{-7} M for Hg^{2+} and Cu^{2+} ions. Finally, the practicability of **N1 (R 1.29)** to quantify Hg^{2+} and Cu^{2+} ions in real water samples was successfully validated by using both the UV–Vis and the smartphone (Anand and Sahoo 2019).
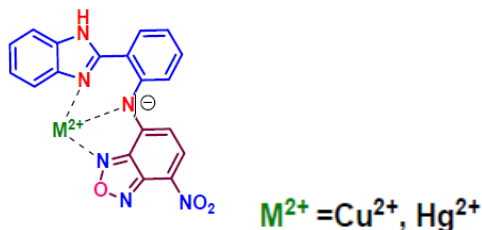
R 1.29

1.5 SCOPE OF WORK

Among the wide range of cations, the detection of environmentally hazardous cations has gained great attention because of its high toxicity and cause serious health illness. Looking at the literatures it can be concluded that the design and synthesis of the receptor is well defined area of supramolecular chemistry. However, majority of investigations are having some drawbacks which includes.

➤ Majority of the receptors are involved complicated molecules which were synthesized and require multistep complicated chemistry. Hence these receptors are not cost effective

➤ Majority of them are based on fluorometric detection. Hence the detection process involves the complicated, confusing equipment

➢ Detection at μM levels still needs to be explored

➢ Majority of receptors works only without real-time applications

1.6 OBJECTIVES

The objectives of the proposal work are as follows,

➢ Synthesis of organic molecules which can show colorimetric cation sensing property even at low concentration of analyte in organic solvents as well as in aqueous media. The synthesized organic molecules were characterized by various spectroscopic techniques. e.g. ^{1}HNMR, ^{13}CNMR, FT-IR, CHNS analysis, LCMS .

➢ Determination of shift in λ_{max} using UV-Vis spectrophotometry

➢ Determination of receptor to cation complexation ratio using Job's plot (with the help of UV-Vis spectrophotometry)

➢ Quantitative analysis of cation concentration using UV-Vis titration

➢ Calculation of binding constant using B-H equation and Bindfit method.

➢ To grow single crystals of the complex molecules (cation-sensor complex) in different solvent systems so that the binding properties of the metal ions to the sensor could be studied in the solid state

1.7 AIM AND OUTLINE OF THE WORK

The present work deals with design, synthesis and characterization of Schiff's base based molecules for ion recognition property sensing. Our design strategy includes the photoactive organic moiety such as pyrene, thiocarbazone, thiazole and quinoline which acts as a signaling unit linked covalently with heterocyclic ring, which act as ionophore for binding of cations and anions. All the synthesized molecules were characterized by spectral techniques and molecular structures of selected molecules have been established by single crystal X-ray study. Further, the interactions of these ionophores with various cations and anions have been investigated in detail and ion recognition process is monitored by ^{1}H NMR, UV-Vis spectral changes. Binding constants have been calculated by B-H plot. Conclusively, in the current research work, four series of receptor molecules were designed, synthesised and characterised as chemosensors for the molecular recognition of cations.

SYNTHESIS OF BENZOTHIAZOLE SCHIFF'S BASE COLORIMETRIC CHEMOSENSOR FOR THE RECOGNITION OF MERCURY ION

Abstract

In this chapter, the design, synthesis and characterizations of new benzothiazole Schiff's base derivatives as colorimetric receptors for the detection of mercury ions have been discussed in detail. The colorimetric cation sensing properties and detection mechanism of these receptors have been incorporated.

2.1. INTRODUCTION

Conservatively the detection of mercury ion is usually expensive as it uses sophisticated instruments, complicated procedures or low sensitivity and selectivity approaches like atomic absorption/emission spectroscopy or inductively coupled plasma mass spectroscopy. For these reasons, the chromogenic chemosensors are especially attractive as they permit naked eye detection of color change without any use of spectroscopic instruments. In addition, these colorimetric sensors ideally have the benefits of low cost, easy synthesis and storage, and more tolerance towards different experimental conditions. The efficient colorimetric sensors could be achieved by designing a host molecule in such a way that binding of the guest molecule, **(Fig.2.0)** transforms into a color change. Based on the literature survey, the receptors based on benzothiazole Schiff's base are effective chemosensors. The presence of hydroxyl group in the receptor helps to form chelation and hence increase the colorimetric sensitivity towards mercury ion.
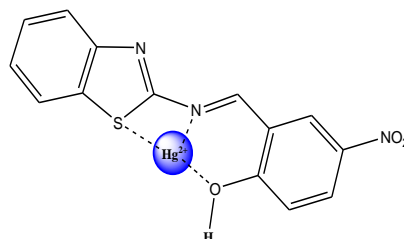
Fig. 2.0. Binding of the guest molecule

2.2. EXPERIMENTAL SECTION

All chemicals were procured from Sigma-Aldrich, Alfa Aesar or from Spectrochem and used without further purification. All the solvents were

procured from Spectrochem, SD Fine, India of HPLC grade and used without further distillation. The ^{1}H NMR spectra were recorded on a Bruker, (400MHz) instrument using TMS as internal reference and DMSO-d_6 as solvent. Resonance multiplicities are labelled as s (singlet), d (doublet), t (triplet) and m (multiplet). Melting points were measured on a Stuart-SMP3 melting-point apparatus in open capillaries. Infrared spectra were recorded on a Perkin-Elmer FT-IR spectrometer; signal designations: s (strong), m (medium) and w (weak). UV-vis spectroscopy was carried out with Analytikjena Specord S600 Spectrometer in standard 3.5 mL quartz cells (2 optical windows) with 10 mm path length.

2.2.1. Synthesis of receptor S1R1, S1R2, S1R3

The receptors (S1R1- S1R3) was designed and synthesized in a single step, through a condensation reaction as shown in (Scheme 2.1). The targeted receptor molecules were synthesized by condensing 0.83 mM of 2-amino benzothiazole with 0.83 mM of respective aldehyde i.e., 5-nitrosalicyaldehyde (for S1R1), benzaldehyde (for S1R2) and biphenyl-4-carboxaldehyde (for S1R3) in ethanol solution at room temperature for 3 hrs and a drop of acetic acid was added as catalyst. After cooling, the solid was filtered and washed with ethanol to get the desired compounds. The obtained products were characterized by ^{1}H NMR, FT-IR spectroscopy, ^{13}C NMR and Mass spectrometry (**Fig. 2.1–2.12**).
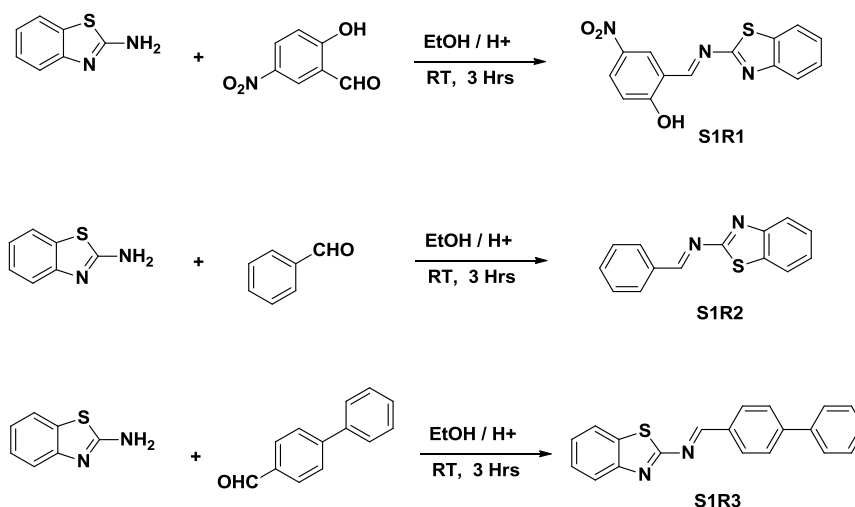
Scheme-2.1: Synthesis of receptors **S1R1, S1R2** and **S1R3**

2.2.2. Characterization data for S1R1, S1R2, S1R3:

2-(Benzothiazol-2-yliminomethyl)-4-nitro-phenol, (S1R1):

Melting range: 247-250˚C; IR (KBr, frequency in cm^{-1}): (C=C) 1463 cm^{-1}, 1526 cm^{-1}, (C=N) 1608 cm^{-1}, (C-H aromatic str) 3075 cm^{-1}, (OH) 3377 cm^{-1}. **^{1}H-NMR (DMSO-d$_6$, δ_{ppm} 400 MHZ)**: 7.44 m (aromatic 4H), 7.96 m (aromatic 1H), 8.39 m (aromatic 2H), 9.26 d (HC=N), 9.91 d Broad (-OH).**^{13}C NMR (DMSO-d$_6$, 100 MHz)** 102.05, 104.95 110.29, 115.41, 119.61, 131.57, 132.86, 135.34, 135.61, 140.79, 154.21, 162.95, 163.90 and 167.03. MS (ESI, m/z) calculated 299.30, observed (M+1) 300. Elemental analysis calculated C-56.18, H- 3.03, N-14.04 Observed C- 56.32, H-3.08, and N-13.85.

Benzothiazol-2-yl-benzylidene-amine (S1R2):

Melting range: 219-224˚C; IR (KBr, frequency in cm^{-1}): (C=C) 1543 cm^{-1}, (C=N) 1615 cm^{-1}, (C-H aromatic str), 3067 cm^{-1}. **^{1}H NMR (400 MHz DMSO-d$_6$, δ_{ppm}):** 6.6 m (aromatic 3H), 7.12 m (aromatic 3H), 8.04 m (aromatic H), 8.09 m (aromatic H), 8.51 s (HC=N). **^{13}C NMR (CDCl$_3$, 100 MHz)** 119.44, 121.04 122.00, 123.69, 124.36 126.03, 128.77, 137.49. MS (ESI, m/z) calculated 238.31, observed (M+1) 239.00. Elemental analysis calculated C-70.56, H- 4.23, N-11.76 Observed C- 70.42, H-4.28, and N- 11.87.

Benzothiazol-2-yl-biphenyl-4-ylmethylene-amine (S1R3):

Melting range: 220-226˚C; IR (KBr, frequency in cm^{-1}): (C=C) 1543 cm^{-1}, (C=N) 1615 cm^{-1}, (C-H aromatic str) 3062cm^{-1}. **^{1}H NMR (400 MHz DMSO-d$_6$, δ_{ppm}):** 7.12 m (aromatic 3H), 7.45 m (aromatic 3H), 7.70 m (aromatic 3H), 8.73 m (aromatic 4H), 9.39 s (HC=N). **^{13}C NMR (CDCl$_3$, 100 MHz)** 117.50, 118.48, 120.99, 122.20, 124.37, 125.53, 130.73, 139.74, 165.70, 166.57. MS (ESI, m/z), calculated 314.40, observed (M+1) 314.00, Elemental analysis calculated C-76.40, H- 4.49, N-8.91 Observed C- 76.32, H-4.41, N- 8.78.
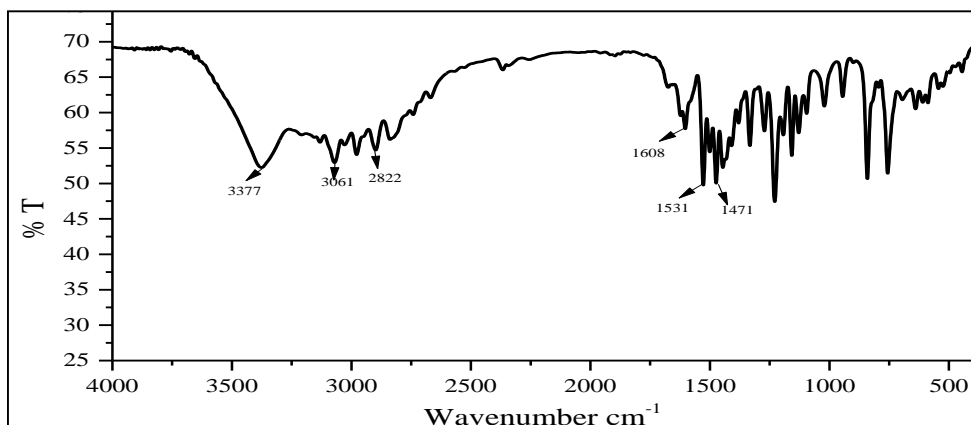
Fig. 2.1: FT-IR Spectrum of receptor **S1R1**
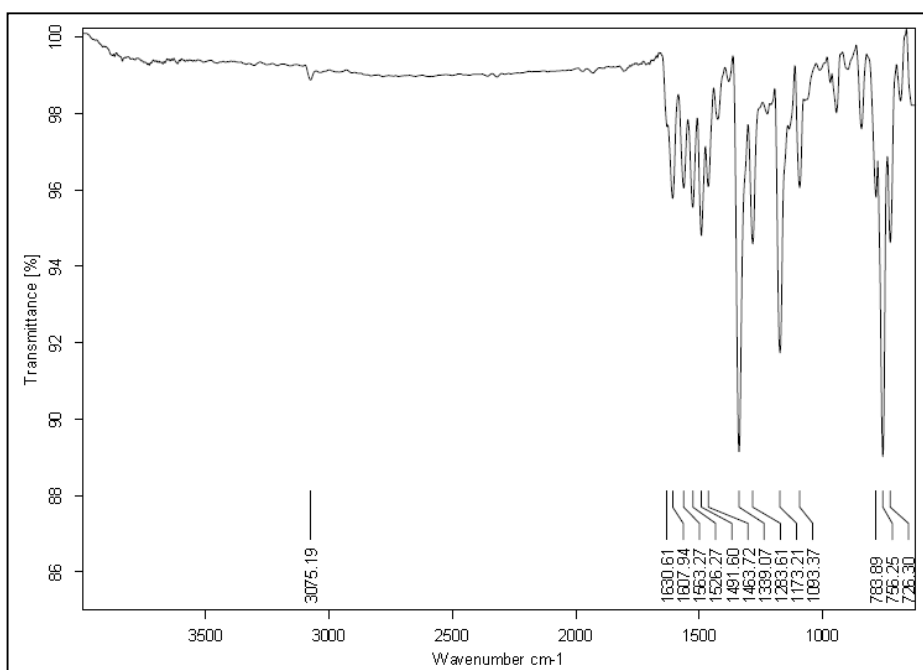
Fig.2.2: FT-IR Spectrum of receptor **S1R2**
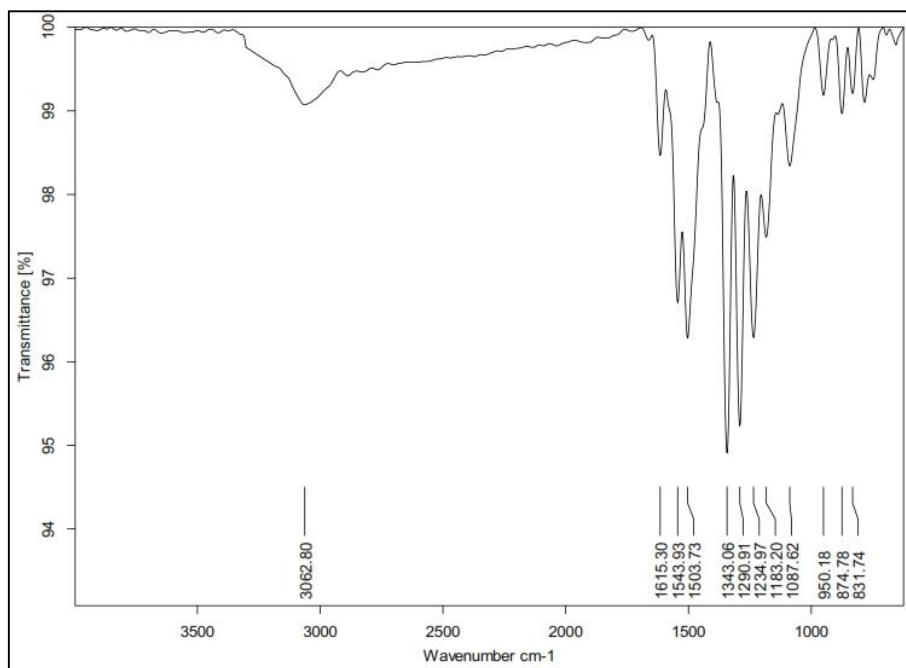
Fig 2.3: FT-IR Spectrum of receptor **S1R3**
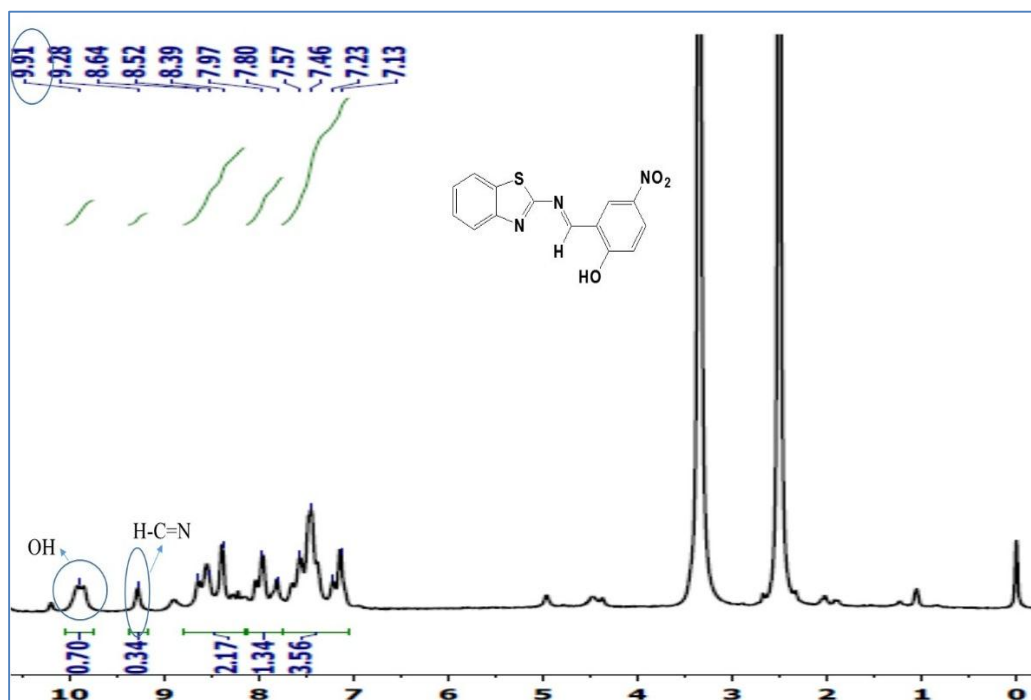
Fig 2.4: ^{1}H NMR spectrum of receptor **S1R1**
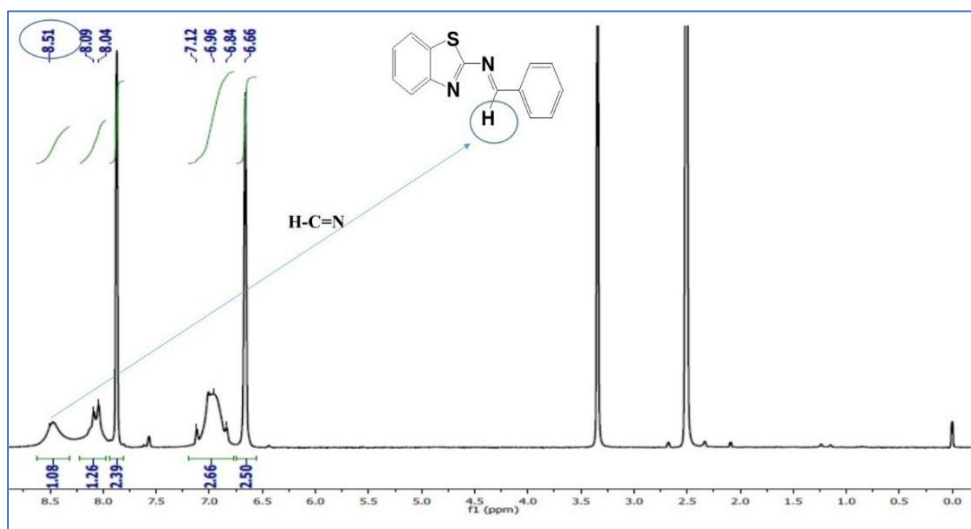
Fig. 2.5: ^{1}H NMR spectrum of receptor **S1R2**
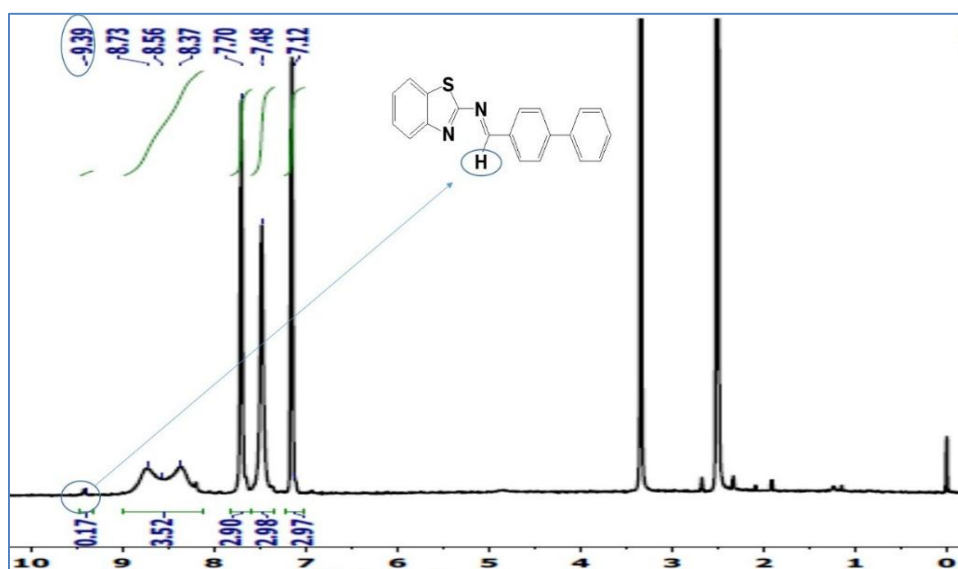
Fig. 2.6: ^{1}H NMR spectrum of receptor **S1R3**
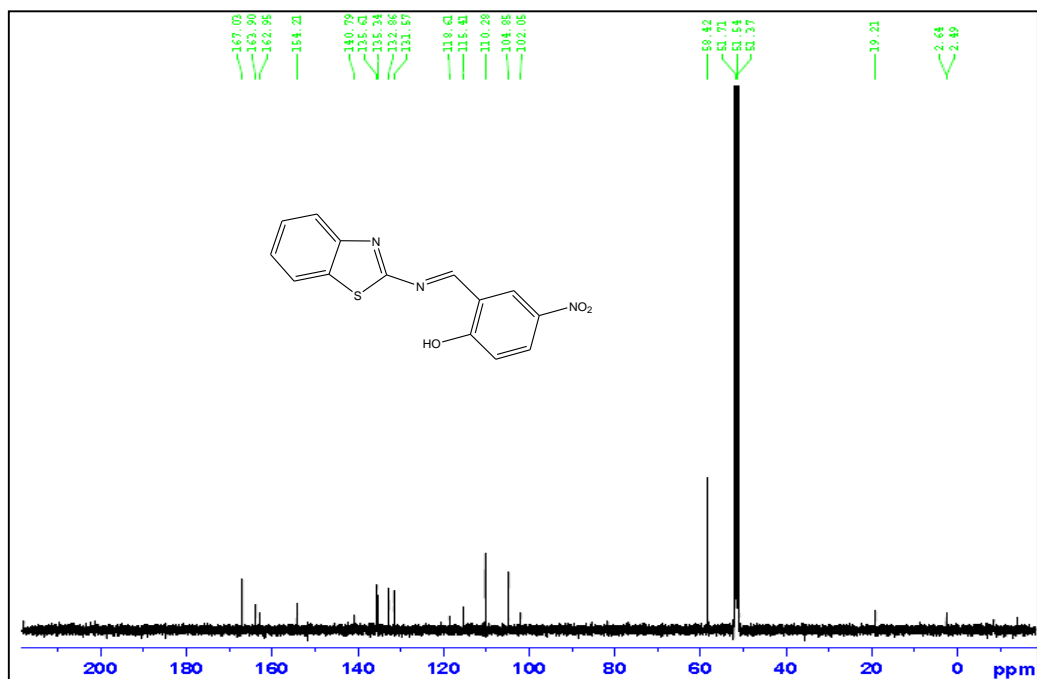
Fig. 2.7. ^{13}C NMR spectrum of receptor **S1R1**
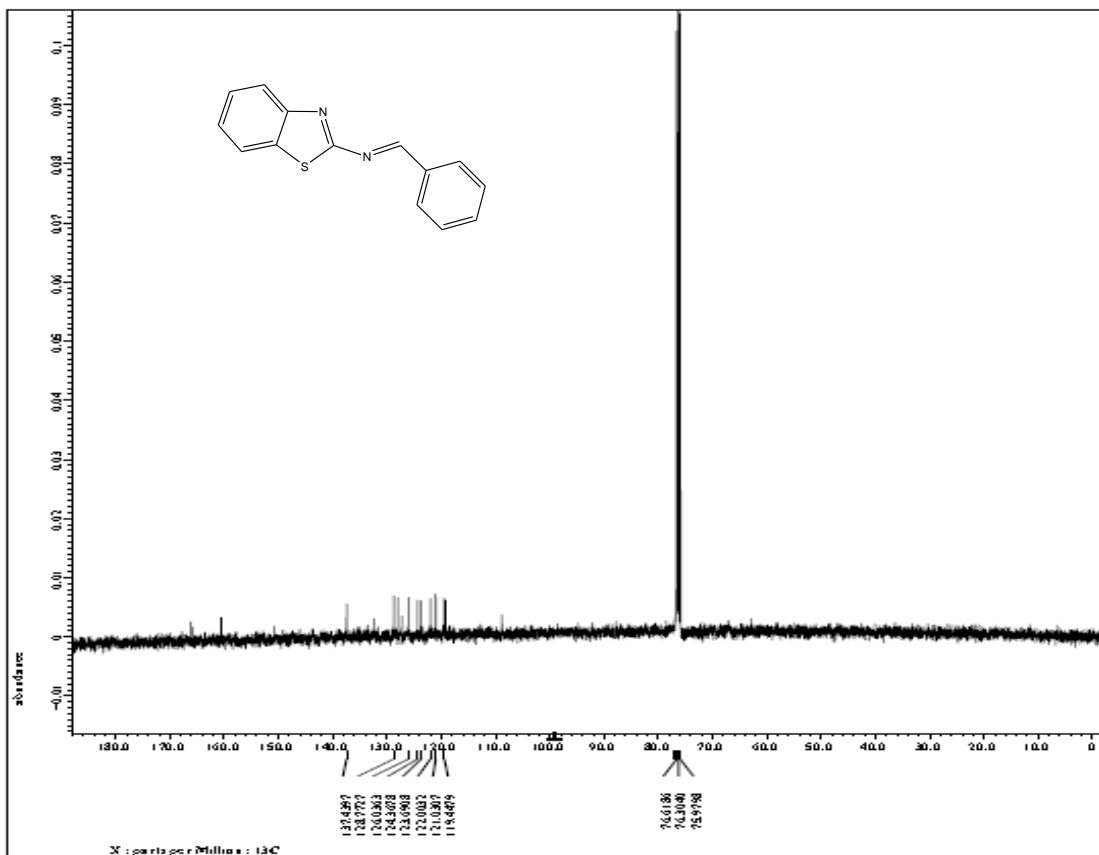
Fig. 2.8. ^{13}C NMR spectrum of receptor **S1R2**

23
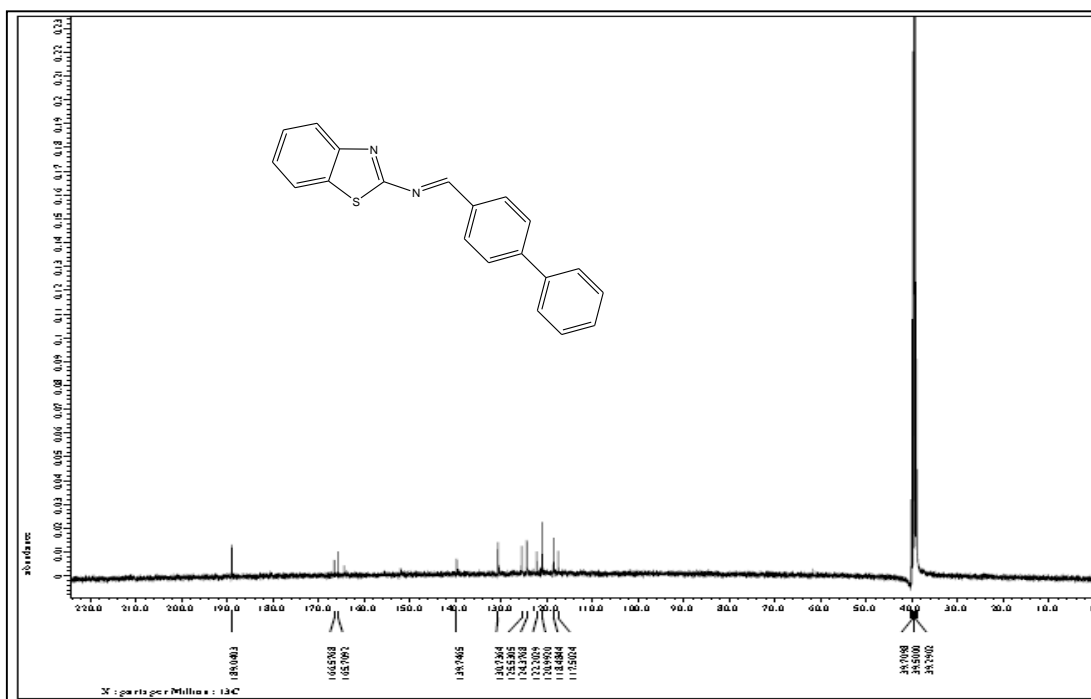
Fig 2.9. ^{13}C NMR spectrum of receptor **S1R3**
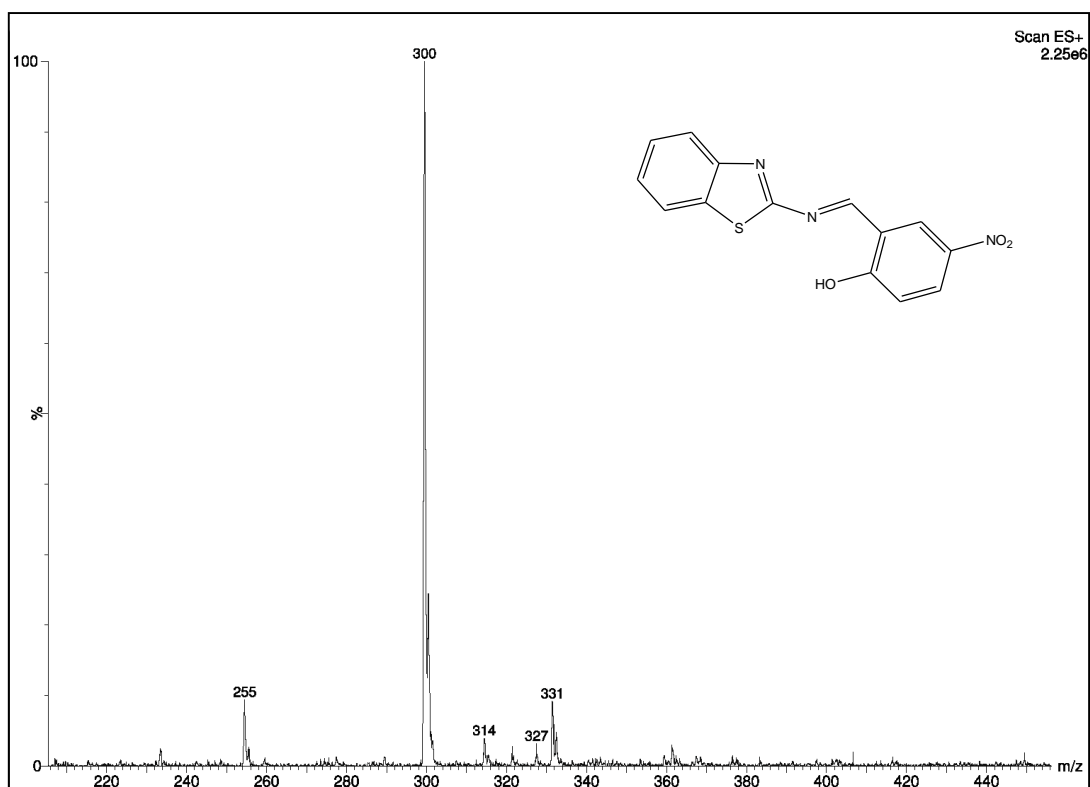
Fig 2.10: ESI-mass spectrum of receptor **S1R1**
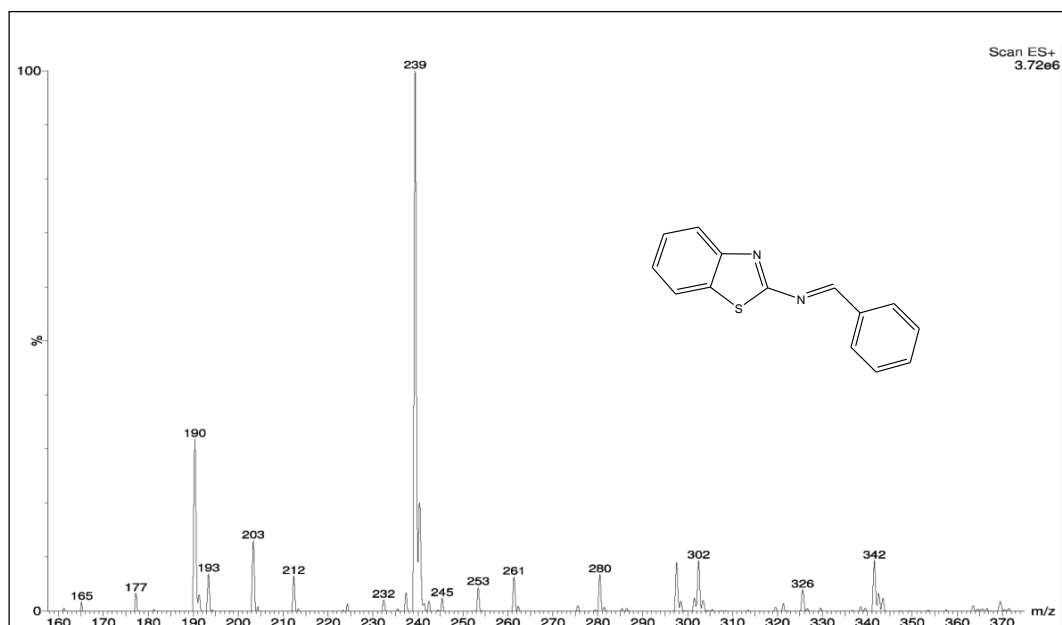
Fig 2.11: ESI-mass spectrum of receptor **S1R2**
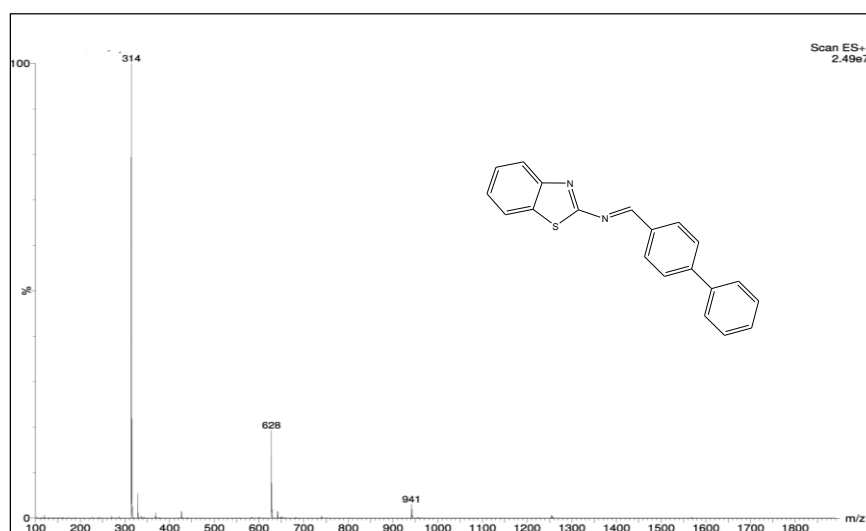
Fig 2.12: ESI-mass spectrum of receptor **S1R3**

2.3. RESULTS AND DISCUSSION

An individual colorimetric studies were conducted for the all synthesized receptors **S1R1, S1R2, S1R3** in DMSO solvent, $(2.5\times10^{-5}$ M) for the detection of different cations such as Ni^{2+}, Hg^{2+}, Pb^{2+}, Cu^{2+}, Co^{2+}, Cr^{3+}, Zn^{2+} and Fe^{2+} in an aqueous solution $(1.0\times10^{-3}$ M). The receptor **S1R1** showed a significant color change from yellow color to color less in the presence of Hg^{2+} ions which can be easily identified by the naked eye. While the **S1R1** did not show any color change in the

25

presences of 3.4 equiv. of other tested cations. It indicates that the receptor **S1R1** has selective and sensitive towards Hg^{2+} ions over the other tested metal ions. In the similar way the receptor **S1R2** and **S1R3** were investigated for colorimetric detection of cations and they did not show any color change in the presence 3.4 equiv. of Hg^{2+} and other tested cations.

The reorganization ability of receptor **S1R1** towards different metal ions investigated by colorimetric as shown in Fig.2.13, receptor **S1R1** did not show any color changes in the presence of 3.4 equiv. of an aqueous solution of different cations such as Ni^{2+}, Hg^{2+}, Pb^{2+}, Cu^{2+}, Co^{2+}, Cr^{3+}, Zn^{2+} and Fe^{2+}. In the presence 3.4 equiv. of Hg^{2+} ions the receptor **S1R1** show a significant color change from yellow to colorless, which could be easily detected by naked-eye as shown **Fig. 2.13**.
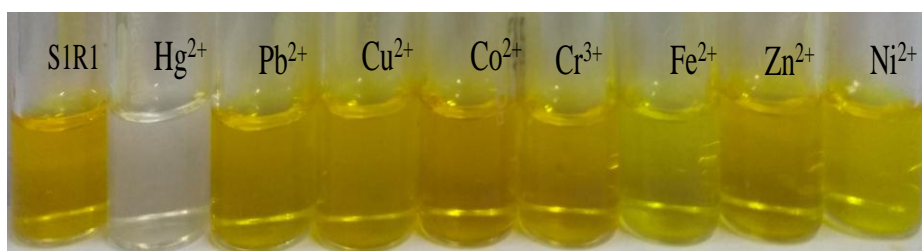
Fig. 2.13. The colorimetric changes observed by naked-eye of receptor **S1R1** upon addition of 3.4 equiv. of various cations in an aqueous solution

2.3.1. UV- Vis spectral studies of receptors

The absorption spectra of receptor **S1R1** in DMSO show major band at 445 nm. The recognition ability of receptor **S1R1** towards different metal ions investigated by UV-Vis measurement as shown in (Fig.2.14a,) receptor **S1R1** did not show any absorption spectra in the presence of 3.4 equiv. of an aqueous solution of different cations such as Ni^{2+}, Hg^{2+}, Pb^{2+}, Cu^{2+}, Co^{2+}, Cr^{3+}, Zn^{2+} and Fe^{2+}. In the presence 3.4 equiv. of Hg^{2+} ions the receptor **S1R1** show a new absorption band at 345 nm and decreased absorption intensity at 445 nm in the UV-Vis absorption spectra (Fig. 2.14a) and the solution of receptor **S1R1-Hg²⁺** showed a significant color change from yellow to colorless, which could be easily detected by naked-eye as shown (Fig. 2.13.) This signifies the interaction between receptor **S1R1** and Hg^{2+} ions and the receptor **S1R1** sense Hg^{2+} in aqueous medium efficiently.
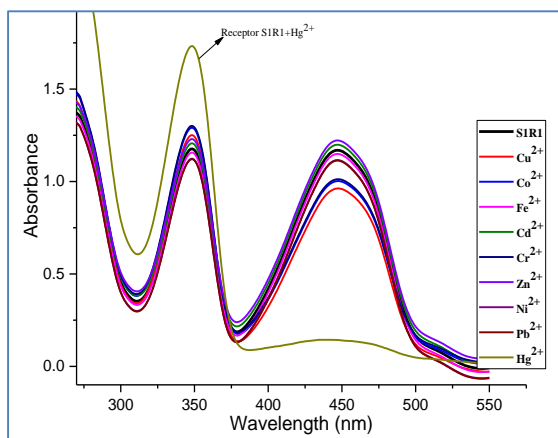
Fig. 2.14a: UV-Vis spectral change of receptor S1R1 (2.5×10^{-5} M in DMSO solvent) in the presence of 3.4 equiv. various metal ions. Insert showing the absorbance of receptor S1R1 and S1R1+Hg^{2+} ions
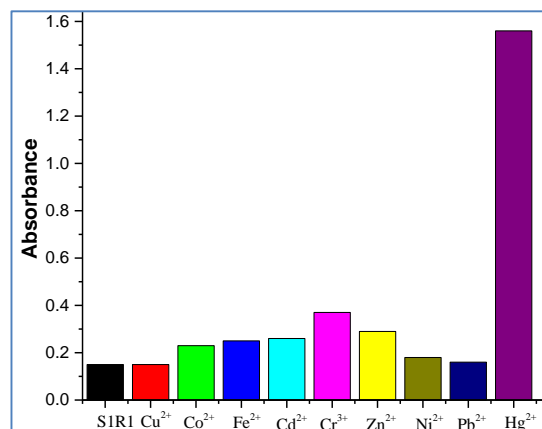
Fig. 2.14b: A bar chart representation of absorption change of S1R1 in the presence of 3.4 equiv. of various metal ions at wavelength 345 nm

To explore the sensing properties of receptor **S1R1** and Hg^{2+}, UV-Vis spectral titration experiment was performed between receptor **S1R1** and Hg^{2+} ions as shown in (Fig.2.15). The incremental addition from 0 to 3.4 equiv. of Hg^{2+} ions (1.0×10^{-3} M in an aqueous solution) to a solution of receptor **S1R1** in (2.5×10^{-5} M in DMSO solution), the absorption intensity band at 445 nm corresponds to –OH group in the receptor **S1R1** gradually decreases and a new band at 345 nm gradually increases. This observation is due to the formation of the complexation of Hg^{2+} ions with receptor **S1R1**, the electron rich hydroxyl group functioned as a donor group and Hg^{2+} accepts electrons. The binding modes of receptor **S1R1** and Hg^{2+} ions were supported by FT-IR studies. The free receptor **S1R1** displayed –OH str. frequency at 3377 cm^{-1} whereas the –OH str. frequency of complex (**S1R1** - Hg^{2+}) almost decreased in the FT-IR spectra (Fig. 2.16), this decrimental –OH str. frequency results suggests that Hg^{2+} ions might bind to the phenolic –OH, and neighboring groups $S_{thiazole}$ and N_{imine}.
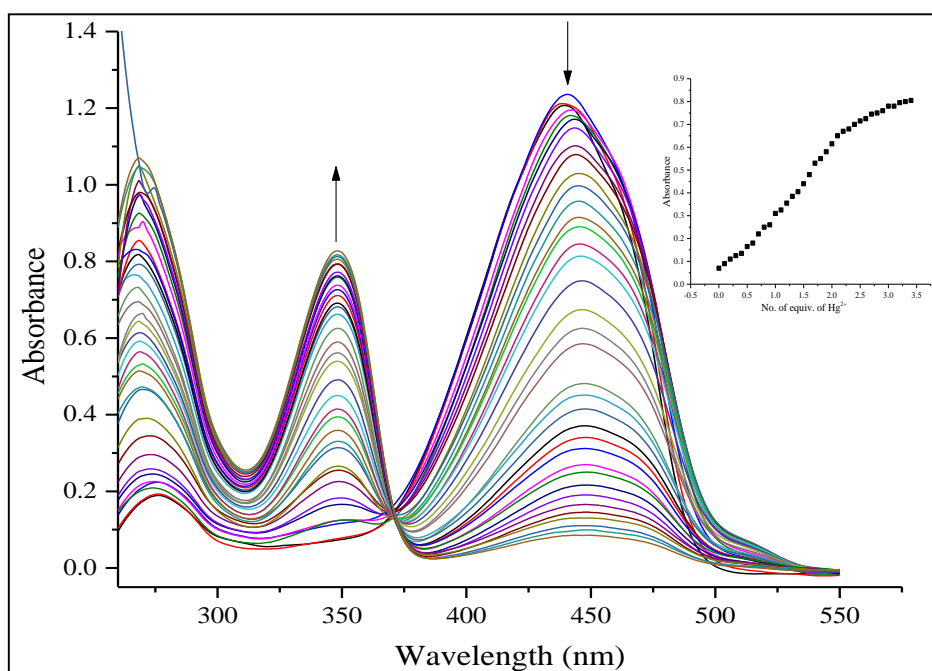
Fig. 2.15: UV–vis spectra of **S1R1** (2.5×10^{-5} M, DMSO) with increasing concentration of Hg^{2+} ions (0 – 3.4 equiv.) in an aqueous medium. Inset graph shows binding isotherm at selective wavelength (345 nm)
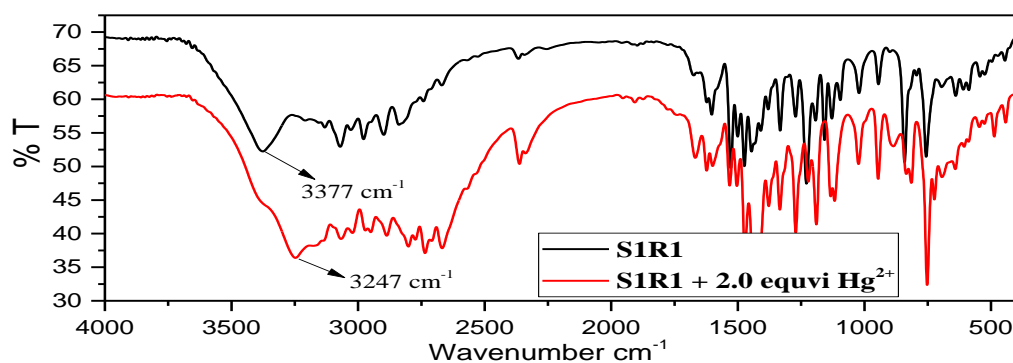
Fig. 2.16: FT-IR Spectra of free receptor **S1R1** and **S1R1** in the presence of 2.0 equvi of Hg^{2+}

The binding stoichiometry between receptor **S1R1** and Hg^{2+} ions was determined by the Benesi-Hildebrand (B-H) method using UV-Vis spectrometric titration data wavelength at 345 nm. The linearity of the graph confirms the formation of stable 1:1 complexation of receptor **S1R1** with Hg^{2+} ions as shown in (Fig. 2.17a). The association constant (K) found to be 6.8×10^{3} M^{-1} using following equation. Further, the stoichiometry and association constant values were determined by Bindfit

28

method given in supramolecular.org (P. Tandarson et al.2010). And results shows 1:1 binding ratio of receptor and metal (Fig. 2.17b).

$$\frac{1}{(A - A_o)} = \frac{1}{\{K (A_{max} - A_o)[M_X^+]^n\}} + \frac{1}{[A_{max} - A_o]}$$

Where, A_0, A, A_{max} are the absorption considered in the absence of Hg^{2+}, at an intermediate, and at a concentration of saturation, K is binding constant, $[M_x^+]$ is concentration of Hg^{2+} ions and n is the stoichiometric ratio.
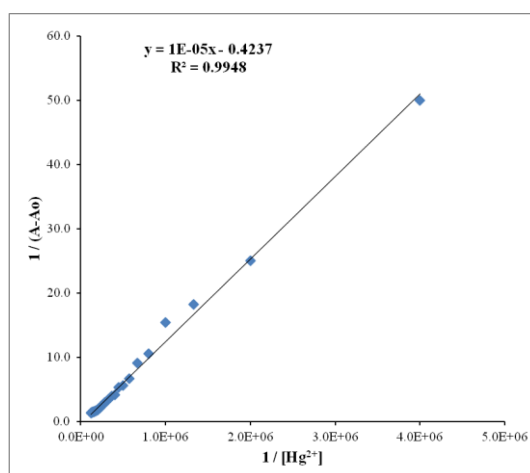
Fig. 2.17a: Benesi–Hildebrand plot of receptor **S1R1** assuming 1:1 binding stoichiometry with Hg^{2+} ions, wavelength at 345 nm
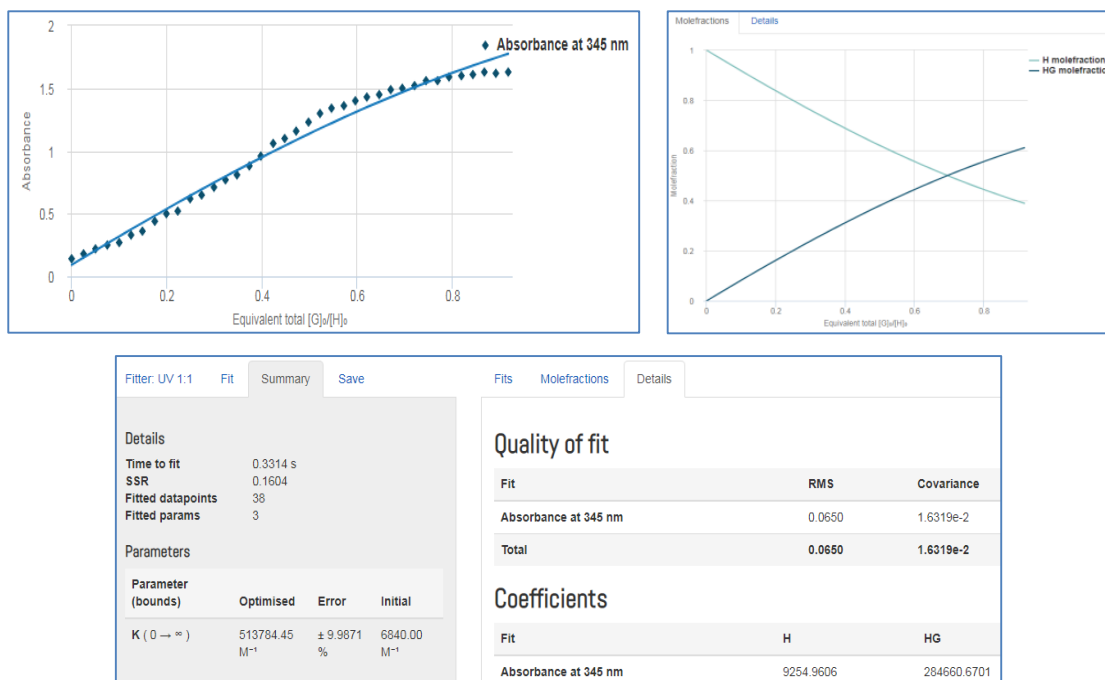
Fig. 2.17b: Bindfit plot of receptor **S1R1** and **Hg^{2+}; S1R1 shows** 1:1 binding stoichiometry with Hg^{2+} ions, wavelength at 345 nm

2.3.2. Detection limit (DL) and quantization limit (QL) determination of Hg^{2+} ions.

The detection limit (DL) and quantization limit (QL) for Hg^{2+} ion was determined using a calibration plot between Hg^{2+} metal ion concentration (range from 2.5×10^{-7} M to 6.0×10^{-6} M) and corresponding absorbance of receptor **S1R1-Hg^{2+}**complex measured wavelength at 345 nm.

The DL and QL were determined based on the standard deviation of the response and the slope using the following equation mentioned by ICH quality guideline Q2R1

$$DL \ or \ QL = \frac{C \times \sigma}{m}$$

Where σ = standard deviation of blank measurement, m = slope of the calibration curve, C = constant (for DL 3.0 and QL 10.0). The calibration plot was drawn between the concentration of metal ion and absorbance using LINEST MS-excel as shown in the (Fig. 2.18). Further, the calculated DL was found to be 0.03 ppm and QL was found to be 0.3 ppm.
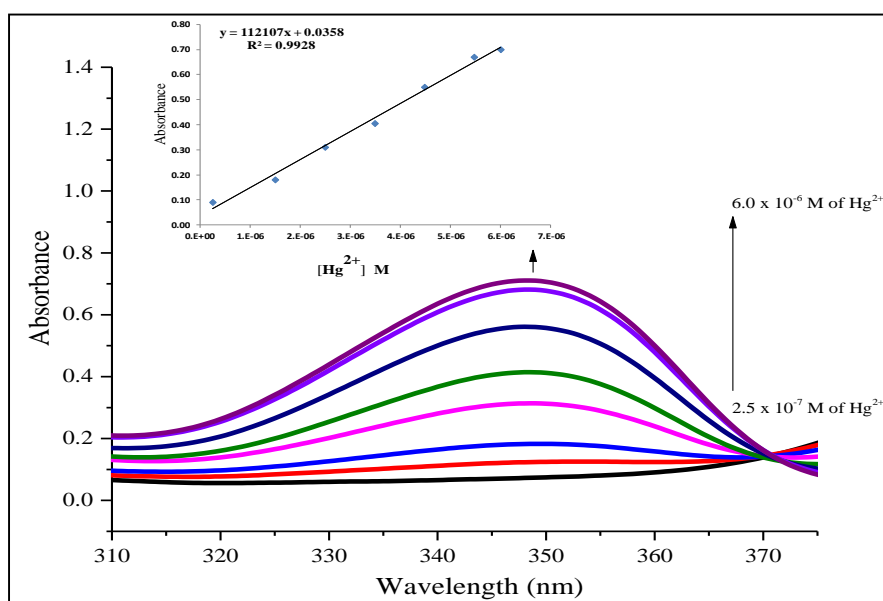
Fig. 2.18: Linearity of UV-Vis spectra of complex (**S1R1**-Hg^{2+}). Inset graph shows   calibration curve plot of absorbance of complex (**S1R1**-Hg^{2+}) vs. concentration of Hg^{2+} ions in M

2.3.3. Binding mechanism

Based on the UV-Vis titration studies experiment, FT-IR and ^{1}H NMR titrations were carried out to further identify the binding mechanism. The Fig 2.19 shows the ^{1}H NMR spectra of receptor **S1R1** (5×10^{-4} M) up on addition of 0-2 equiv. of Hg^{2+}. When treated with 1.0 equvi of Hg^{2+}, the peak of phenol –OH up field shifted from 9.0 ppm to 8.8 ppm, while it completely disappeared after adding 2.0 equiv. of Hg^{2+} ion at the same time the aromatic proton signals were also affected which underwent a concomitant up field shift. When the concentration of metal ion increases the lone pair of electron (non-bonded electrons) on oxygen which are responsible for formation of metal- ligand complex. In that case the bond length between the oxygen and Hydrogen become weaker so the bond between oxygen and hydrogen acts as partial bond as this result the hydroxyl proton signal is disappears. These observations clearly supported the –OH group involved in the binding mechanism. The binding mechanism of the Hg^{2+} ions to the receptor **S1R1** can be proposed as showed in **Fig 2.20.** The FT-IR spectrum were recorded for the free receptor **S1R1** and the mixture of **S1R1** – 2.0 equvi of Hg^{2+} complex individuality, the observation reveals that the –OH Str. frequency of receptor **S1R1** almost diminished in the presence 3.4 equiv. of Hg^{2+} ions, as shown in Fig. 2.16. From the UV-Vis titration and FT-IR studies results reveals that -OH group present in receptor **S1R1** responsible for binding of Hg^{2+} ions.
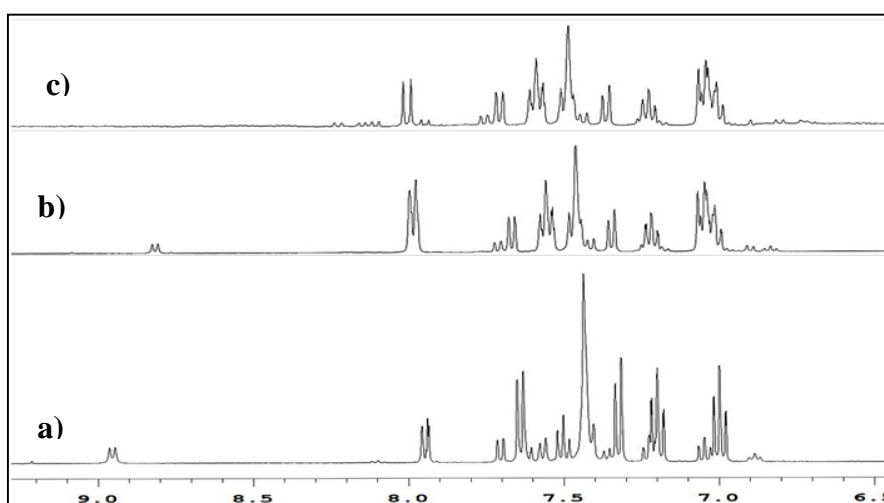
Fig 2.19: ^{1}H NMR titration of receptor **S1R1** with Hg^{2+} ions. (a). Free receptor **S1R1**, (b). **S1R1** and 1.0 Equiv. of Hg^{2+}, (c). **S1R1** and 2.0 Equiv. of Hg^{2+} ions
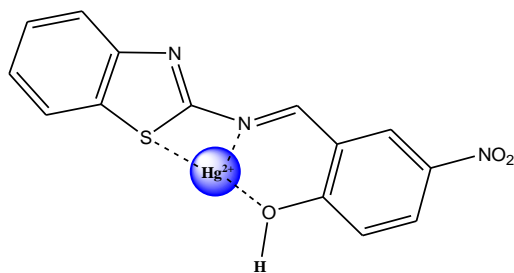
Fig 2.20: Proposed binding mechanism of Hg^{2+} ions with receptor **S1R1**

2.4. CONCLUSION

To summarize, the design and synthesis of receptors molecules **S1R1-S1R3** as a potential candidate for chemo sensors. Among the tested receptors, the molecule **S1R1** showed effective and selective sensing ability for the colorimetric detection of Hg^{2+} ions over other tested cations. The phenolic–OH functional group of **S1R1** as a binding site showed a significant colour change from yellow colour to colourless, selectively in the presence of Hg^{2+} ions which can be easily identified by the naked-eye, where as other tested cations failed to show any significant colour change. This colour change was due to the formation of complex between Hg^{2+} ions and receptor **S1R1**, which was confirmed by UV-Visible spectral titrations, ^{1}H NMR and solid state FT-IR studies. The receptor **S1R1** showed a reasonable detection limit of 0.03 ppm and a quantization limit of 0.3 ppm for Hg^{2+} ions.

NEW THIOCARBAZONE SCHIFF'S BASE COLORIMERIC CHEMOSENSORS FOR DETECTION OF Hg^{2+}, Cu^{2+}, AND Cd^{2+} IONS

Abstract

In this chapter, the design, syntheses and characterizations of new heterocyclic thiocarbazone Schiff's base derivatives as efficient colorimetric receptors for Cu^{2+}, Hg^{2+}, and Cd^{2+} metal ions have been discussed in detail. The colorimetric cation sensing properties and detection mechanism of these receptors have been incorporated.

3.1. INTRODUCTION

The designing of new capable colorimetric receptors for selective recognition of biologically and environmentally important metal ions, such as Cu^{2+}, Hg^{2+}, and Cd^{2+}, have attracted much attention globally. In addition, the application for new colorimetric receptors has extensively improved, mostly because it involves the detection through a less expensive technique in which the analyte is detectable by a color change noticeable by direct optical observation. Nevertheless, colorimetric techniques also offer several advantages in comparison with others, such as high sensitivity, quick response and they are non-destructive. Hence many artificial organic receptor molecules containing different channels such as imine, (Azadbakht et al.2013; Ermakova et al. 2013; Jiang et al.2012; Lauwerys et al.1994; Choi et al. 2014), coumarine, (Beer and Gale 2001; Que et al.2008) quinolines (Jiang et al.2011), (Vinod Kumar and Anthony2014) and rhodamine (Labbe et al. 1999), (Zhang et al.2015) have been developed as colorimetric cation sensors. Metal ions have a very important role namely in stabilization and reactivity of proteins. However, for human and environmental well-being, they must occur in optimal quantities. Otherwise, they can promote metabolic disorders since they are easily fascinated and accumulated from the environment (Zhang et al.2015; Wu et al.2016). Metal ions, for instance Hg^{2+}, Pb^{2+} and Cd^{2+} are extremely toxic and pollutant and once present in water they are carcinogenic. Recently, Udaya Kumari et al. 2014 developed an innovative Schiff base molecular sensor **1** for different metal ions using signaling channels based on a

carbazole backbone which showed a highly selective colorimetric response to Hg^{2+}, Cu^{2+}, and Co^{2+} ions in DMSO solvent.

With this background, herein we reported the thiocarbazide group into the sensor molecule so that it can strengthen transition and heavy metals coordination ability. These receptor moieties comprise thio group (–C=S–) and imine group (–C=N) groups as a binding site for cation detection. The receptors were designed on the binding site spacer and signaling unit methodology, which are used for the recognition of different heavy metal ions. The binding of Hg^{2+} ions to the receptor **S2R1** shows significant enhancement in a visible color change from colorless to yellow color, **S2R2** shows colorless to yellow color with Cu^{2+} ions, **S2R3** colorless to pale pink with Cd^{2+} ions.

3.2. EXPERIMENTAL SECTION

3.2.1. Materials, spectroscopic and physical methods

All chemicals and metal nitrate salts were purchased from commercial suppliers and used without any further purification. The synthetic and HPLC grade solvents were used for synthesis and UV-Vis titrations without any further purification. ^1H NMR spectra were recorded on a Bruker-400MHz spectrometer. Single crystal X-ray diffraction (SC-XRD) data for synthesized molecules collected on a Bruker Apex II duo diffractometer with a CCD detector. As a source of radiation for the experiment, monochromatic Molybdenum (Mo) Kα radiation (λ=0.7107Å) was used. Data collection was done at ambient temperature (296K). All the crystal structures were solved by direct methods using SHELXL-2007/2014 software and the refinement was carried out by full-matrix least-squares technique using SHELXL-2007/2014. For all the non-hydrogen atoms anisotropic displacement parameters were calculated. Melting point was recorded on Stuart-SMP3 melting-point apparatus in open capillaries and are uncorrected. Fourier Transform Infrared (FT-IR) Spectra was recorded on a Bruker Alpha which is equipped with silicon carbide as IR source. All sample spectra were recorded using KBr pellet media. The samples under study were recorded with 16 scans with the sample resolution of 4 cm^{-1}. The background data collection was done with KBr pallet prior to the analysis of samples. The UV-Vis

titrations were carried out on UV-Vis spectrophotometer (Analytikjena Specord S600) in standard 3.0 mL quartz cells (2 optical windows) having a path length of 1.0 cm.

3.2.2. Colorimetric and UV–Vis studies

A Stock solution of various metal ions as their nitrate salts (1.0×10^{-2} M) was prepared in de-ionized water. An individual receptor stock solution of **S2R1- S2R3** (1.0×10^{-3} M) were prepared in dimethyl sulphoxide (DMSO). The stock solutions **S2R1- S2R3** were further diluted to 2.5×10^{-5} M with the same solution. In colorimetric and UV-Vis titration experiments, metal ions were added by using a micropipette to a receptor solution **(S2R1-S2R3)**. UV-Vis spectral data were recorded after the addition of the metal ions using 3.0 mL quartz cells (2 optical windows) having a path length of 1.0 cm.

3.2.3. General synthesis procedure for receptor S2R1- S2R3

A Schiff base reaction was conducted for amine and aldehydes in 1:2 molar ratio into a six individual solution of thiocarbohydrazide in ethanol (15 mL) and thiophene-2-carboxaldehyde, 5-phenyl thiophene-2-carboxaldehyde, furfural-2-carboxaldehyde, 5-Nitro furfural-2-carboxaldehyde, pyrrol-2-carboxaldehyde and 8-hydroxy quinoline-2-carbaldehyde was added slowly and a catalytic amount of acetic acid was added, then stirred the reaction mixture for 3 hours at room temperature. After obtaining, the precipitates ensured the absence of starting materials absence in the reaction mass. The precipitates were filtered and washed with ethanol and dried under hot air oven, then cooled and recorded the weight and calculated the % yield of synthesized chemosensors. The synthesis method is shown in the **(Scheme 3.1)**
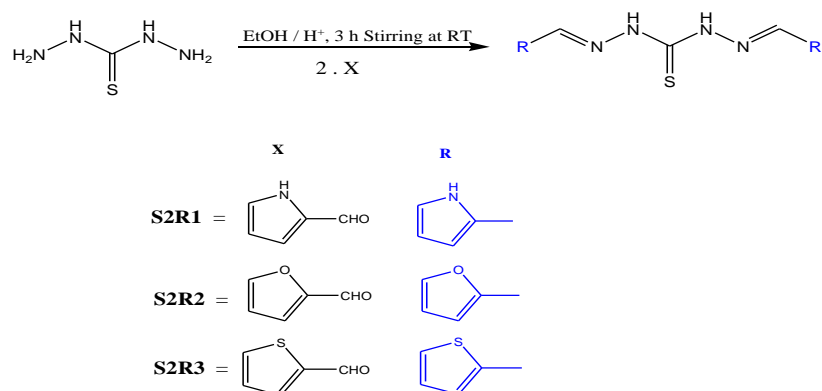
Scheme 3.1: Synthesis route for compounds **S2R1- S2R3**

3.2.4. Characterization data for S2R1, S2R2, S2R3

(E)-2-((1H-pyrrol-2-yl)methylene)-N'-((E)-(1H-pyrrol-2-yl)methylene)hydrazine-1-carbothiohydrazide, (S2R1): Melting point: 257˚C. FT-IR (KBr, cm^{-1}): 3377, 3063, 1611, 1608, 1470, 838. ^{1}H-NMR (**400MHz**, DMSO-d$_6$, δ_{ppm}): 6.30-6.32 (d, aromatic, 2H), 6.5-6.7 (m, aromatic, 2H), 8.0-8.2 (s, imine, 2H), 11.2 (s, NH of heterocyclic nitrogen, 2H), 11.5 (s, NH of carbazine Nitrogen, 2H). ^{13}C NMR (**100Mz** DMSOd$_6\delta_{ppm}$)167.03,163.09,162.95,154.21,135.34,132.86,131.57,115.41,110.28,104.85. LC-MS (ESI) m/z: Calculated for C$_{11}$H$_{12}$N$_6$S, 260.32, found, 261.20 (M+1). From the crystallography data the receptor **S2R1** was unsymmetrical molecule and the 4 protons of –**NH** are in different chemical environment so it shows different chemical shift values in ^{1}H- NMR spectra.

(E)-N'-((E)-furan-2-ylmethylene)-2-(furan-2-ylmethylene)hydrazine-1-carbothiohydrazide, (S2R2): Melting point: 252˚C. FT-IR (KBr, cm^{-1}): 3371, 3076, 1611, 1600, 1456, 835. **^{1}H-NMR (500 MHz DMSO-d$_6$, δ_{ppm}):** 7.25 (m, aromatic 2H), 7.4 (m, aromatic 2H), 7.8 (m, aromatic 2H), 8.20 (s, imine, 2H), 10.31 (s, N-H), 10.18 and (s, NH). ^{13}CNMR (**100Mz,** DMSO-d$_6$ δ_{ppm}) 179.08, 149.21, 144.32, 143.54,138.08,137.65,131.90,130.92,128.16,127.91,126.71.LC-MS (ESI) m/z: Calculated for C$_{11}$H$_{10}$N$_4$O$_2$S$_2$, 262.29, found, 263.10 (M+1). From the crystallography data the receptor **S2R2** was unsymmetrical molecule (Due to bulky molecules) and the 2 protons of –**NH** are in different chemical environment one –NH is near to sulphur and other –NH is far away to sulphur so it shows different chemical shift values in ^{1}H- NMR spectra.

(E)-N'-((E)-thiophen-2-ylmethylene)-2-(thiophen-2-ylmethylene)hydrazine-1-carbothiohydrazide (S2R3): Melting point: 278˚C. FT-IR (KBr, cm^{-1}): 3334, 3066, 1626, 1615, 1494, 840. **^{1}H-NMR (500 MHz DMSO-d$_6$, δ_{ppm}):** 7.0 (m, aromatic 2H), 7.4 (m, aromatic 2H), 7.8 (m, aromatic 2H), 8.21 (s, imine, 2H), 10.32 (s, N-H), 10.21 and(s,NH).^{13}CNMR(**100Mz**DMSOd$_6\delta_{ppm}$)157.41,140.72,138.41,131.55,128.35,127.92,126.91,122.56,113.32,109.25. LC-MS (ESI) m/z: Calculated for C$_{11}$H$_{10}$N$_4$S$_3$, 294.42, found, 295.10 (M+1). the receptor **S2R3** was expected to be unsymmetrical molecule (Due to bulky molecules) and the 2 protons of –**NH** are in different

chemical environment one –NH is near to sulphur and other –NH is far away to sulphur so it shows different chemical shift values in ^{1}H- NMR spectra.

The characteristic spectra of receptors S2R1, S2R2, S2R3 have been given below **(Fig. 3.1- 3.9).**
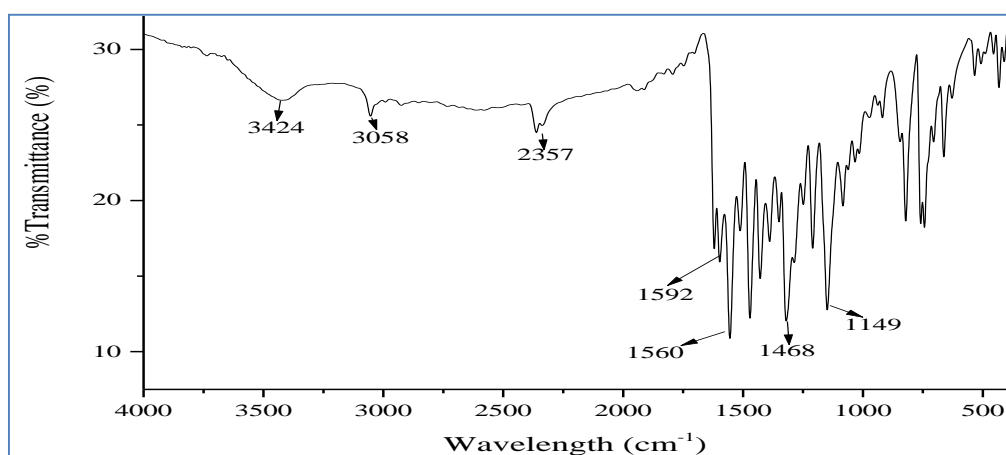
Fig. 3.1: FT-IR Spectrum of receptor S2R1
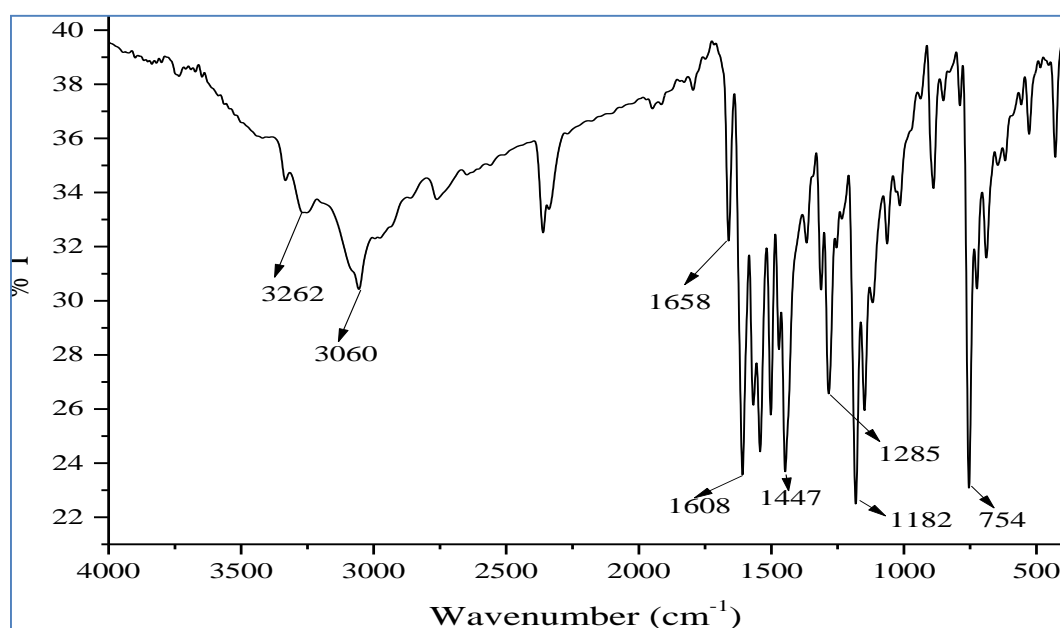
Fig. 3.2: FT-IR Spectrum of receptor S2R2
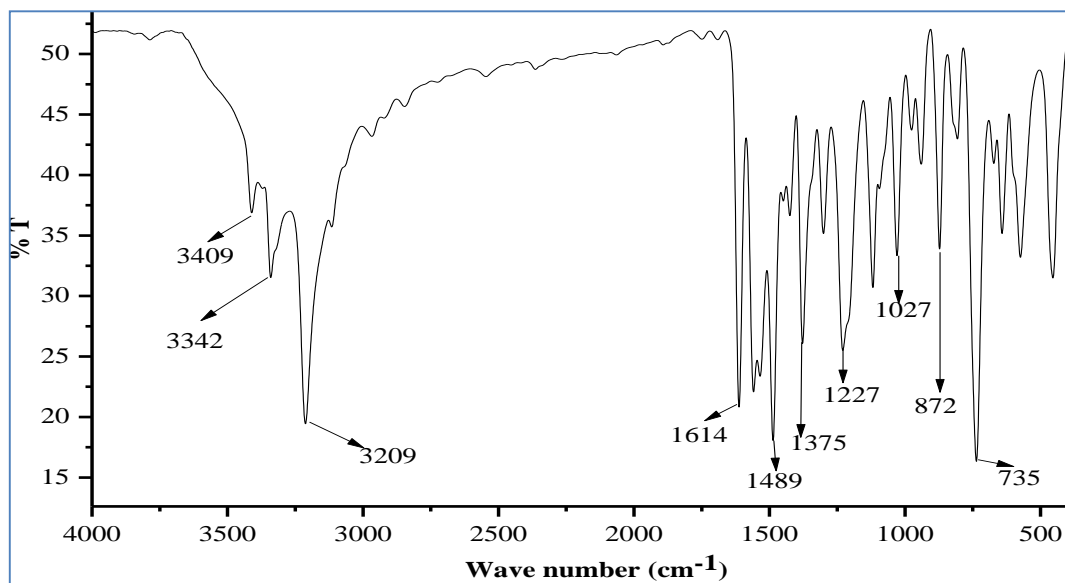
Fig. 3.3: FT-IR Spectrum of receptor S2R3
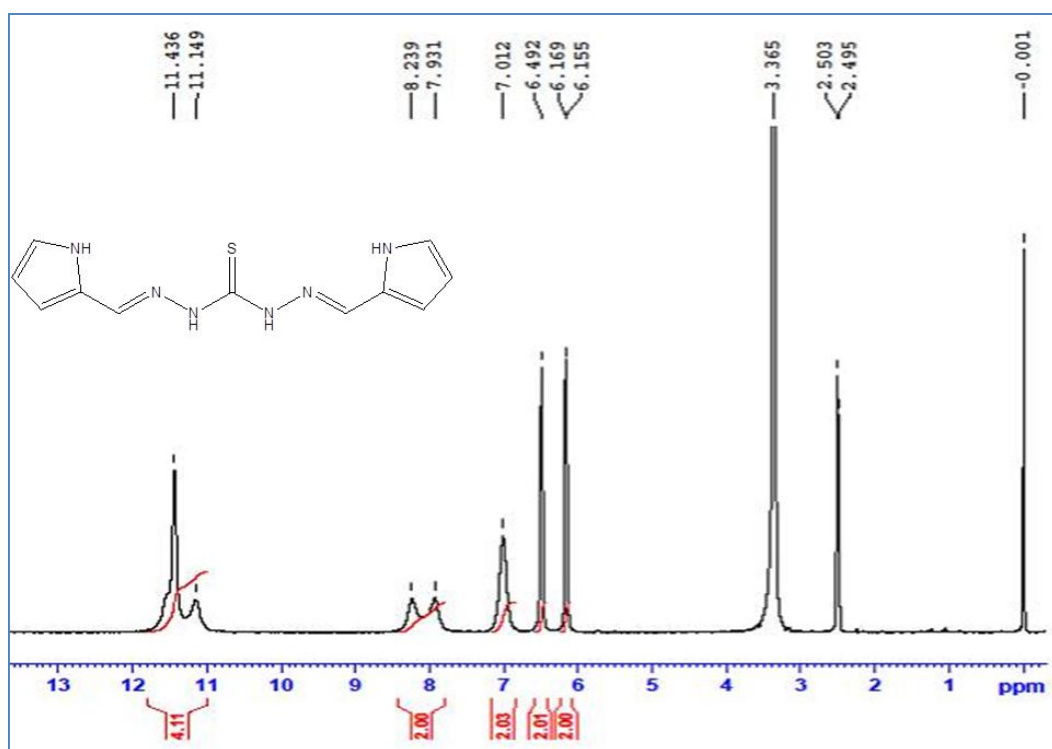
Fig. 3.4: ^{1}H NMR spectrum of receptor **S2R1**
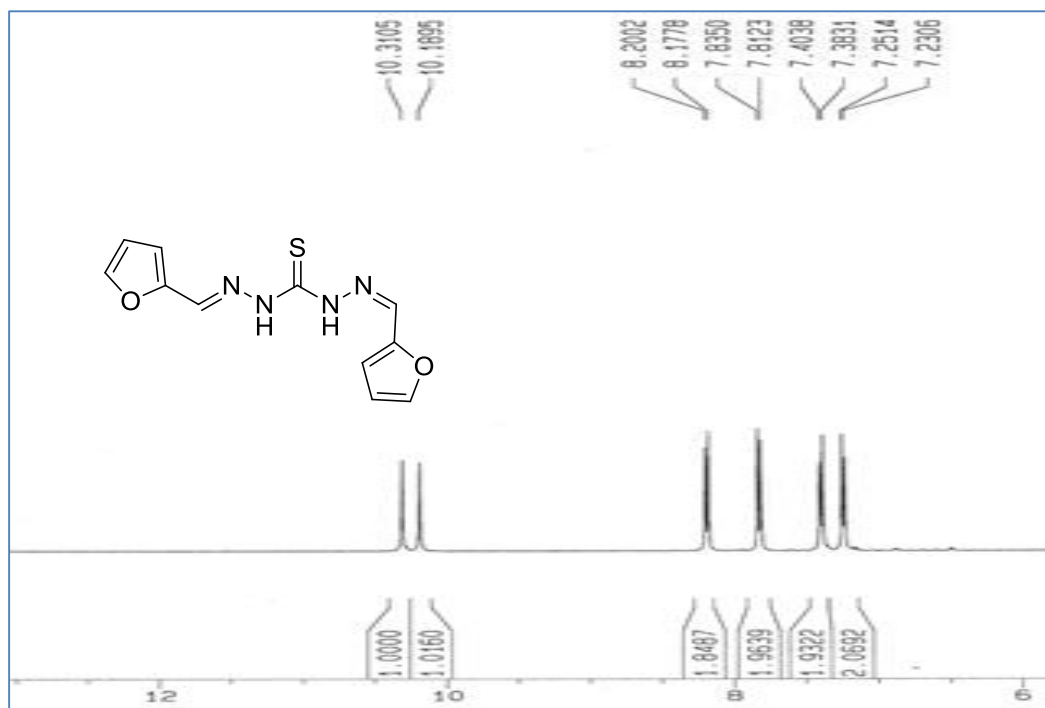
Fig. 3.5: ^{1}H NMR of spectrum receptor **S2R2**
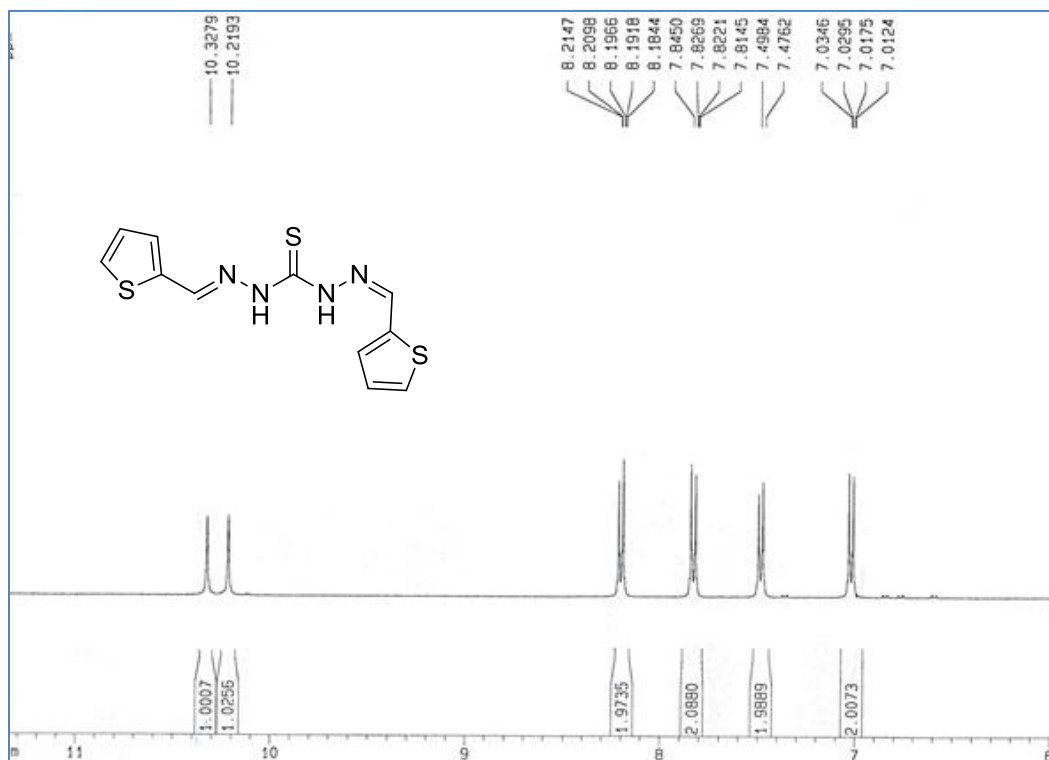
Fig. 3.6: ^{1}H NMR spectrum of receptor **S2R3**
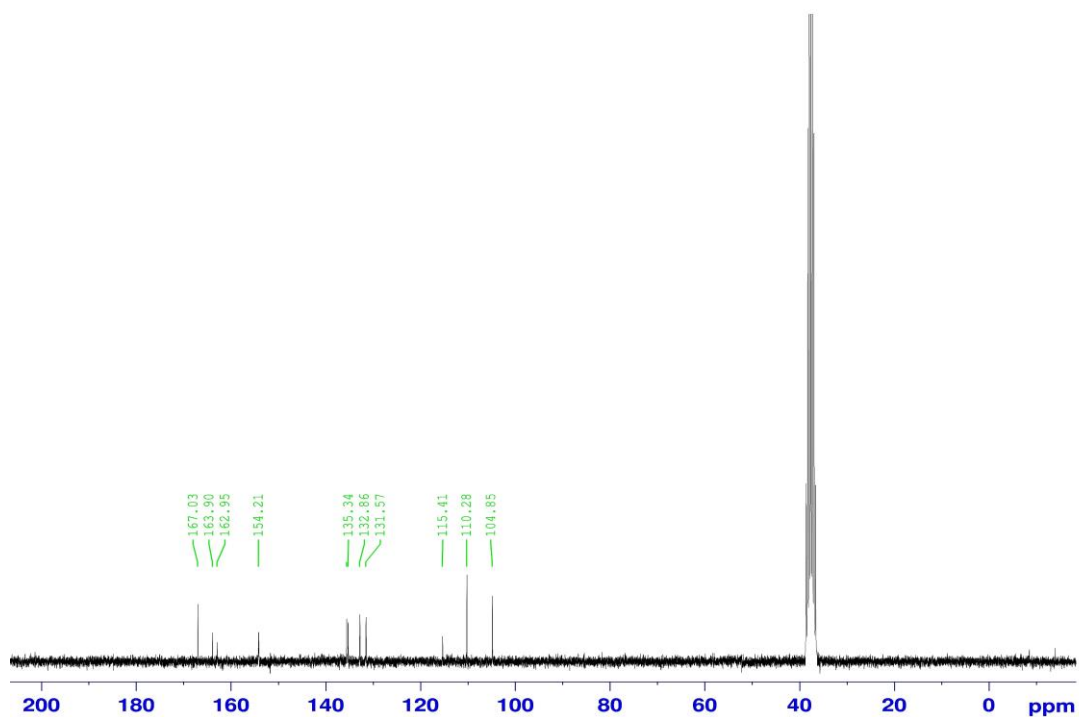
Fig. 3.7: ^{13}C NMR spectrum of receptor **S2R1**
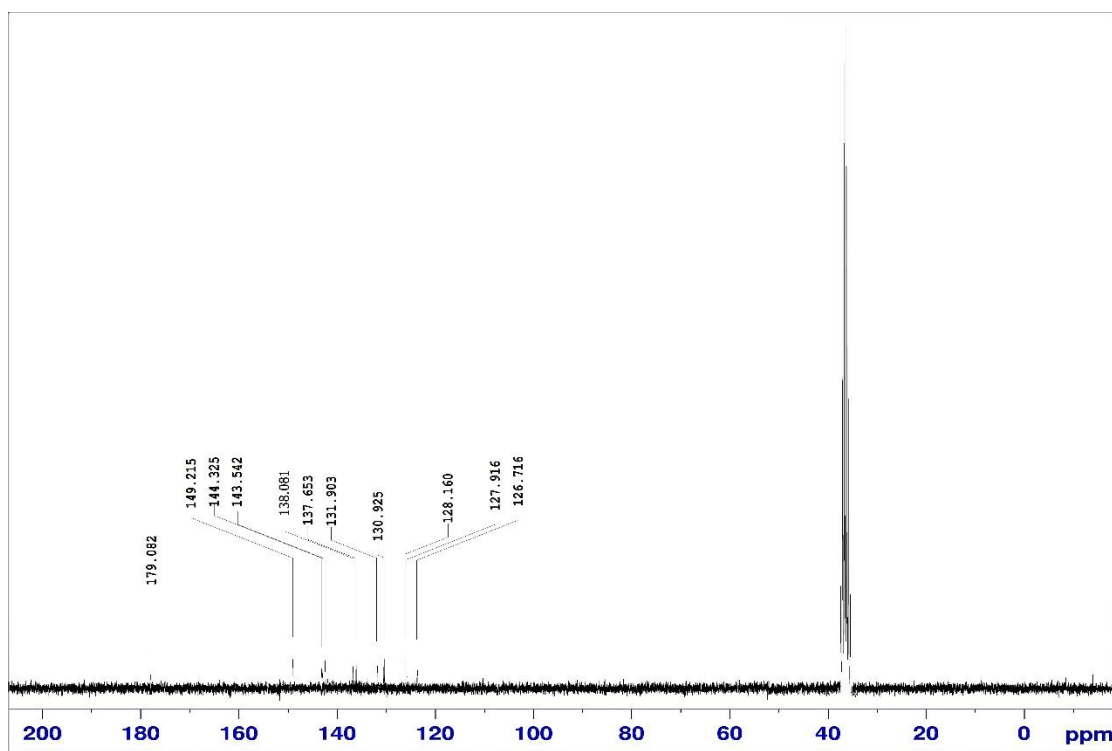
Fig. 3.8: ^{13}C NMR spectrum of receptor **S2R2**
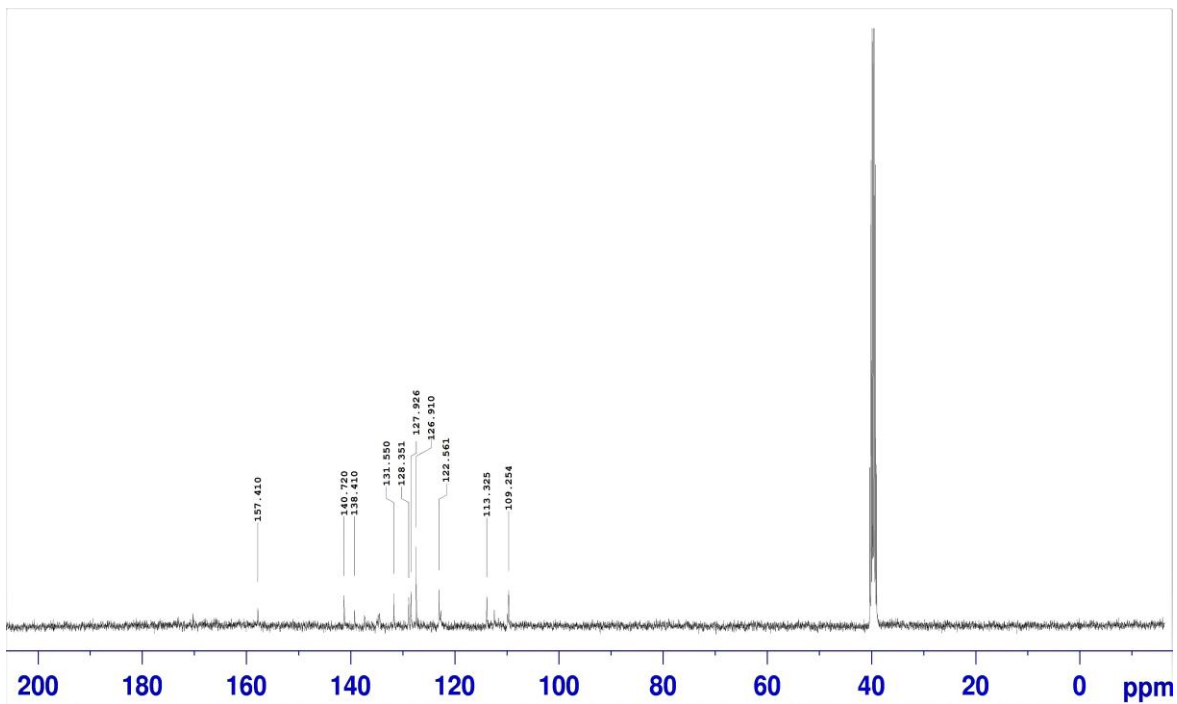
Fig. 3.9: ^{13}C NMR spectrum of receptor **S2R3**
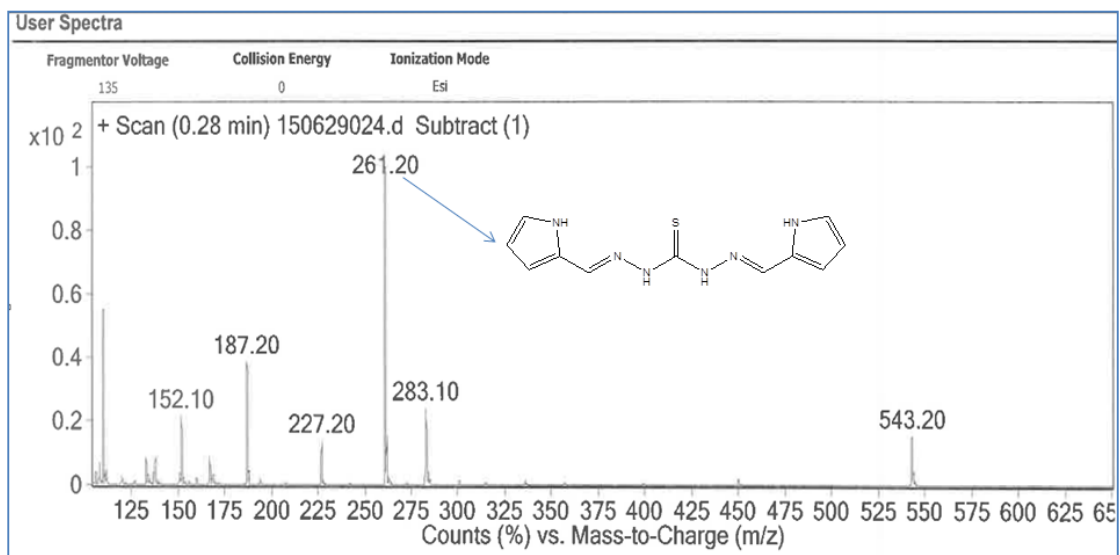
Fig. 3.10: ESI-mass spectrum of receptor **S2R1**
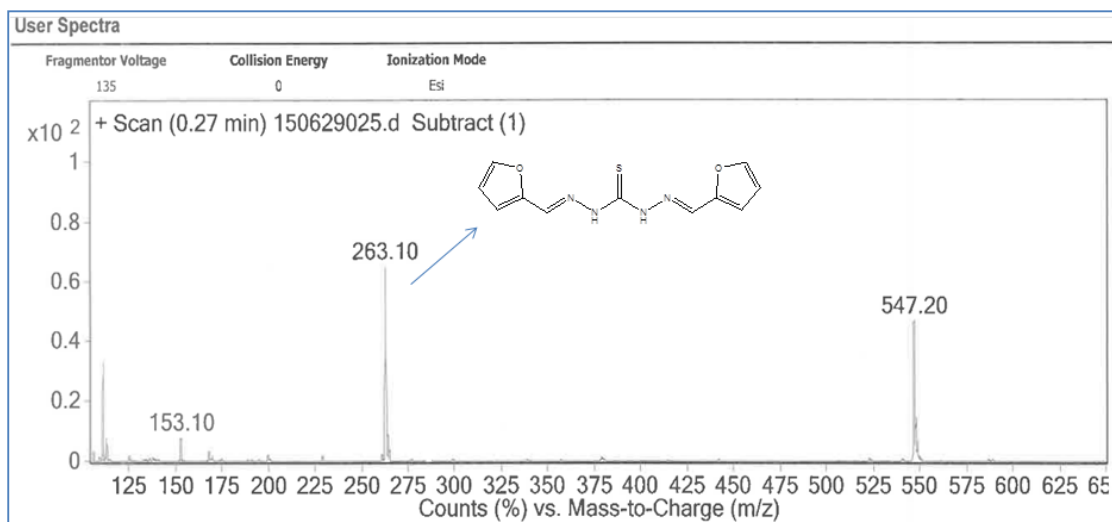
Fig. 3.11: ESI-mass spectrum of receptor **S2R2**
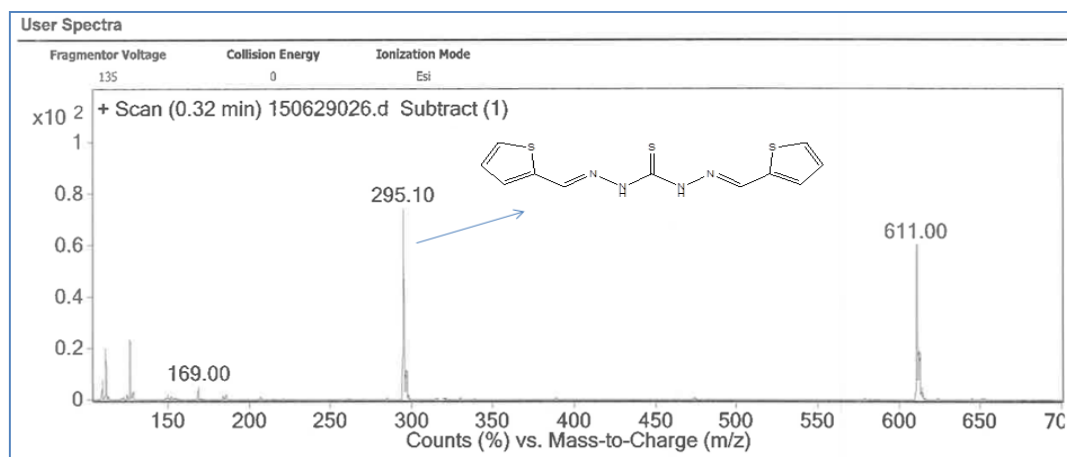
Fig. 3.12: ESI-mass spectrum of receptor **S2R3**

3.3. RESULTS AND DISCUSSION

A high-quality brown and yellow color single crystals of receptors **S2R1**and **S2R2** were grown by slow evaporation in solution with 1:1 ethanol-DMSO binary solvent mixture at room temperature. The obtained crystals was suitable for SC-XRD studies and it was subjected to SCXRD studies and collected crystallographic data are presented in **Table 3.1**. The SC-XRD analysis revealed that the receptor **S2R1** crystallizes in monoclinic crystal system space group P21/c with the cell parameters, a = c = 90 (Å), b = 92.541(2) Å, and Z = 4**.** Similarly the receptor **S2R2** crystallizes in orthorhombic crystal system space group Pbca with the cell parameters, a = b =c= vcxw

42
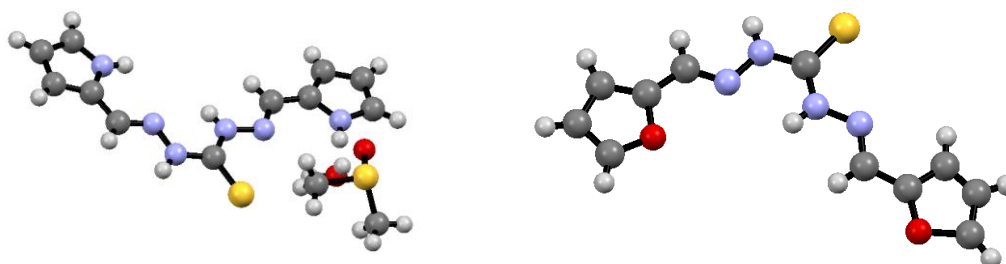
S2R1   **S2R2**

Fig. 3.13. Crystal structure of receptor **S2R1** and **S2R2**

Table 3.1. Crystallographic data of receptor **S2R1** and **S2R2**

Parameters	Receptor S2R1	Receptor S2R2
CCDC NO.	1423244	1423409
Chemical formula	$C_{13} H_{20} N_6 O_2 S_2$	$C_{11}H_{10}N_4O_2S_1$
Formula weight	356.47	262.29
Crystal system	Monoclinic	Orthorhombic
Space group	P21/c	Pbca
α (^{0})	9.9682(4)	17.8981(5)
β (^{0})	7.5071(3)	7.8487(2)
γ (^{0})	23.7036(10)	18.0695(5)
a [A^0]	90	90
b[A^0]	92.451(2)	90
c [A^0]	90	90
V [A^0]	1772.17(13)	2538.35(12)
Z	4	8
Z^1	0	0
Reflections	3485	514
Unique rflns	2875	499
Parameters	288	163
Crystal color	Brown	yellow
T/$^{\circ}$K	296(2)	296(2)
$M(M_0 K_{\alpha})[mm^{-1}]$	0.71073	0.71073
Crystal shape	Flakes	Flakes

R1(I>2σ)	0.0790	0.1220
wR2(I>2σ)	0.1665	0.0387
Goodness of fitness (GooF)	1.345	1.045
R- Factor (%)	0.0617	0.0378

3.3.1. Colorimetric studies

The colorimetric sensing abilities were initially examined by adding various nitrate salts of cations such as Cu^{2+}, Hg^{2+}, Cr^{3+}, Fe^{2+}, Co^{2+}, Zn^{2+}, Ni^{2+}, Cd^{2+} and Pb^{2+} ions to receptors **S2R1 – S2R3** (**Fig. 3.14** in shown below). **S2R1** did not show any color change in the presence of above-tested cations except Hg^{2+} ions, whereas in the presence of Hg^{2+} ions, it showed a significant color change. **S2R2**, did not show any significant color change in the presence of Hg^{2+}, Cr^{3+}, Fe^{2+}, Co^{2+}, Zn^{2+}, Ni^{2+}, Cd^{2+} and Pb^{2+} ions apart from Cu^{2+} ions. **S2R3** did not show any color change in the presence of Cr^{3+}, Fe^{2+}, Co^{2+}, Zn^{2+} and Ni^{2+} ions, however in presence of Cd^{2+} ions, it showed colorless to pink. The color change of receptor **S2R1 – S2R3** in the presence of different metal ions is displayed in **Table 3.2**.
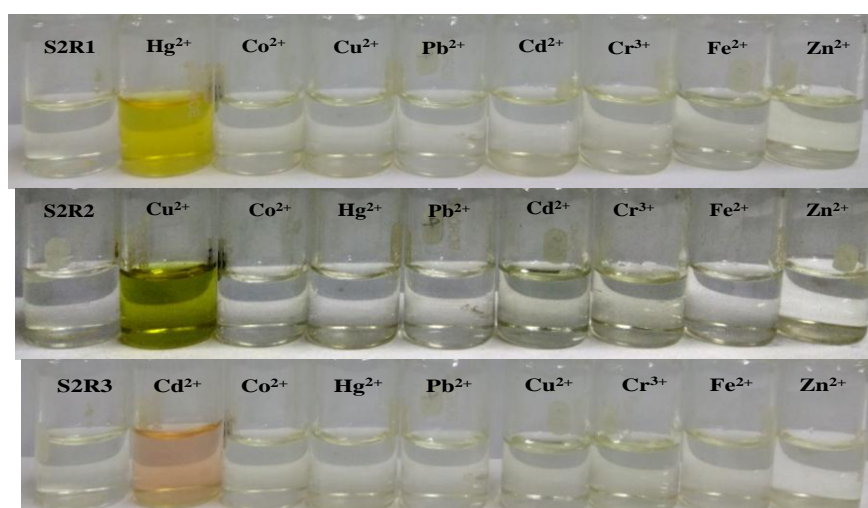
Fig. 3.14. The colorimetric changes observed by naked-eye of receptor **S2R1**- **S2R3** upon addition of 2.0 equiv. of various cations in an aqueous solution

Table 3.2: Color change of receptor **S2R1- S2R3** in the presence 2.0 equivalence of different metal ions

Receptor	Con. (M) of Receptor(DMSO)	Color of the Receptor	Volume of Receptor	Metal ion	Color change
S2R1	2.5×10^{-5}	Colorless	2.0 mL	Hg^{2+}	Yellow
S2R2	2.5×10^{-5}	Colorless	2.0 mL	Cu^{2+}	Yellow
S2R3	2.5×10^{-5}	Colorless	2.0 mL	Cd^{2+}	Light pink

3.3.2. UV- Visible absorption studies

All the analytical solution was prepared as mentioned in the experimental section of colorimetric and UV–Vis studies. A detailed UV-vis titration and comparative study experiment were conducted to investigate the selectivity and binding properties of receptor **S2R1- S2R3** towards active and inactive metal ions based on the observation of colorimetric study. **(Fig. 3.15-3.17**). Receptor **S2R1** showed absorption band at 350 nm, corresponding to n-π* transitions of the HC=N group. Upon the addition of mercury ions to receptor **S2R1**, it showed a significant red shift by 50 units in the absorption spectra in the presence of Hg^{2+} ions. The bands at 350 nm decrease and band at 400 nm increase with the gradual increment of Hg^{2+} ions to the **S2R1 (Fig. 3.17a).** The increase in absorbance and red shift of the band at 400 nm is highly indicative of the formation of a charge transfer complex between Hg^{2+} and the receptor **S2R1.** The selective detection of Hg^{2+} ions is mainly due to thiophillic nature of **S2R1**. In a similar way the receptor **S2R2** showed the band at 342 nm, corresponding to n-π* transitions of HC=N group, In the presence of Cu^{2+} ions, receptor **S2R2** showed a red shift in the absorption spectra by 53 units increment. With the incremental addition of Cu^{2+} ions to the **S2R2**, there was decrease in the absorption intensity at 342 nm and new band appeared at 395 nm with gradual increment in absorption, which is due to formation of complex between Cu^{2+} and the **S2R2**.**(Fig. 3.17b).** The selective detection of Cu^{2+} ions is mainly due to the high affinity of furfural group present in receptor **S2R2**. The receptor **S2R3** showed absorption at 395 nm in the absence of metal ions, whereas with the addition of Cd^{2+} ions resulted in the generation of the new absorption band at 579 nm (red shift by 184 nm increment) **(Fig. 3.17c).** With the incremental addition of Cd^{2+} ions to the receptor

S2R3 solution, the absorbance band at 395 nm decrease gradually and simultaneously, the absorption band at 579 nm progressively increased owing to the formation of the complex between **S2R3** and the Cd^{2+} ions. All the receptors showed a clear isobestic point at 387 nm, 378 nm and 502 nm with the gradual increment of Hg^{2+}, Cu^{2+} and Cd^{2+} ions respectively in the absorption spectrum, which indicates that the receptors forms complex with those metal ions.
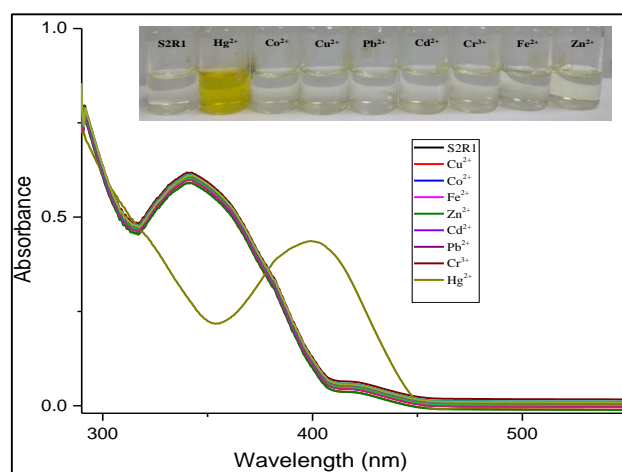
Fig. 3.15: Comparative UV-Vis spectrum of receptor **S2R1** (2.5 x 10^{-5} M, DMSO) in the presence of 2.0 equvi. of other cations. Insert shows colorimetric changes observed by naked-eye
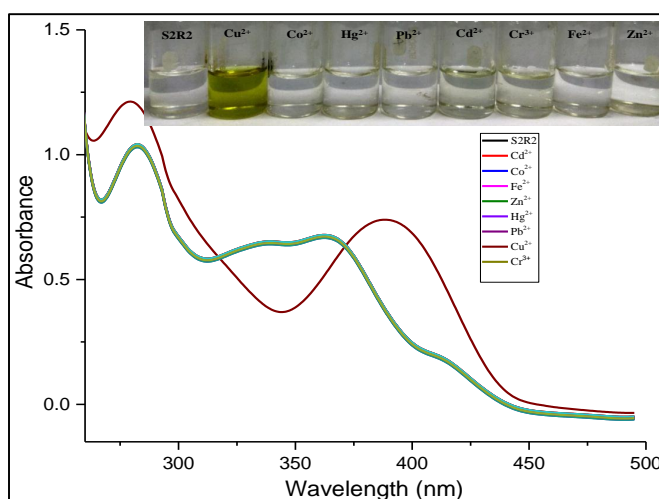
Fig. 3.16: Comparative UV-Vis spectrum of receptor **S2R2** (2.5 x 10^{-5} M, DMSO) in the presence of 2.0 equvi. Of other cations Insert shows colorimetric changes observed by naked-eye
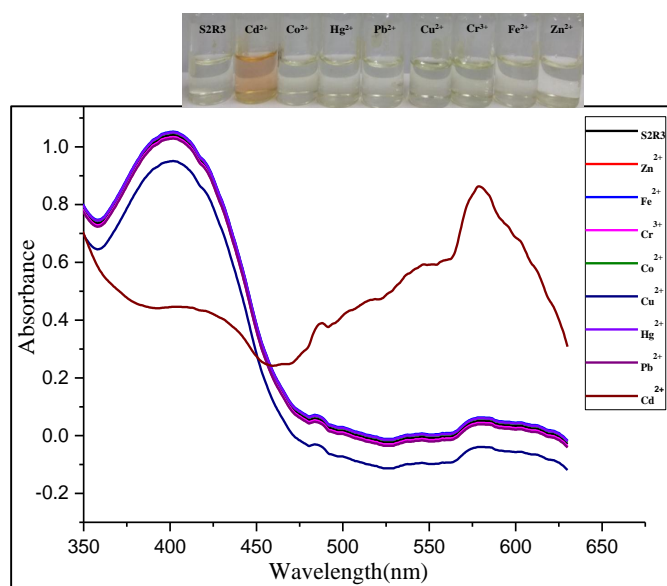
Fig. 3.16: Comparative UV-Vis spectrum of receptor **S2R3** (2.5 x 10⁻⁵ M, DMSO) in the presence of 2.0 equvi. of other cations. Insert shows colorimetric changes observed by naked-eye
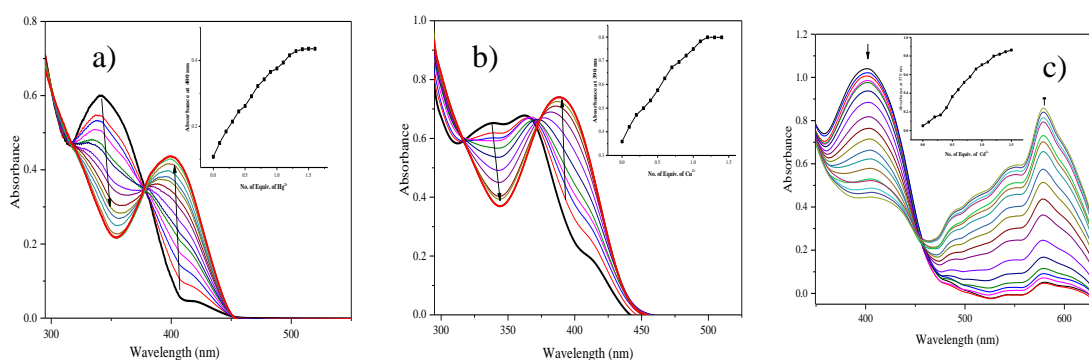
Fig. 3.17: UV–Vis titration and color change of **S2R1, S2R2** and **S2R3** (2.5×10⁻⁵ M, DMSO) with increasing concentration of metal ions (0 – 1.5 equiv.) in an aqueous medium. Inset graph shows binding isotherm at selected wavelength. **a).** **S2R1** vs. Hg²⁺ ions, selected wavelength at 400 nm. **b).** **S2R2** vs. Cu²⁺ ions, selected wavelength at 390 nm, **c).** **S2R3** vs. Cd²⁺ ions, selected wavelength at 579 nm

3.3.3. Selectivity of receptor S2R1- S2R3 towards metal ions

The selectivity of receptors was confirmed by UV-Vis spectroscopy in the presence of different cations such as Cu^{2+}, Hg^{2+}, Cr^{3+}, Fe^{2+}, Co^{2+}, Zn^{2+}, Ni^{2+}, Cd^{2+} and Pb^{2+} ions. Interestingly, all the receptor was selective towards the Cu^{2+}, Hg^{2+} and Cd^{2+} metal ions. The receptors S2R1 have showed selectivity recognition towards for Hg^{2+} ions in the presence of other tested ions (**Fig. 3.15**). While, **S2R2,** exhibited selectivity towards Cu^{2+} ions in the presence of other tested cations (**Fig. 3.16**). The receptor **S2R3** has revealed a clear new

47

absorption band in the presence of Cd^{2+} ions and did not shown any absorption changes with the other tested ions (**Fig. 3.17**). The high affinity of receptor **S2R1-S2R3** towards Hg^{2+}, Cu^{2+} and Cd^{2+} ions than other tested metal ions were supported by ionic radii, electronegativity and HSAB theory (**Fig. 3.18 &3.19**).
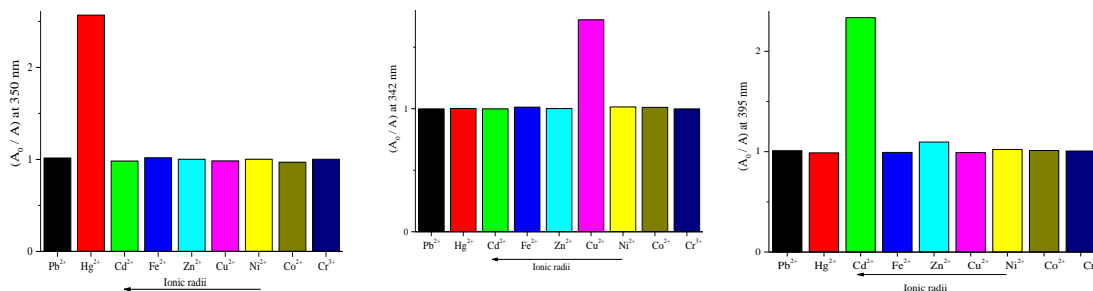
Fig 3.18: Absorbance response (A_0/A) of SR1-R3 at selected wavelength (400 nm, 395 nm and 579 nm) plotted against ionic radii (pm) of cations in decreasing order
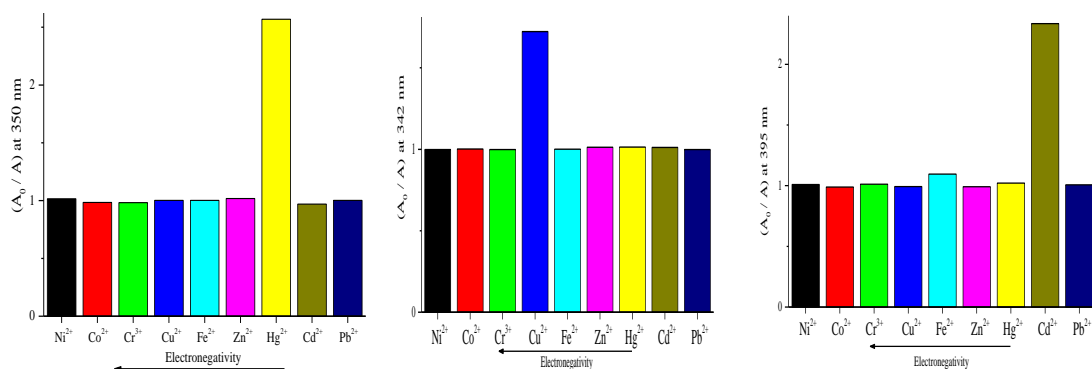
Fig.3.19: Absorbance response (A_0/A) of SR1- **S2**R3 at selected wavelength (400 nm, 395 nm and 579 nm) plotted against electronegativity of cations in decreasing order

3.3.4. Binding constant and detection limit determination

The binding stoichiometry between receptor **S2R1-S2R3** with the different metal ions was determined by the Benesi-Hildebrand (B-H) method using UV-Vis spectrometric titration. The B-H plot confirms that all the receptors form 1:1 complexation with the metal ions **(Fig 3.20a-c)**. The association constant (K) was calculated for all the receptor metal complexes using B-H equation and results are tabulated in **table 3.3.** Further, the stoichiometry and association constant values were determined by Bindfit method given in supramolecular.org (P. Tandarson et al.2010). And results shows 1:1binding ratio of receptor and metal (**Fig. 3.21a-c**).
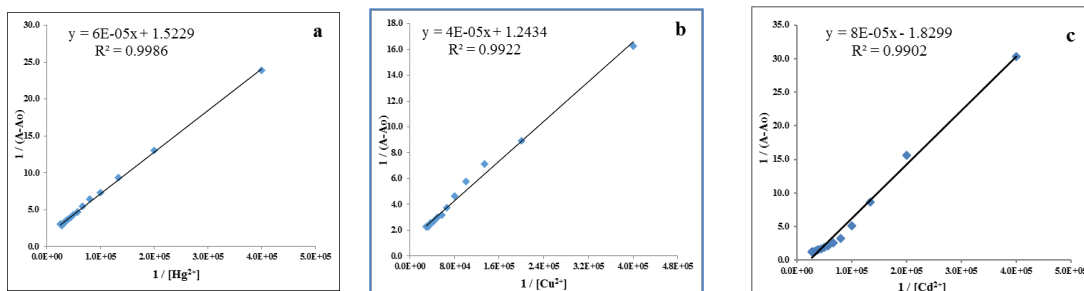
Figure 3.20: Benesi-Hildebrand (B-H) plot of receptor binding with metal ions associated with absorbance change at selective wavelength. **a).** S2R1 (2.5 x 10^{-5} M, DMSO) with Hg^{2+} ions at 400 nm, **b).** S2R2 (2.5 x 10^{-5} M, DMSO) with Cu^{2+} ions at 390 nm, **c).** S2R3 (2.5 x 10^{-5} M, DMSO) with Cd^{2+} ions at 579 nm
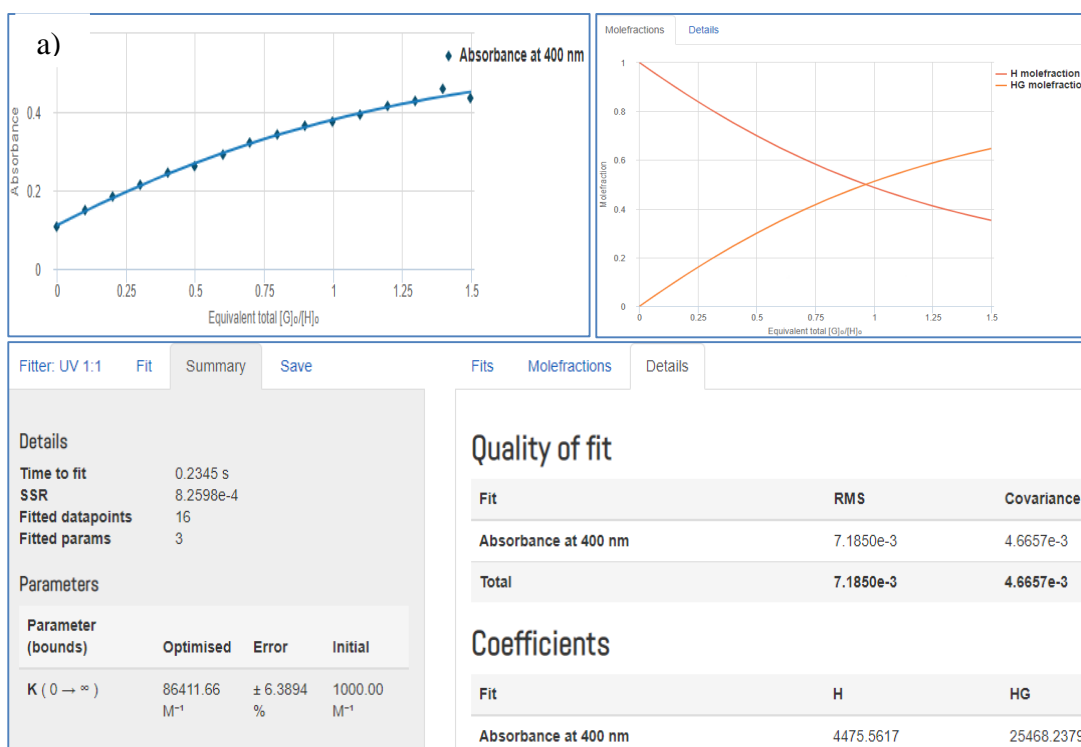
Figure 3.21a: Bindfit plot of receptor **S2R1** (2.5 x 10^{-5} M, DMSO) and **Hg^{2+}; S2R1 shows** 1:1 binding stoichiometry with Hg^{2+} ions, at 400nm.
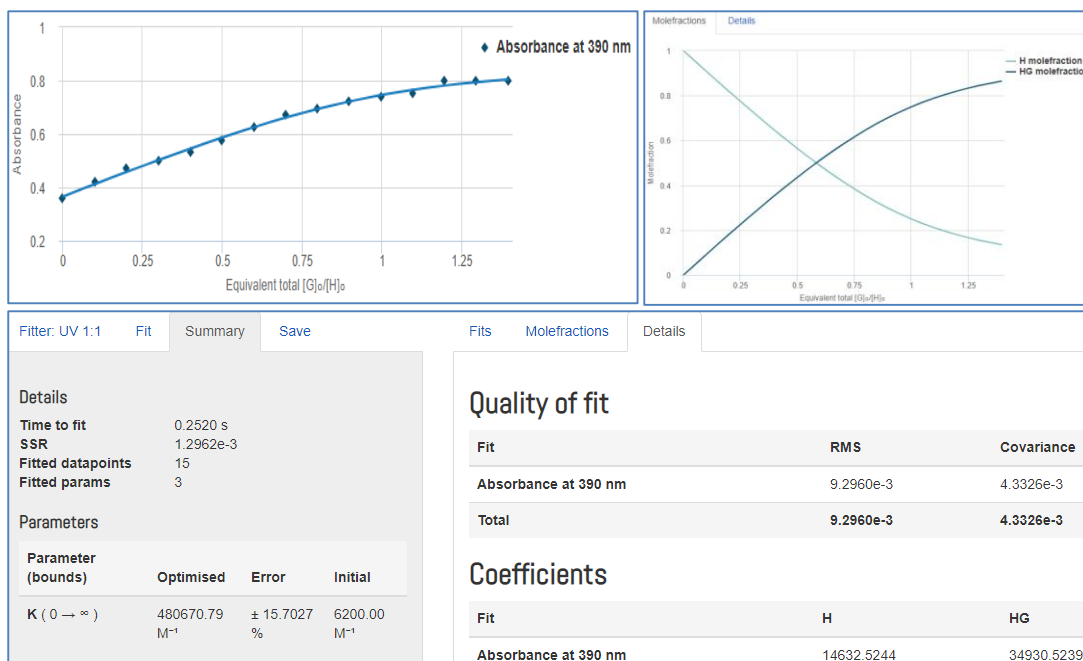
Figure 3.21b: Bindfit plot of receptor **S2R2** (2.5×10^{-5} M, DMSO) and Cu^{2+}; **S2R2** shows 1:1 binding stoichiometry with Cu^{2+} ions, at 390nm
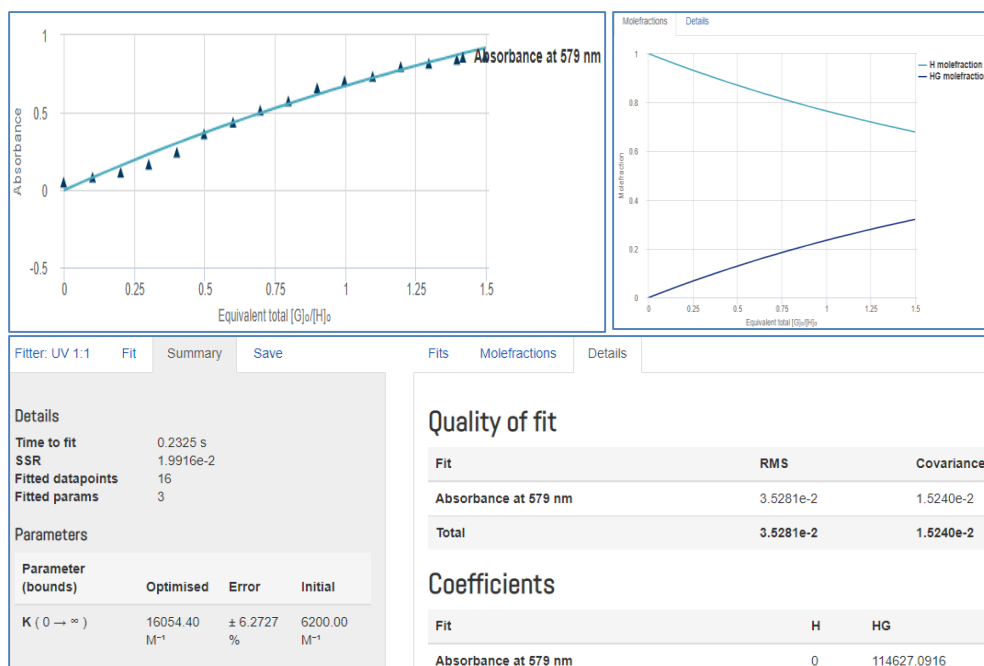
Figure 3.21c: Bindfit plot of receptor **S2R3** (2.5×10^{-5} M, DMSO) and Cd^{2+}; **S2R3** shows 1:1 binding stoichiometry with Cd^{2+} ions, at 579nm

The detection limit (DL) for Hg^{2+}, Cu^{2+} and Cd^{2+} ions were determined using the calibration plot between metal ion concentration and the corresponding

absorbance of receptor-metal complex measured at selective wavelengths (**Fig. 3.22a-c**).

The DL were calculated based on the standard deviation of the measurement and the slope using the following equation mentioned by ICH quality guideline **Q2R1.**

$$DL = \frac{C \times \sigma}{m}$$

Where, σ = standard deviation of the measurement, m = slope of the calibration curve, C = constant (3.0). Further, the calculated DL values, regression analysis data and detection limit of Hg^{2+}, Cu^{2+} and Cd^{2+} ions by the proposed receptors **S2R1-S2R3** tabulated in **table 3.3**.
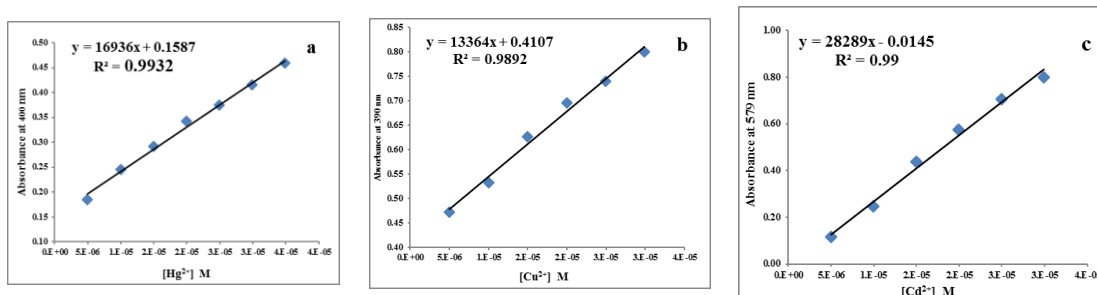
Figure 3.22: Calibration curve plot of absorbance of complex (Receptor-metal) verses concentration of metal ions in M. **a). S2R1**- Hg^{2+} vs. Hg^{2+} ions, **b). S2R2**-Cu^{2+} vs Cu^{2+} ions **c). S2R3**- Cd^{2+} vs. Cd^{2+} ions

Table 3.3: Regression analysis data, stoichiometry, binding constant and detection limit of receptor S2R1-S2R3 with metal ions.

Receptor	Metal ion	Stoichio metry	Binding constant (K) M^{-1}	Linear range (µM)	R^2	Detection limit (ppm)
S2R1	Hg^{2+}	1:1	1.0 x 10^3	5.0 – 38.9	0.9932	0.55
S2R2	Cu^{2+}	1:1	6.2 x 10^3	5.0 – 29.9	0.9892	0.21
S2R3	Cd^{2+}	1:1	6.2 x 10^3	5.0 – 29.9	0.9900	0.36

3.4. CONCLUSIONS

To summarize, herein we have developed three thiocarbohydrazide based receptors **S2R1- S2R3** for the selective detection of Hg^{2+}, Cu^{2+} and Cd^{2+} ions over other tested cations. Among synthesized receptor. The **S2R1** selectively binds Hg^{2+} ions with the good detection limit (0.55 ppm**)**. The **S2R2** shown colorimetric response towards Cu^{2+} ions with μM detection limit (0.21ppm**)** and **S2R3** specifically binds Cd^{2+} ions with the detection limit of (0.36ppm), All the receptors **S2**R1- **S2**R3 exhibited good binding consent (10^3μM) and 1:1 stoichiometric binding ratio with that of metal ions, based on the correlation study (absorption (A_0/A) versus ionic radii, electronegativity), comparative study results, high affinity of receptor **S2R1-S2R3** was confirmed towards Hg^{2+}, Cu^{2+} and Cd^{2+} than other tested cations. Among the all synthesized receptors, **S2R1** and **S2R3** is versatile in its function binding Hg^{2+}, Cd^{2+} ions with distinct colorimetric response in an aqueous medium. Sensing activity of **S2R1** and **S2R3** gains significance in the field of colorimetric chemosensors for heavy metal ions detection. All the reported receptors have good linear range from 0 to 10^{-6} M, it reveals that the receptors can be used for quantitative determination of heavy metal ions in water media.

CHAPTER-4

CATION SENSING PROPERTIES OF NEW HETEROCYCLIC LIGANDS BASED ON ELECTRON RICH THIOPHENE

Abstract

In this chapter, the design, synthesis and characterizations of new heterocyclic ligands as colorimetric receptors for cations have been discussed in detail.

4.1. INTRODUCTION

Development of receptors which can detect and possible extraction of precious metal ions from various sources including natural origin is also industrially important because of the commercial reasons. Highly toxic metal ions such as Hg^{2+}, Pb^{2+} and Cd^{2+} are of special interest because of clinical and environmental reasons, and their early detection in the environment is desirable. Heavy metal ions in drinking water is a serious problem and a lot of efforts are going on for their detection at low concentration and development of chemical processes for their removal. Most of the receptors bearing amide, thiourea, imidazole, indole carbazole, calixarene subunits which can detect cations. However, these molecules are structurally complicated and hence required skilled labor to synthesize the receptors. The receptors based on heterocyclic Schiff's base (**S3R1** and **S3R2**) were synthesized barring hydroxyl and nitro groups. These receptors were synthesized to check the role of –OH group and –NO_2 group in detection process an additional receptor **S3R3** which does not contain any hydroxy group was synthesized to justify the binding site of receptors.
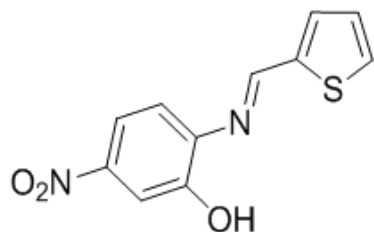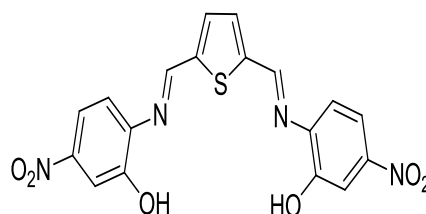
S3R1   S3R2

4.2. EXPERIMENTAL SECTION

4.2.1. Materials, method and instruments

All the chemicals used in the present study were procured from Sigma-Aldrich and Alfa Aesar and were used as received without further purification. All the solvents were purchased from SD Fine, India was of HPLC grade and used without further distillation.

^{1}H NMR (400MHz, DMSO-d$_6$) and ^{13}C NMR (100MHz, DMSO-d$_6$) spectra were recorded on a Bruker-400MHz spectrometer. Chemical shifts are reported in ppm downfield from tetramethylsilane (TMS, δ scale with solvent resonances as internal standards). Single crystal X-ray Diffraction (SC-XRD) data for synthesized molecules collected on a Bruker Apex II duo diffractometer with a CCD detector. As a source of radiation for the experiment, monochromatic Molybdenum (Mo) Kα radiation (λ=0.7107Å) was used. Data collection was did at ambient temperature (≈23° C). The crystal structure of receptor **S3R3** was solved by direct methods using SHELXL-2007/2014 software and the refinement was carried out by full-matrix least-squares technique using SHELXL-2007/2014. For all the non-hydrogen atoms anisotropic displacement parameters were calculated. Melting points were recorded on Bio-cote (SMP10) instrument in open capillary and are uncorrected. Fourier transform infrared (FT-IR) spectra were recorded on a Bruker Alpha which is equipped with silicon carbide as IR source. All sample spectra were recorded using KBr pellet media (16 scans with the sample resolution of 4 cm^{-1}). The background data collection was did with KBr pallet before the analysis of samples. The UV-Vis titrations were carried out on UV-Vis spectrophotometer (Analytikjena Specord S600) in standard 3.0 mL quartz cells (2 optical windows) having a path length of 1.0 cm.

4.2.2. Synthesis of receptors S3R1–S3R3

The general scheme of synthesis of new receptors **S3R1**, **S3R2** and **S3R3** are represented in **Scheme 4.1.** The chemical structures of all the receptors were confirmed by ^{1}H NMR, ^{13}C NMR, FT-IR and Mass spectrometry. (**Fig. 4.2-4.13**) The receptor S3R3 was recrystallized in 1:1 ethanol-DMSO binary solvent mixture by

slow evaporation method for SC-XRD studies and its crystallographic data are provided in **Table 4.1**.
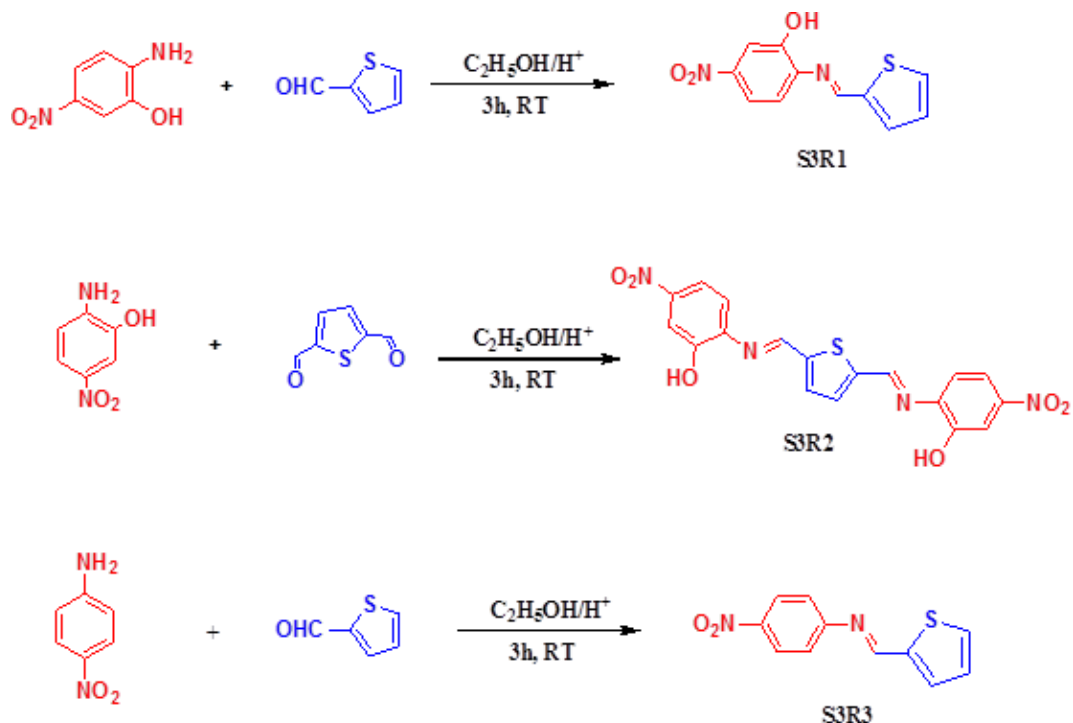
Scheme 4.1: General scheme of synthesis of receptors **S3R1**, **S3R2** and **S3R3**

(E)-5-nitro-2-((thiophen-2-ylmethylene) amino) phenol (S3R1):

Taken 3.2 mmol (0.5g) of 4-nitro-2-hydroxy aniline and 3.2 mmol of thiophene-2-carboxaldehyde (0.36g) into 10 mL of ethanolic solution and drop of glacial acetic acid (catalyst) was added. Further, the reaction mixture was stirred at room temperature ($\approx$25°C) for 3h. Confirmed the absence of starting materials in reaction mass by TLC. Finally, filtered the yellow colored precipitate and dried. **Yield:** 89 %; **melting point:** 219°C-223°C; **FT-IR (KBr, cm^{-1}):** 3423(O–H str.), 3062 (Ar. C–H str.), 1666 (Imine C=N str.), 1578 (N–O Asymmetric str.) and 1288 (N-O symmetric str.); **^{1}H NMR (400MHz, DMSO-d$_6$, δ_{ppm}):** 7.6 (m, aromatic 2H), 7.85 (m, aromatic 1H), 7.1 (m, aromatic 1H), 6.9 (m, aromatic1H), 8.94 (s, 1H, O–H), 6.9 (m, aromatic, 1H), 8.12 (m, 1H, N–H). **^{13}C NMR (100MHz, DMSO-d$_6$, δ_{ppm}):** 179.45, 153.87,145.24,142.28, 134.38,125.84,124.33,121.56,118.62**; LC-MS (ESI) m/z:** Calculated for $C_{11}H_8N_2O_3S$, 248.00, found, 249.033 (M+1), **Elemental Analysis** calculated for $C_{11}H_8N_2O_3S$ C, 56.88; H, 3.47; N, 12.06 Observed C, 56.48; H, 3.27; N, 11.92.

6,6'((((1E,1'E)thiophenE2,5diylbis(methanylylidene))bis(azanylylidene))bis(3nitro phenol),(S3R2):

To a 3.2 mmol (0.5g) of 4-nitro-2-hydroxy aniline, 1.6 mmol (0.225g) of thiophene-2,5- dicarboxaldehyde was taken into a 10 mL of ethanol solution. To this, a drop of glacial acetic acid (catalyst) was added and the reaction mixture was stirred at room temperature for 3h. After 3h the reaction mixture was tested and find the absence of starting materials by TLC method. Finally, filtered the yellow colored precipitate and dried. **Yield:** 86 %; **Melting point:** 243˚C-245˚C; **FT-IR (KBr,cm^{-1}):** 3367(O-H str.), 3079 (Ar. C-H str.), 1650 (Imine C=N str.), 1560 (N-O Asymmetric str) and 1391(N-O symmetric str.); **^{1}H-NMR (400 MHz, DMSO-d$_6$, δ$_{ppm}$):** Actually this S3R2 should show 6 sets in the ^{1}H NMR due to symmetry. But the ^{1}H NMR of S3R2 shows 10 set of signals with slight variation in their chemical shifts; this is due to presence of E geometrical isomer. (Due to bulky groups on both sides) 7.01-7.25 (m, aromatic 2H), 7.1 (m, aromatic 2H), 7.4 (m, aromatic 2H), 7.7 (m, aromatic 2H), 8.7 (s, imenic, 2H), 11.8 (s, 2H of -OH). **^{13}C-NMR (100 MHz, DMSO-d$_6$, δ$_{ppm}$):** 206.63, 180.99, 146.96, 144.40, 130.22, 125.55, 123.12; **HRMS (ES) m/z:** Calculated for C$_{18}$H$_{12}$N$_4$O$_6$S, 412.40, found, 413.17 (M+1); **Elemental Analysis:** calculated for C$_{18}$H$_{12}$N$_4$O$_6$S C, 52.43; H, 2.93; N, 13.59 Observed C, 52.17; H, 2.87; N, 13.37.

(E)-N-(4-nitrophenyl)-1-(thiophen-2-yl) methanimine, (S3R3):

To a 3.34 mmol (0.18g) of 4-nitroaniline, 3.34 mmol (0.374g) of thiophene 2-carboxaldehyde was taken into a 10 mL of ethanol solution. To this, a drop of glacial acetic acid (catalyst) was added and the reaction mixture was stirred at room temperature for 3h. After 3h the reaction mixture was tested and find the absence of starting materials by TLC method. Finally, filtered the yellow colored precipitate and dried. Yield 86%; **Melting point:** 195˚C -198˚C. **FT-IR (KBr, cm^{-1}):** 3160 (Ar C–H str.), 1594 (Imine C=N str.), 1510 (N–O Asymmetric str.) and 1340 (N–O symmetric str.). **^{1}H-NMR (500 MHz,CDCl$_3$-, δ$_{ppm}$):** 7.53 (m, aromatic, 2H), 7.1 (m, aromatic, 3H), 6.8 (m, aromatic 1H), 6.9 (m, aromatic 1H) and 8.78 (s, iminic, 1H);(Solvent CDCl$_3$ peak 7.26ppm) **^{13}C-NMR (100 MHz, DMSO-d$_6$, δ$_{ppm}$):**152.22, 152.01, 146.42, 140.94, 134.40, 125.01, 120.47, 118.83, 117.40; **LC-MS (ESI) m/z:** Calculated for C$_{11}$H$_8$N$_2$O$_2$S, 232.35, found, 233.10 (M+1); **Elemental Analysis**

calculated for $C_{11}H_{12}N_2O_2S$ C, 62.32; H, 3.92; N, 6.06. Observed C, 62.02; H, 3.72; N, 6.01.

4.2.3. Characterization data of receptors S3R1–S3R3

SCXRD Studies

A high-quality brown color single crystal of receptor S3R3 was grown by slow evaporation its solution with 1:1 ethanol-DMSO binary solvent mixture at room temperature. The obtained crystal was suitable for SC-XRD studies and it was subjected to SCXRD studies and collected crystallographic data are presented in **Table 4.1**. The SC-XRD analysis revealed that the receptor **S3R3** crystallizes in monoclinic crystal system space group C2/C with the cell parameters, a = c = 90 (Å), b = 94.233(3) Å, and Z = 8. The ORTEP diagram (50% probability) of receptor **S3R3** is displayed in **Fig 4.1**.
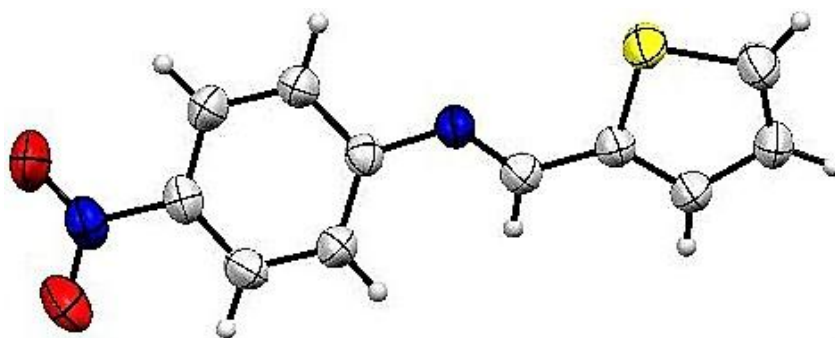
Fig. 4.1: SC-XRD structures of **S3R3**

Table 4.1: Crystallographic data of receptor S3R3

Parameters	Receptor S3R3
CCDC NO.	1423016
Chemical formula	$C_{11}H_8N_2O_2S$
Formula weight	232.25
Crystal system	Monoclinic
Space group	C2/C
α (^{0})	9.4829(4)
β (^{0})	12.0732(4)
γ (^{0})	18.6703(8)
a [A^0]	90

b[A^0]	94.233(3)
c [A^0]	90
V [A^0]	1772.17(13)
Z	8
Z^1	0
Reflections	2100
Unique rflns	1928
Parameters	178
Crystal color	Brown
T/$^\circ$K	296(2)
M(M$_0$ K$_\alpha$)[mm^{-1}]	0.71073
Crystal Shape	Flakes
R1(I>2σ)	0.1010
wR2(I>2σ)	0.0961
Goodness of fitness (GooF)	1.075
R- Factor (%)	0.0368
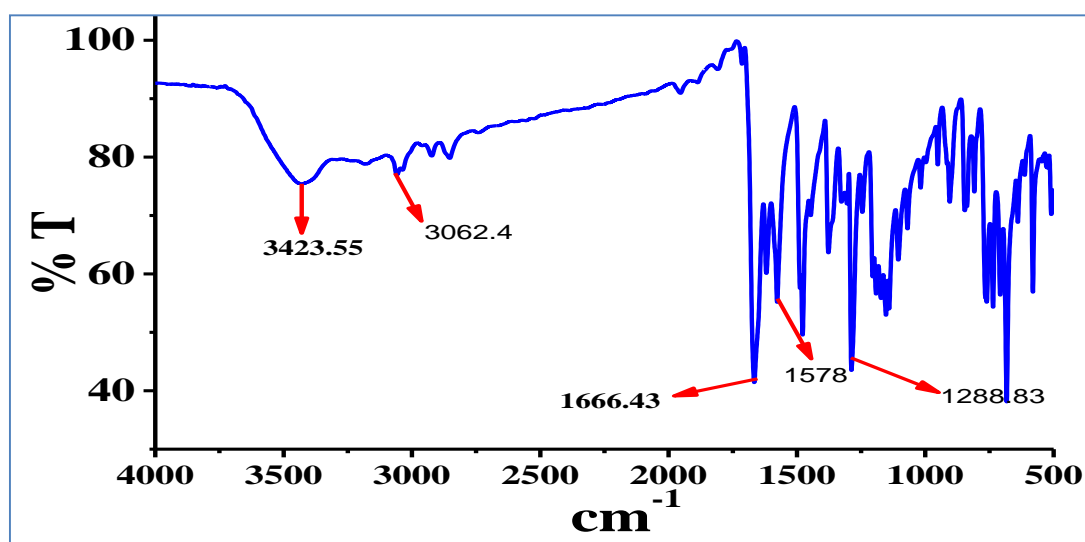
Fig. 4.2. FT-IR Spectrum of receptor S3R1

58
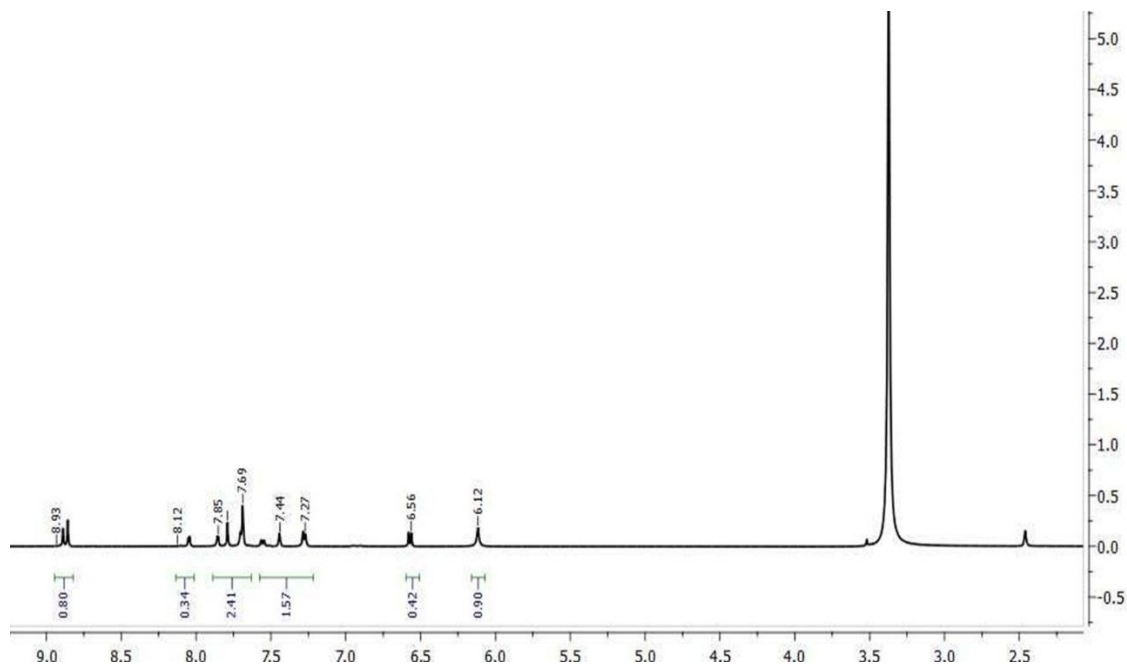
Fig. 4.3. ^{1}H NMR spectrum of receptor S3R1
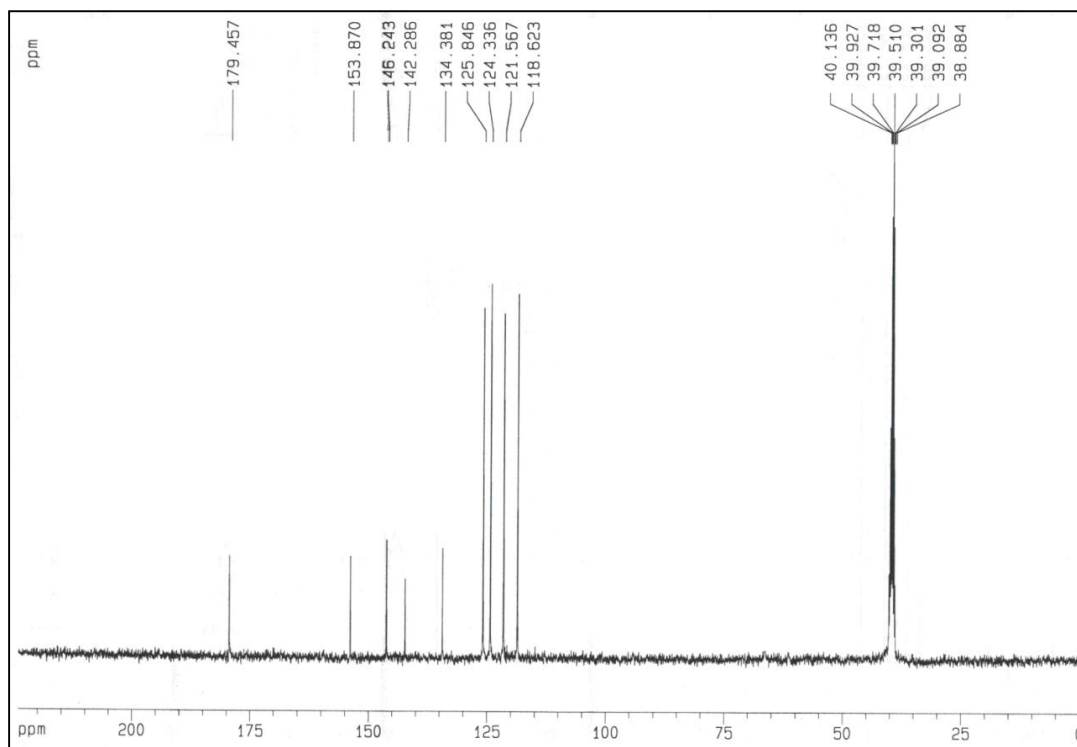
Fig. 4.4. ^{13}C NMR of spectrum receptor S3R1
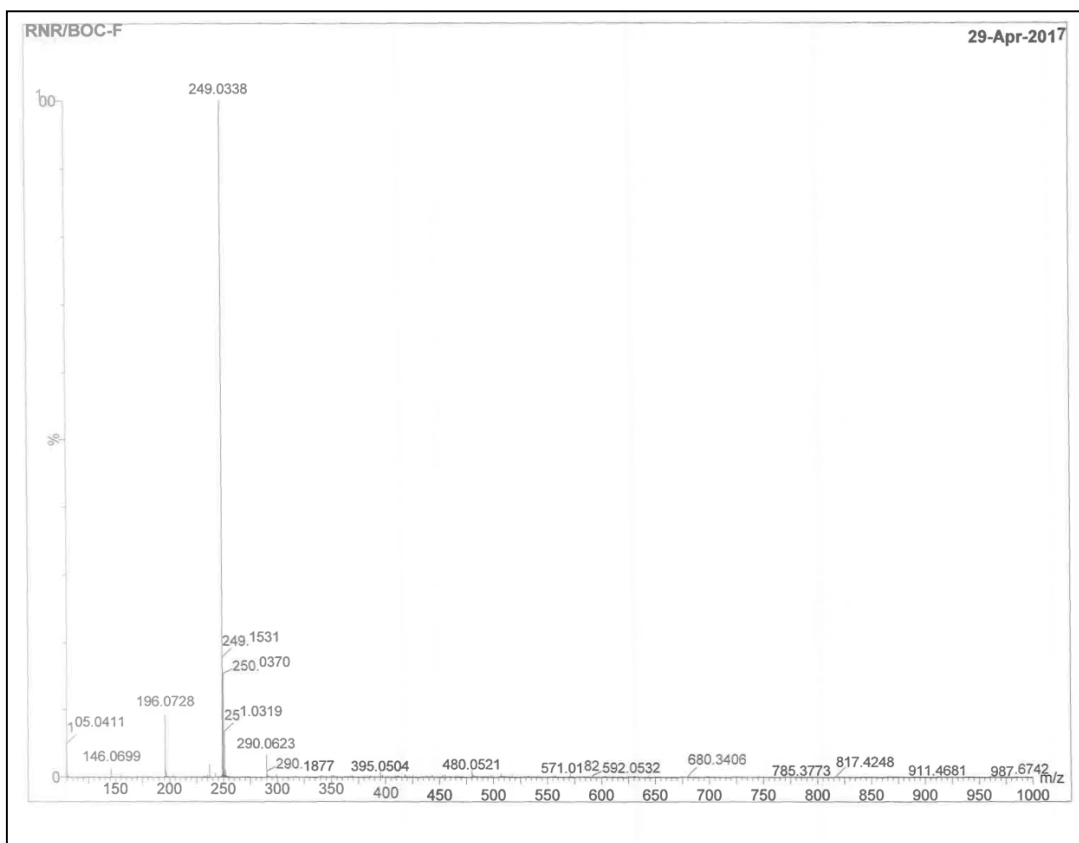
Fig. 4.5. HRMS spectrum of receptor S3R1
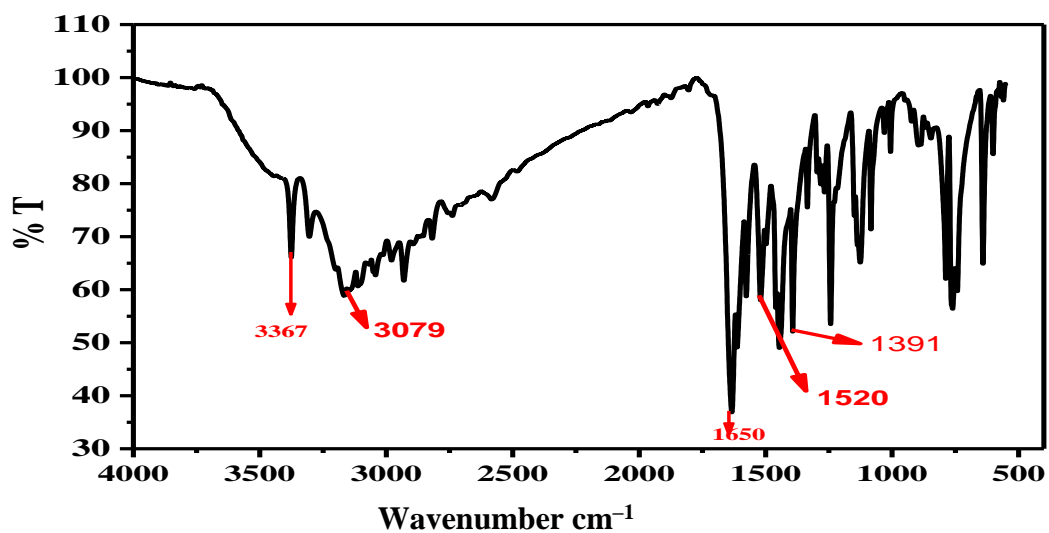
Fig. 4.6. FT-IR Spectrum of receptor S3R2

60
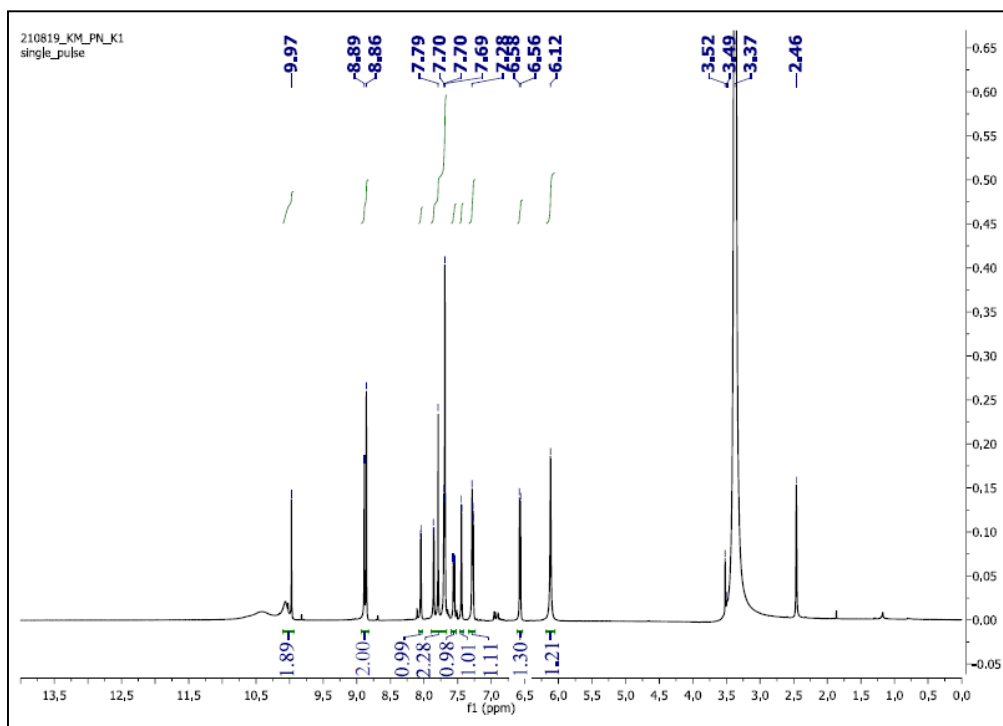
Fig. 4.7. ^{1}H NMR spectrum of receptor S3R2
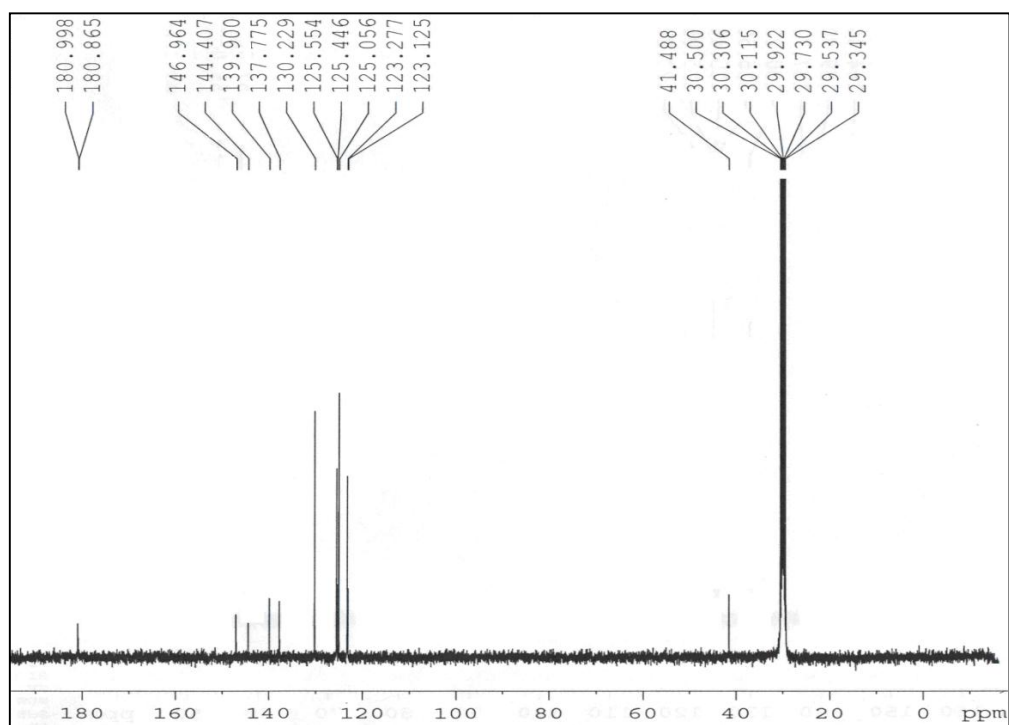
Fig. 4.8. ^{13}C NMR spectrum of receptor S3R2
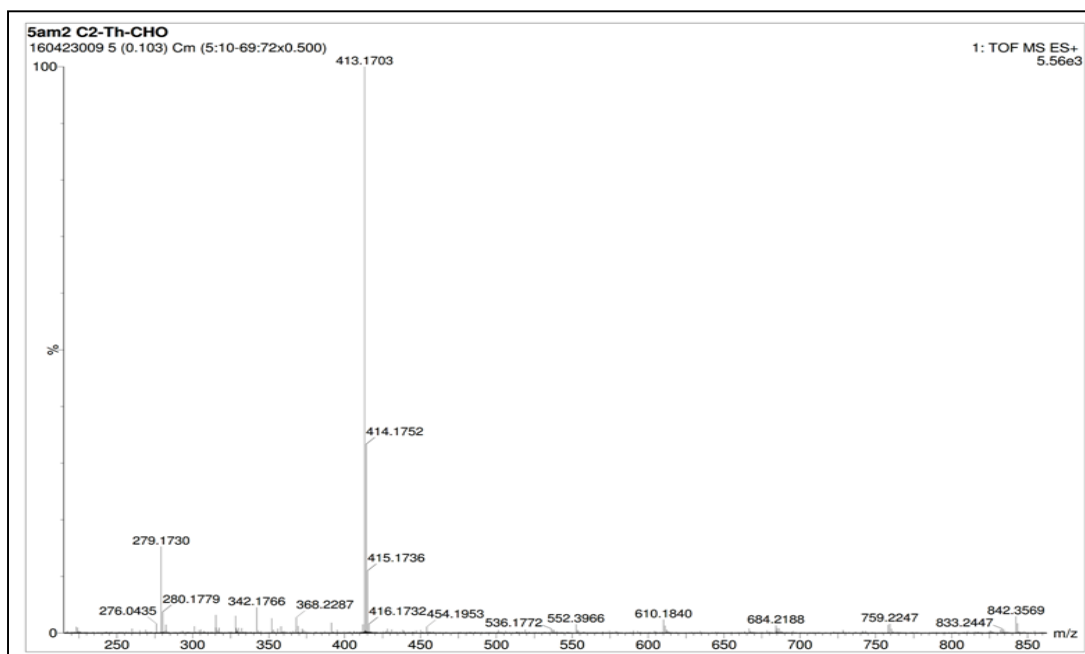
Fig. 4.9. HR-MS spectrum of receptor S3R2
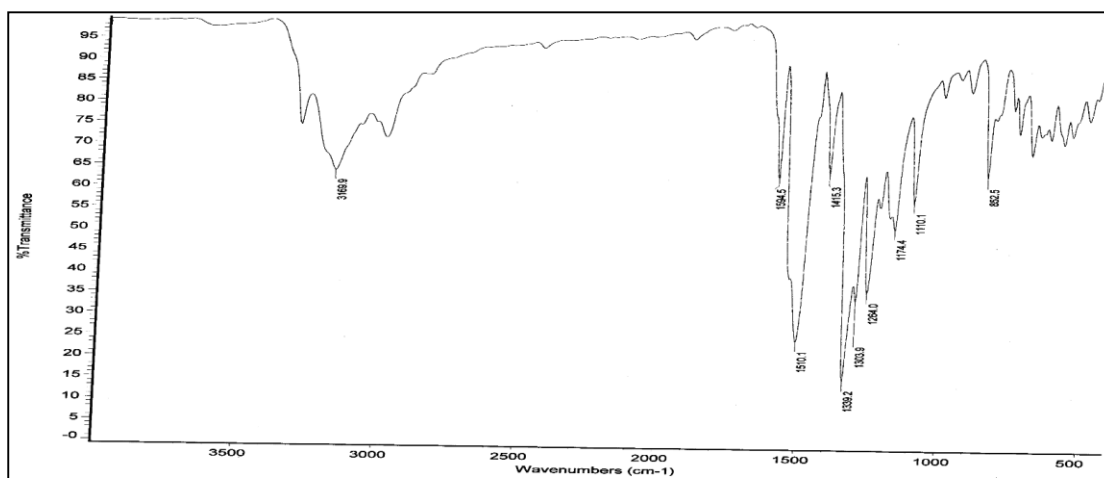
Fig. 4.10. FT–IR spectrum of receptor S3R3
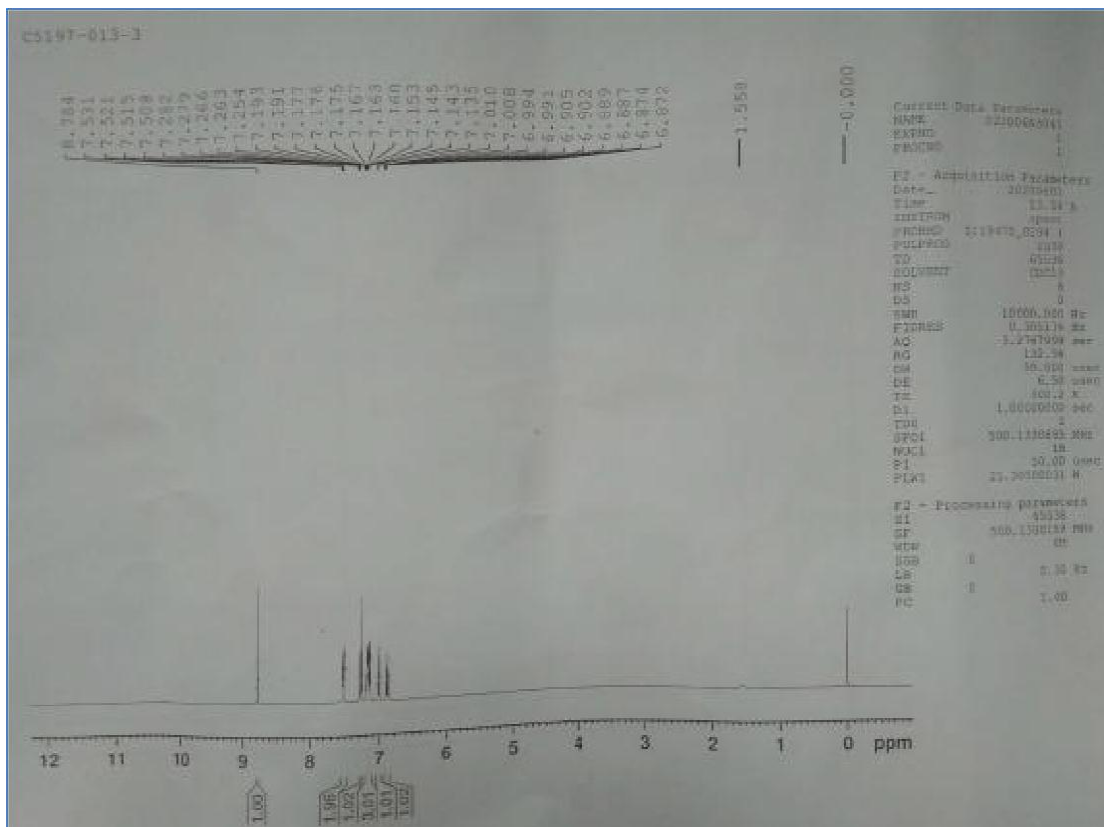
Fig. 4.11: ^{1}H NMR spectrum of receptor S3R3 in CDCl$_3$, 500 MHz
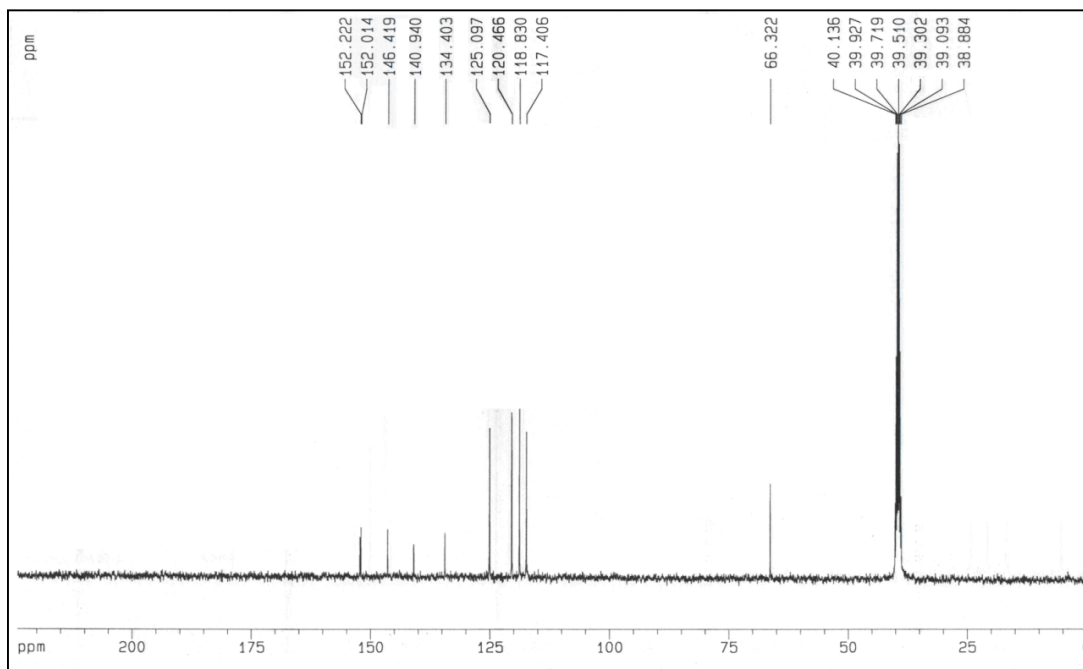
Fig. 4.12. ^{13}C NMR spectrum of receptor S3R3
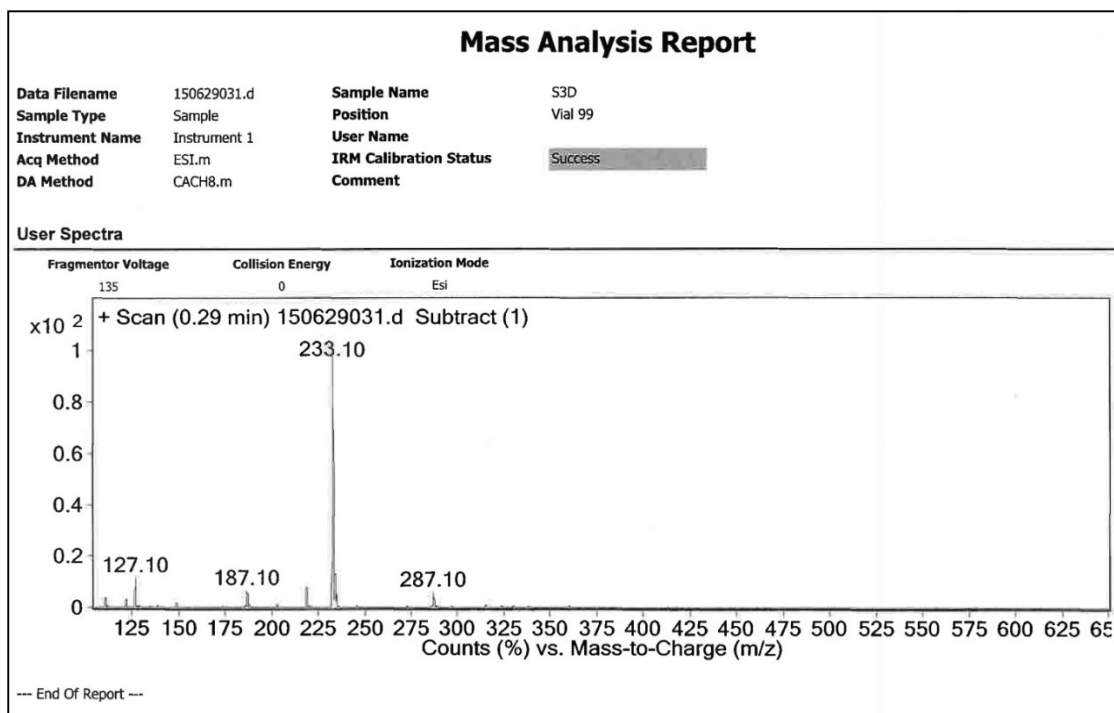
Fig. 4.13. ESI-Mass spectrum of receptor S3R3

4.3. RESULTS AND DISCUSSION

4.3.1. UV–Vis spectroscopic studies

The presence of heteroatoms on the receptors drives in the possibility to envisage the coordinating ability with metal ions. With this in view, the cation binding ability of the receptors S3R1, S3R2 and S3R3 have been investigated with the addition of 2 eq. of nitrate salts of cations such as Cu^{2+}, Hg^{2+}, Cr^{3+}, Fe^{2+}, Co^{2+}, Ni^{2+}, Cd^{2+} and Pb^{2+} ions in de-ionized water. Receptor S3R3 did not exhibit any significant colorimetric response with the addition of test cations used in the present study (**Fig. 4.14**). Receptors S3R1 and S3R2 (2.5×10^{-5} M in DMSO) exhibited a color change from pale yellow to colorless in the presence of Hg^{2+} ions (**Fig. 4.14**). Further, the selectivity of receptor S3R1-S3R2 towards Hg^{2+} ions was confirmed by UV-Vis studies with the addition of 2 equiv. of other competitive tested cations used in the present study. (**Fig. 4.15–4.16**).

There was no significant change in the absorption spectra of S3R1 and S3R2 with the addition of 2 eq. of Cu^{2+}, Cr^{3+}, Fe^{2+}, Co^{2+}, Ni^{2+}, Cd^{2+} and Pb^{2+} ions, whereas

64

with the addition of Hg^{2+} ions it showed a significant change in the absorption spectra of S3R1 and S3R2. This significant absorption change indicates the high selectivity of both the receptor S3R1 and S3R2 towards the Hg^{2+} ions. The decreasing the absorption at 400 nm in S3R1 and S3R2 upon addition of Hg^{2+} ions is responsible for the color changes.
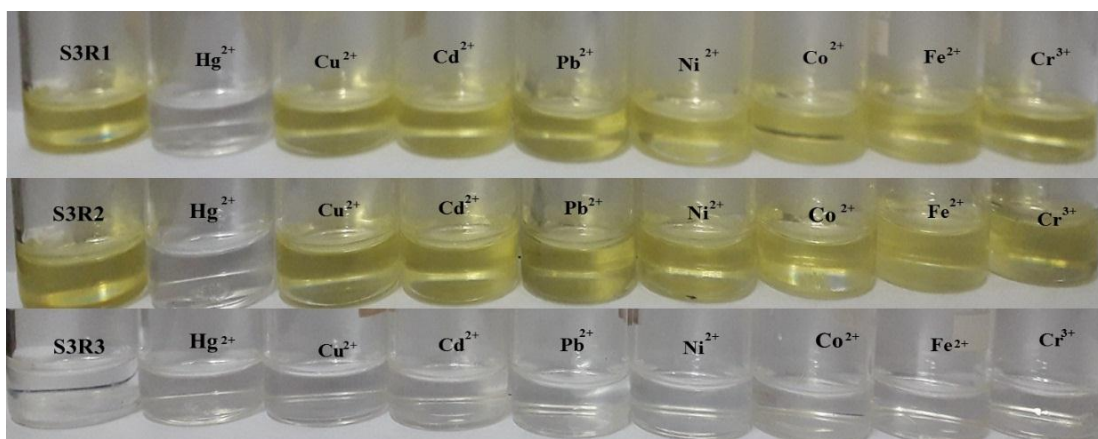
Fig. 4.14. The colorimetric changes of receptors S3R1–S3R3 upon addition of 2 equiv. of various cations in an aqueous solution
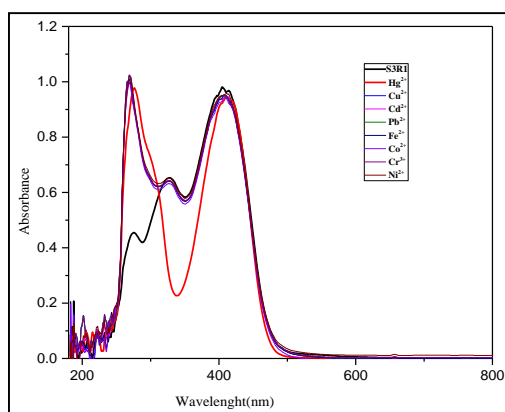
Fig. 4.15. UV-Vis spectral change of receptor S3R1 (2.5×10^{-5} M in DMSO solvent) in the presence of 2.0 equiv. various metal ions
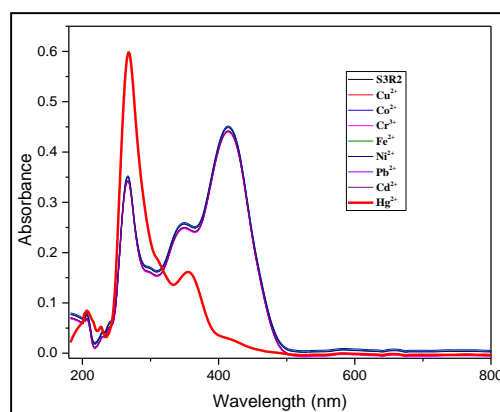
Fig. 4.16. UV-Vis spectral change of receptor S3R2 (2.5×10^{-5} M in DMSO solvent) in the presence of 2.0 equiv. various metal ions

UV-Vis titration studies have been performed with the incremental addition of Hg^{2+} ions (0–2.0 equiv) to confirm the cation binding properties of receptors **S3R1** and **S3R2**. The receptor **S3R1** (2.5 × 10^{-5} M, DMSO) exhibited absorption bands at 276 nm, 338 nm and 406 nm corresponding to the π–π*, n–π* transitions of the –CH=N and –OH moiety respectively (D Renuga et al. 2012). With the incremental

addition of Hg^{2+} ions to S3R1, the band at 276 nm increased in its intensity at the same time the band at 338 nm decreased with its intensity, and it indicates that the formation of a complex between Hg^{2+} and the receptor S3R1 (**Fig. 4.17**). The peak at 406 nm did not alter in its intensity during the titration. The appearance of a clear isobestic point at 310 nm indicates the transition state between free receptor and metal complex formation. The saturation point was attained with the addition of 2 eq. of Hg^{2+} ions (**Fig. 4.17**).
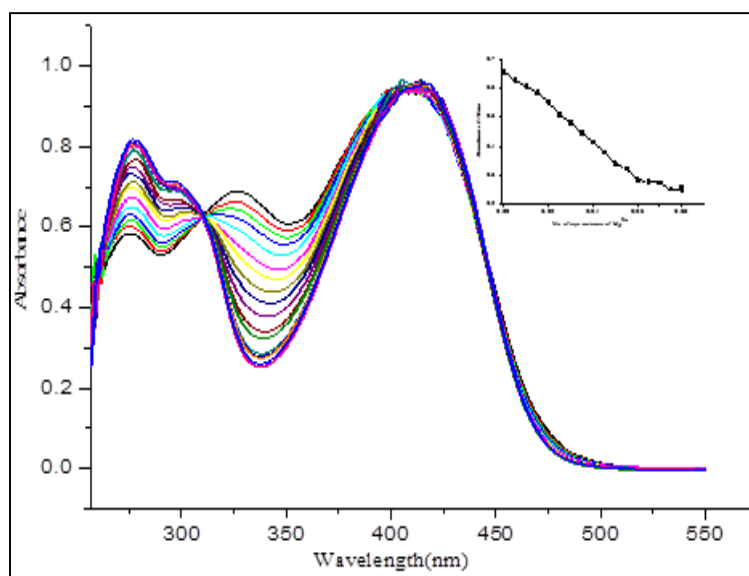
Fig. 4.17: UV–Vis titration of S3R1 (2.5×10^{-5} M, DMSO) with increasing concentration of Hg^{2+} ions (0 – 2.0 equiv.) in an aqueous medium. Inset graph shows binding isotherm at 338 nm wavelength

Receptor S3R2 (2.5×10^{-5} M, DMSO) exhibited absorption bands at 338 nm and 414 nm representing $\pi–\pi^{*}$, $n–\pi^{*}$ transitions of the –CH=N and –OH moiety respectively (D Renuga et al. 2012). With the incremental addition of Hg^{2+} ions to S3R2, the band centered at 338 nm decreased in its intensity along with minute red shift differing by ~17 nm. With the subsequent addition of Hg^{2+} ions, the band centered at 414 nm decreased in its intensity and completely diminished with the addition of 1.5 eq. of Hg^{2+} ions indicating the attainment of saturation point. The isobestic point was centered at 319 nm. The titration profile is shown in **Fig. 4.18.** The selective detection of Hg^{2+} ions is mainly due to the high affinity of the thiophilic group and hydroxyl group present in receptors S3R1 and S3R2.

66
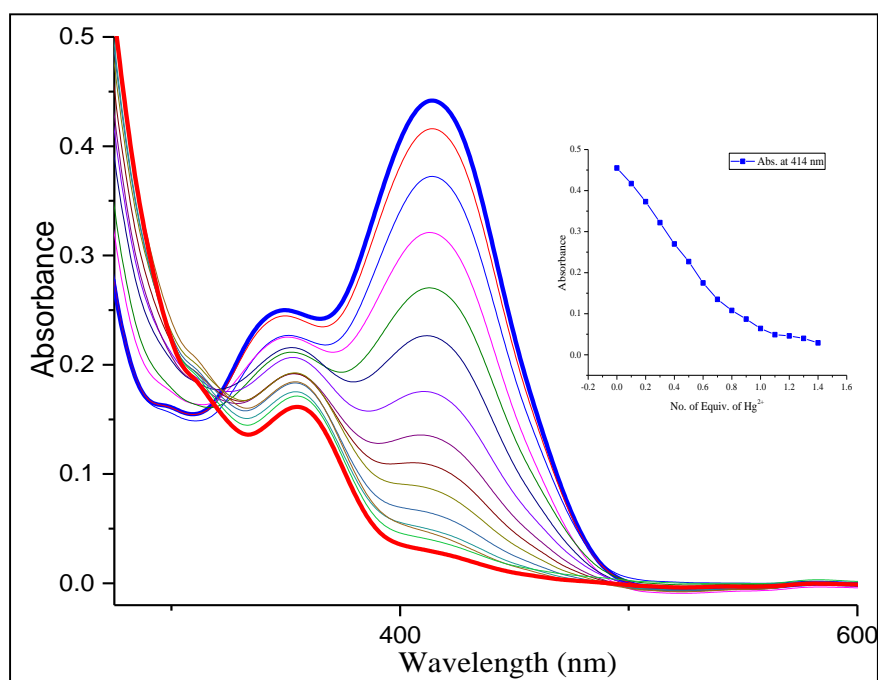
Fig. 4.18: UV–Vis titration and of S3R2 (2.5×10^{-5} M, DMSO) with increasing concentration of cations ($0 - 2.0$ equiv.) in an aqueous medium. Inset graph shows binding isotherm at 414nm wavelength

4.3.2. B-H plot and detection limit calculation

The binding stoichiometry between receptor **S3R1-S3R2** and Hg^{2+} ions was determined by the Benesi-Hildebrand (B-H) method using UV-Vis titration data. The linearity of the graph confirms the formation of stable 1:1 complexation of receptor **S3R1-S3R2** with Hg^{2+} ion as shown in **Fig. 4.19a-b**. The association constant (K) was calculated using the following equation.

$$\frac{1}{(A - A_o)} = \frac{1}{\{K \ (A_{max} - A_o)[M_X^+]^n\}} + \frac{1}{[A_{max} - A_o]}$$

Where, A_0, A, A_{max} are the absorption considered in the absence of Hg^{2+}, at an intermediate, and at a concentration of saturation, K is binding constant, $[M_x^+]$ is a concentration of Hg^{2+} ions and n is the stoichiometric ratio. The determined association constant (K) to be 1.6×10^4, 1.0×10^3 M^{-1} for S3R1–Hg^{2+} and S3R2–Hg^{2+}, respectively. The B-H plots indicated a 1:1 binding ratio between receptors (S3R1& S3R2) and Hg^{2+} ions **(Fig. 4.19a–b).** Further, the stoichiometry and association constant values were determined by Bindfit method given in supramolecular.org (P.

Tandarson et al.2010). And results shows 1:1binding ratio of receptor and metal (**Fig. 4.20a-b**).
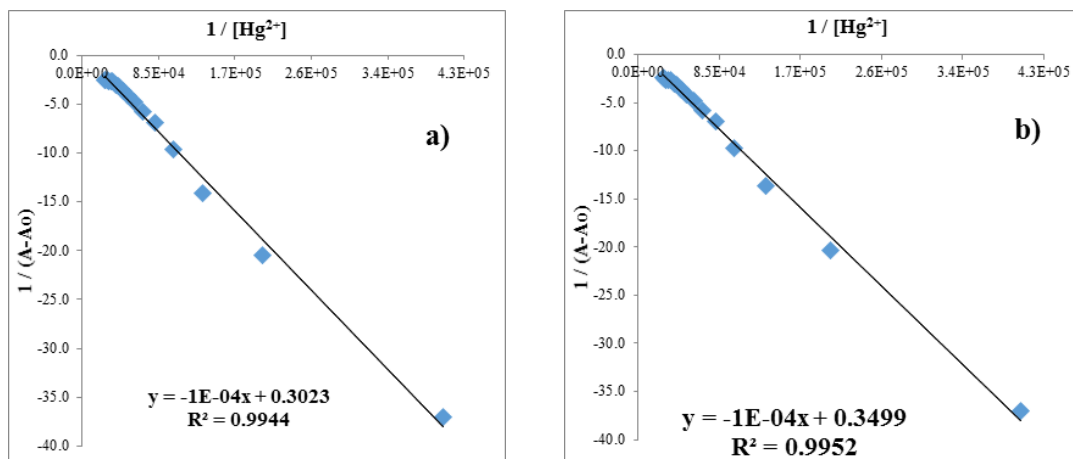
Fig. 4.19: Benesi-Hildebrand (B-H) plot of receptor a). S3R1 and b). S3R2 binding with Hg^{2+} ions
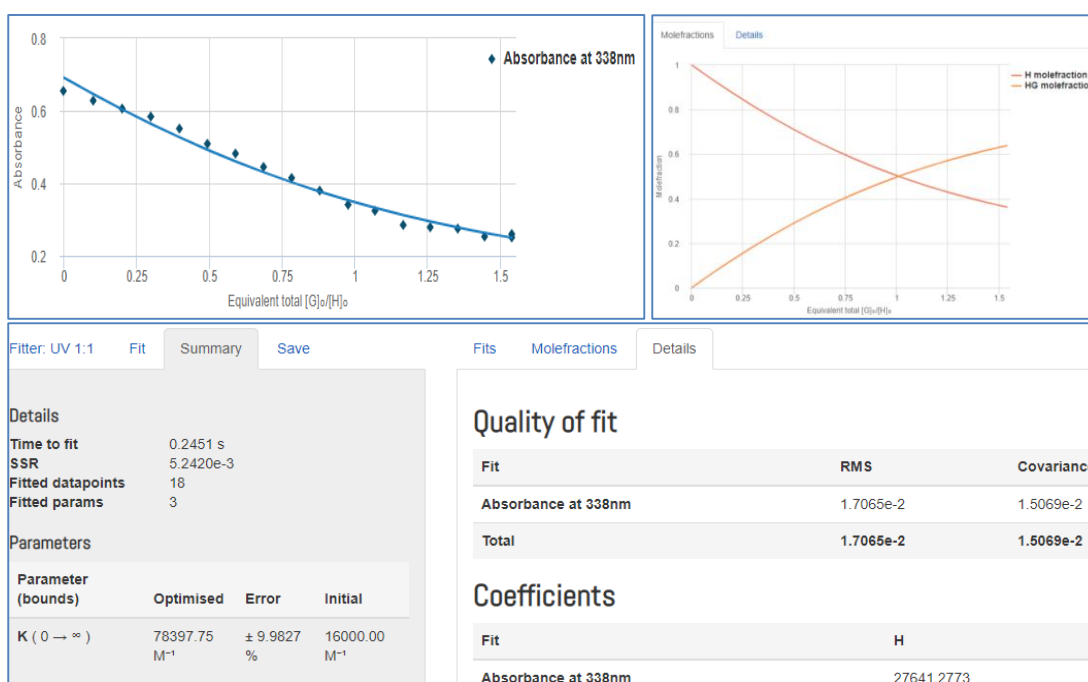
Figure 4.20a: Bindfit plot of receptor **S3R1** (2.5×10^{-5} M, DMSO) and **Hg^{2+}; S3R1 shows** 1:1 binding stoichiometry with Hg^{2+} ions, at 338nm
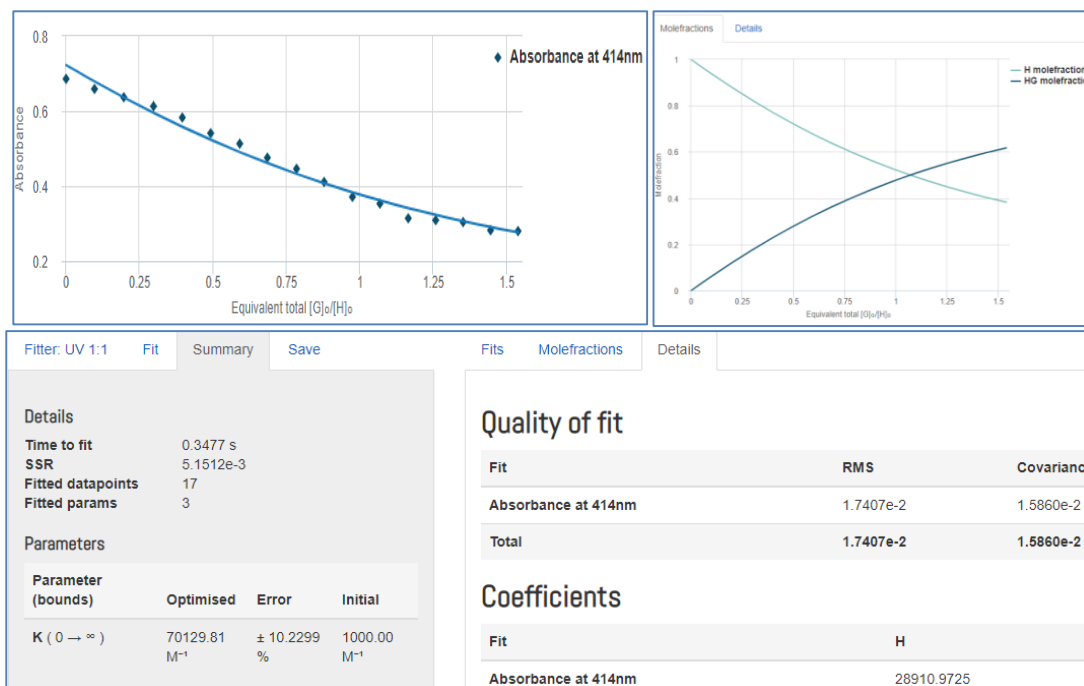
Figure 4.20b: Bindfit plot of receptor **S3R2** (2.5×10^{-5} M, DMSO) and **Hg^{2+}; S3R2 shows** 1:1 binding stoichiometry with Hg^{2+} ions, at 414nm

Further, the calibration plots were drawn between concentrations of Hg^{2+} ions vs. absorbance of receptor complexes (Hg^{2+} vs. S3R1–Hg^{2+} and S3R2–Hg^{2+}). The R^2 value >0.99 indicates well the linear relationship between concentration and its response of the complexes **(Fig. 4.21a-b).** The DL was determined based on the standard deviation of the response and the slope using the following equation mentioned by ICH quality guideline Q2R1.

$$DL = \frac{C \times \sigma}{m}$$

Where,

σ = standard deviation of blank measurement**,**

m = slope of the calibration curve,

C= constant (for DL 3.0). (ICH Q2R1 guidelines).
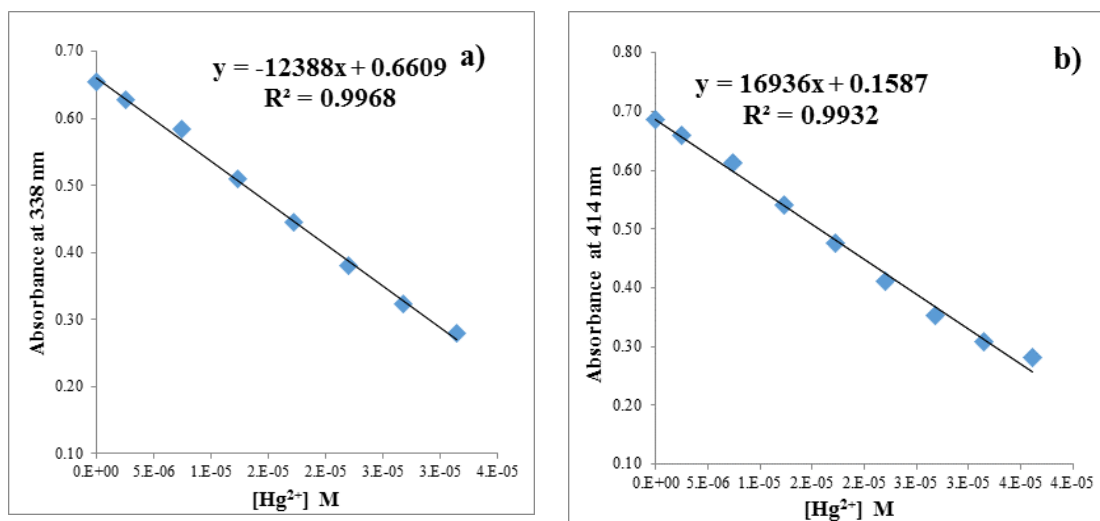
Fig. 4.21: Calibration plot of absorbance of complex (Receptor-Hg^{2+}) versus the concentration of Hg^{2+} ions. **a).** S3R1-Hg^{2+} vs. Hg^{2+} and **b).** S3R2-Hg^{2+} vs. Hg^{2+} ions

The calculated DL values were found to be 0.28 ppm, 0.45 ppm for Hg^{2+} ions using receptors S3R1 and S3R2, respectively.

4.3.3. Binding studies by FT-IR analysis

To find the binding sites in the receptors S3R1 and S3R2 the FT-IR analysis was performed for free receptor and receptor metal complex. When compared the FT-IR spectra of free receptors (S3R1& S3R2) with that of complexes a significant vibration changes were observed for the functional groups –OH and –C=N as shown in **Fig 4.22.** The –OH frequency almost decreased in complexes of S3R1–Hg^{2+} & S3R2–Hg^{2+}, similar observation have been observed for the –C=N group. It indicates that the significant role of these functional groups in binding with Hg^{2+} ions.
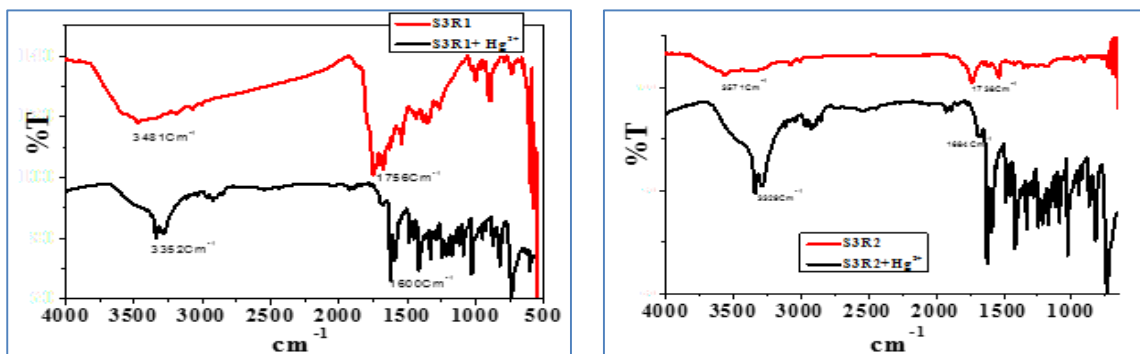
Fig. 4.22 FT-IR spectrum of receptors S3R1, S3R2, S3R1+ Hg^{2+} & S3R2+ Hg^{2+}

70

4.3.4. Theoretical study

The density functional theory (DFT) calculations were performed to get clear understanding of the complexation. We have used Gaussian09 (Schlegel et.al 2009) package to optimize the structure of the metal complexes, S3R1+ Hg^{2+}, S3R2+Hg^{2+}. The exchange-correlation functional B3LYP with the basis sets 6-31G(d,p) for S, O, C, N and H atoms and LANL2DZ for Hg^{2+} were used to optimize the metal complex structures. The optimized structure of the metal complexes, S3R1+ Hg^{2+}, S3R2+Hg^{2+} is shown in the below **Fig. 4.23**. The optimized S3R1 and S3R2 receptor structure provide a pseudo cavity to form complex with Hg^{2+} ion with three donor atoms (O, S and N atoms) and four donor atoms (two Oxygen and two Nitrogen atoms), respectively as in **Fig. 4.23b** and **Fig. 4.23d**. The HOMO and LUMO orbitals of the receptors and complexes are shown in **Fig. 4.24a and 4.24b**.

The HOMO and LUMO are delocalized on the entire bare receptor S3R1 and S3R2. In S3R1, the formerly observed electron density on the moiety (S atom one) in HOMO is accumulated on the metal atom upon binding with the complex, whereas the electron density distribution on LUMO is remain similar to the bare receptor LUMO. The localization of HOMO on the metal atom and LUMO on the receptor molecule suggests the charge transfer from the metal center to the ligand i.e. metal to ligand charge transfer (MLCT). In S3R2 receptor, the HOMO and LUMO are delocalized on the entire molecule similar to the S3R1 receptor. The HOMO is mainly localized on the receptor similar to the HOMO of the bare S3R2 receptor, whereas the LUMO mainly concentrated on the metal atom indicating the ligand to metal charge transfer attributed by nitrile functionalities. The HOMO, LUMO energy levels and band gap energy of the S3R1 and S3R2 receptors and the complexes (S3R1-H^++Hg^{2+} and S3R2-H^++Hg^{2+}) is shown in the **Table 4.1**. The energy bandgap of the S3R1-H^++Hg^{2+} and S3R2+Hg^{2+} metal complexes is significantly reduced by 2.07 eV and 1.1 eV, respectively, compared to the energy band gap of bare receptors due to the charge transfer among the moieties and metal atoms. This bandgap reduction upon complexation is responsible for color changes, this theoretical reduction of bandgap in the complex well concordant with that of the experimental results of S3R1+Hg^{2+} and S3R2+Hg^{2+} metal complexes.
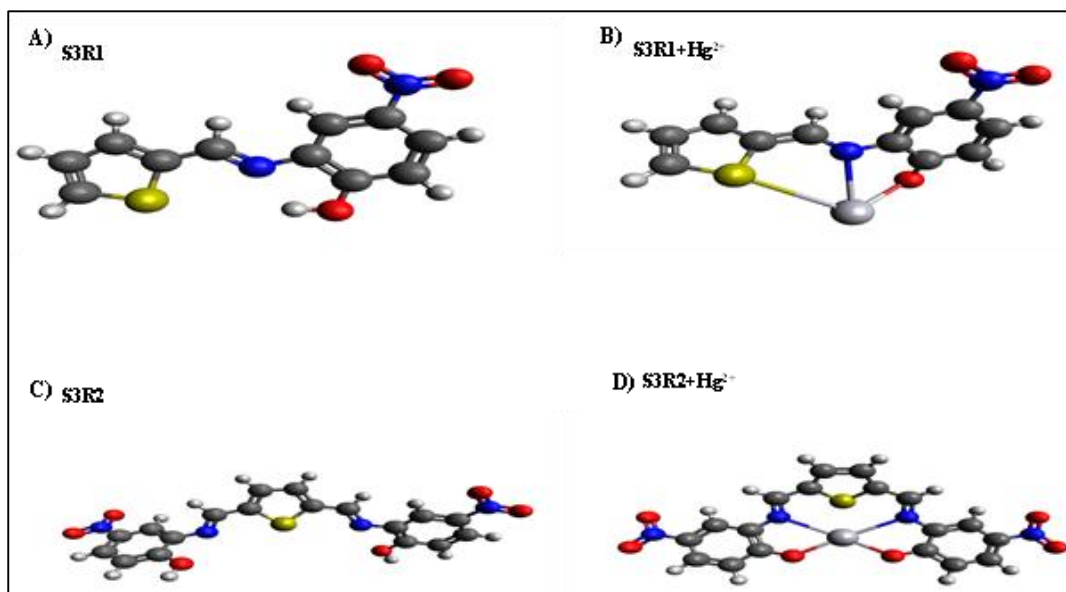
Fig. 4.23. Optimized structure of (a) S3R1 (b) S3R2+ Hg^{2+} (c) S3R2 (d) S3R2+ Hg^{2+}
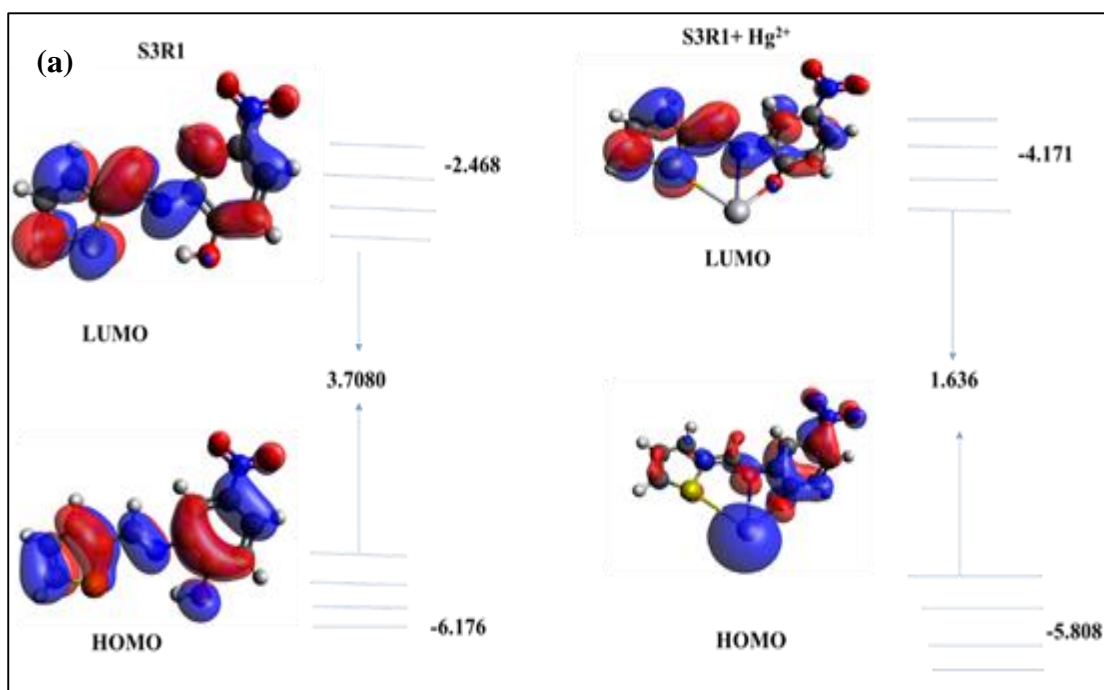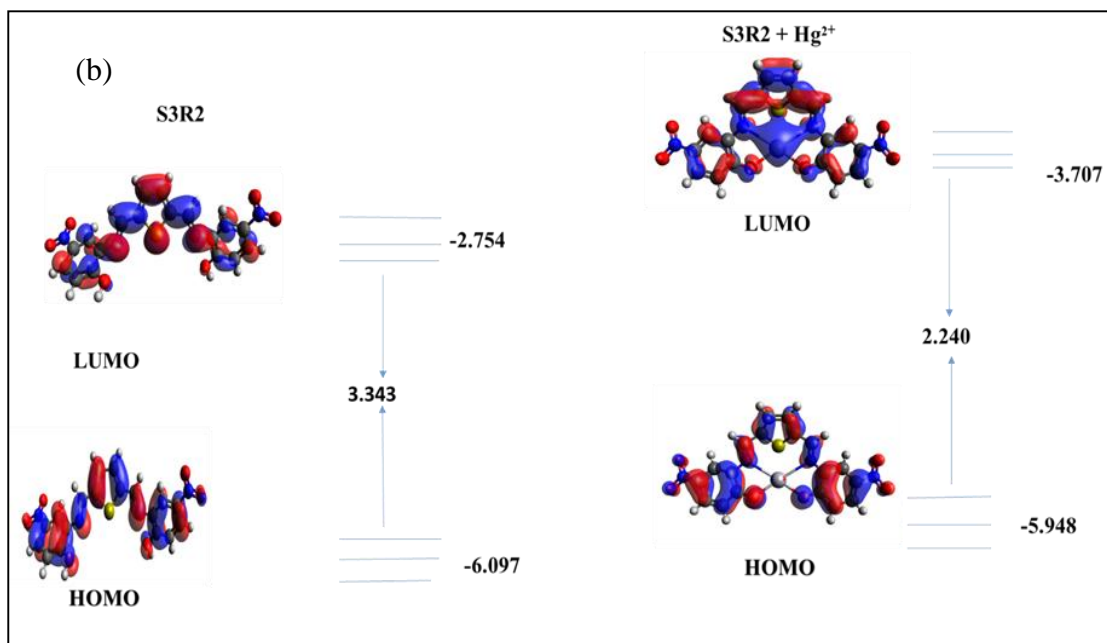
Fig. 4.24. **(a)** Energy levels of various HOMO and LUMO of S3R1 in the absence and presence of Hg^{2+} **(b)** Energy levels of various HOMO and LUMO of S3R2 in the absence and presence of Hg^{2+}

Table 4.1: Energies of HOMO and LUMO of the receptors and complexes

Ligand and metal complexes	HOMO (eV)	LUMO (eV)	ΔE(eV)
S3R1	-6.176	-2.468	3.708
S3R1-H^++Hg(II)	-5.808	-4.171	1.636
S3R2	-6.097	-2.468	3.343
S3R2-H^++Hg(II)	-5.948	-3.707	2.240

4.3.5. ^{1}H NMR Titration

To support the binding interaction between receptors S3R1, S3R2 and Hg^{2+} ions, we carried out ^{1}H NMR titrations of receptors S3R1, S3R2 in the presence of Hg^{2+} (0.0, 0.5 and 1.0 equivalences). As shown in **Fig. 4.25** and **Fig. 4.26** the characteristic aromatic phenolic –OH proton signal (9.34 ppm and 9.0ppm) were completely disappeared upon addition of 1.0 equivalent of Hg^{2+} ion. These observations confirmed that the deprotonation of the phenol OH group which increases the electron density on the phenyl ring, enhanced the charge transfer (CT) and resulted in colorimetric changes. It seems that the interaction between receptor

73

S3R1 and Hg^{2+} involves the deprotonation of phenol OH. The acidity and high hydrogen bonding donor ability of the phenol OH group have made it preferable to undergo deprotonation,
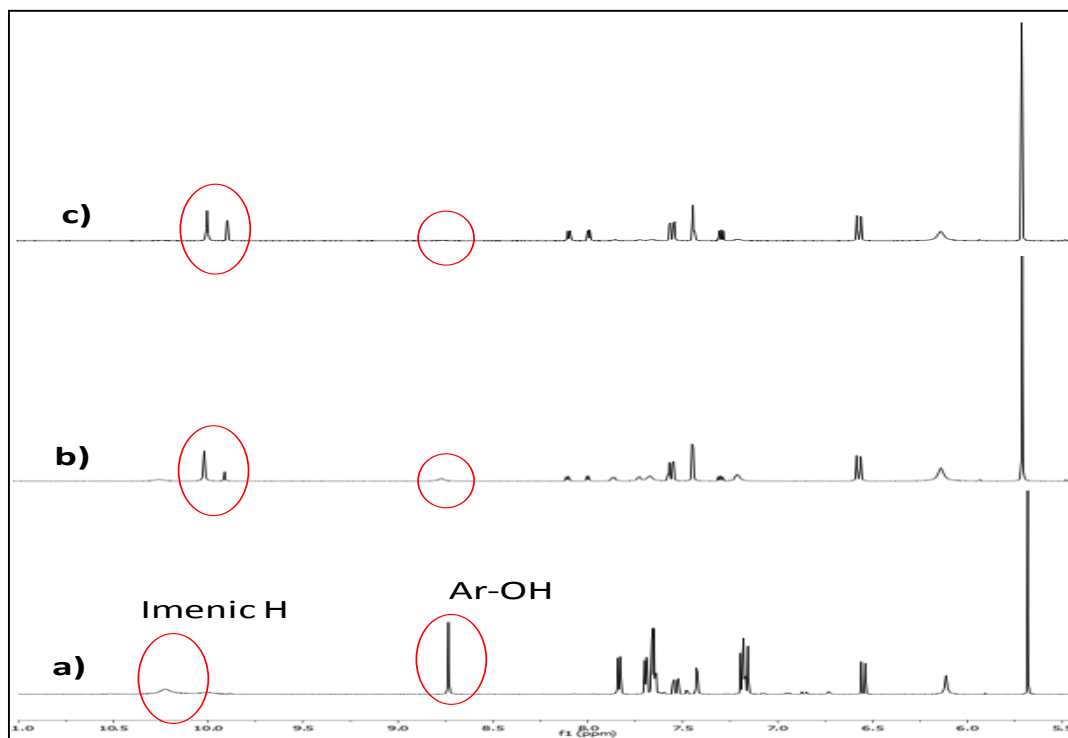
Fig.4.25. ^{1}H-NMR titration of receptor S3R1 with Hg^{2+} ions, **a).** S3R1, **b).** 0.5 Eq. S3R1-Hg^{2+}, **C).** 1.0 Eq. S3R1-Hg^{2+}
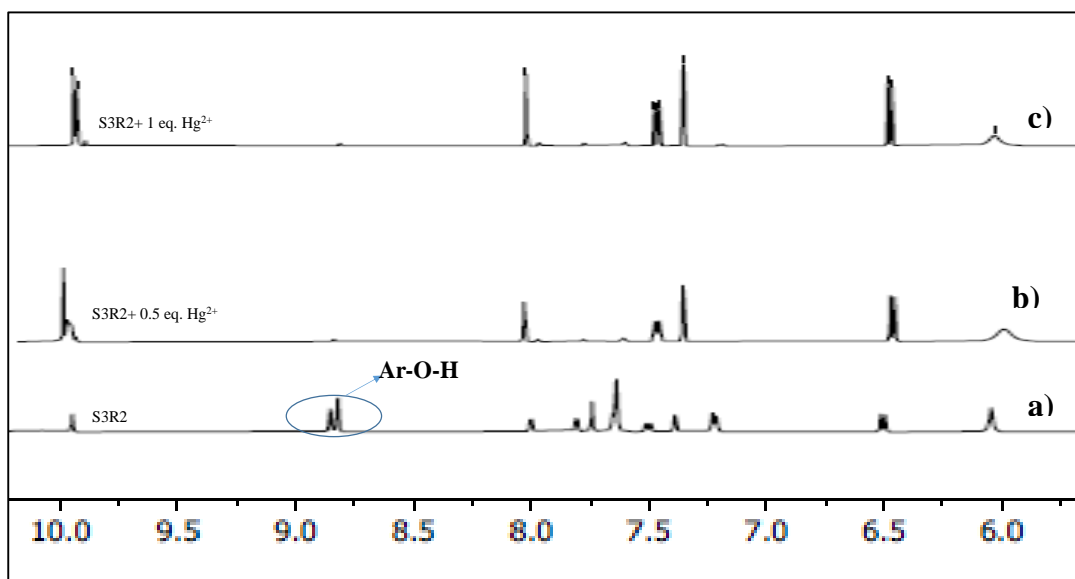
Fig.4.26. ^{1}H-NMR titration of receptor **a)** S3R2 and **b)** 0.5 Eq. S3R2-Hg^{2+} **c)** 1. Eq. S3R1-Hg^{2+}

4.4. CONCLUSION

An easy-to-make Hg^{2+} colorimetric receptors S3R1 and S3R2, bearing electron rich thiophene, imenic and hydroxyl moieties as the binding site which can be explained through FT-IR studies and nitrophenyl moiety as the signal group, was designed and synthesized. These receptors showed specific selectivity for Hg^{2+} in an aqueous media. Comparison with sensor S3R3 indicated that the hydroxyl moiety acted as a strong binding group along with electron-rich thiophene, imenic groups present in S3R1 and S3R2 played a crucial role in the process of colorimetric recognition. Investigation of the recognition mechanism indicated that the receptors S3R1 and S3R2 recognized Hg^{2+} by forming a stable 1:1 ratio receptor and metal complexes (S3R1-Hg^{2+} and S3R2-Hg^{2+}). Moreover, the detection limit of the receptors S3R1 and S3R2 towards Hg^{2+} found to be 0.28 ppm and 0.45 ppm respectively. The receptors displayed good linearity (R2 >0.99) with the linear range of 0.0 to 3.2×10^{-5} M. This indicated that the receptors S3R1 and S3R2 may be useful as a colorimetric receptor for monitoring Hg^{2+} levels in environmental systems.

QUINOLINE SCHIFF'S BASE CHEMOSENSOR FOR COLORIMETRIC DETECTION OF Cd^{2+} IONS

Abstract

In this chapter, the design syntheses and characterizations of new quinoline Schiff"s base derivatives for colorimetric detection of cadmium ions over other cations have been discussed in detail.

5.1 INTRODUCTION

The development of new colorimetric receptors for selective recognition of heavy metal ions have received a considerable concentration in the past few decades. Certain metals when going beyond permissible limit, become very toxic and perilous to mankind. Among various heavy metal ions cadmium, lead and mercury ions are well known for their high toxicity towards the environment and human health. Among them, cadmium is one of the carcinogenic metals. A major exposure source is smoking and through food, but the inhalation of cadmium-containing dust is the most dangerous route. Cadmium can be found in electroplated steel, pigments in plastics, electric batteries and so on. A high exposure level of cadmium is allied with increased risks of cardiovascular diseases, cancer mortality and damage to liver and kidney. Knowing the seriousness of the problem, significant research efforts have been dedicated to improving heavy metal ion detection. Current industrial approaches count on costly, sophisticated instruments, complicated procedures or low sensitivity and selectivity approaches like atomic absorption/emission spectroscopy or inductively coupled plasma mass spectroscopy. For these reasons, chromogenic chemo-sensors are especially attractive because they permit naked eye detection of color change without any use of spectroscopic instruments. Also, these colorimetric sensors ideally have the benefits of low cost, easy synthesis and storage, and more tolerance towards different experimental conditions. Therefore, many researchers have focused on "colorimetric," and fluorometric chemo-sensors in this research area, for the detection of heavy metals.

The quinoline moiety as a receptor, 2-amino thiophenol as chromophore has been frequently used for the colorimetric chemosensors (Wu, F. Y et al. 2006). Therefore, we planned to incorporate the hydroxyquinoline moiety into 2-amino thiophenol moiety to develop a novel chemosensor, 2-[(2Mercapto-Phenylamino)-methyl] Quinoline8-ol. Herein, we report a simple and reliable colorimetric chemosensor for the detection of Cd^{2+} ions in aqueous media. This work was motivated by the fact that most organic molecules reported as Cd^{2+} chemosensors perform the sensing process in a medium different than water, which limits their function in environmental and life sciences. This new sensor is based on a Schiff base derivative, this has been described as important tools for a long time, but their usage as a signaling subunit in chemosensors is limited due to their low solubility in aqueous media.
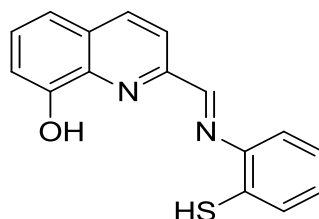
5.2. EXPERIMENTAL SECTION

5.2.1 Materials, methods and instruments

All chemicals were procured from Sigma-Aldrich, Alfa Aesar or spectrochem and used without further purification. All the solvents were procured from spectrochem, SD Fine, India of HPLC grade and used without further distillation. The ^{1}H NMR and ^{13}C NMR spectra were recorded on a Bruker, (400MHz) instrument using TMS as an internal reference and DMSO-d_6 as solvent. Resonance multiplicities are labeled as s (singlet), d (doublet), t (triplet) and m (multiplet). Melting points were measured on a Stuart- SMP3 melting-point apparatus in open capillaries. Infrared spectra were recorded on a Perkin-Elmer FT-IR spectrometer; signal designations: s (strong), m (medium) and w (weak). UV-Vis spectroscopy was carried out with Analytik Jena Specord S600 spectrometer in standard 3.0 mL quartz cells (2 optical windows) with 10 mm path length. The Agilent 6410 series Liquid

chromatography with triple Quadrupole mass detector (Agilent LC/MS/MS model 6410, Agilent Technologies Inc., Santa Clara, CA, USA) with Electrospray ionization source was used in positive polarity. The source temperature was put tom 350 °C and the Capillary voltage put on 4000 volts. The Nitrogen gas was used for nebulization with 10 mLmin^{-1} flow. The additional nitrogen was used for the MS/MS studies of Oxidative impurities and process impurities. The range of mass selected was 100 Da to 1000 Da, the fragmentor was 135 and the scan time was 500 min. The Mobile phase A as 10 mM Ammonium acetate at 4.0 pH adjusted by using the acetic acid and Mobile phase B as Acetonitrile and Methanol as 50:50: %v/v. The injection load was 20 microliter. The column used as Xbridge C18 150 mm x 4.6 mm x 3.5 μm. The data compilation was done by using Mass Hunter software.

5.2.2 Synthesis of receptors S4R1–S4R3:

The general schemes of synthesis of new receptors S4R1–S4R3 are represented in **Scheme 5.1.** Confirmed the chemical structures of all the receptors by ^{1}H NMR, ^{13}C NMR, FT–IR, and Mass spectrometry (**Fig. 5.1–5.12**).
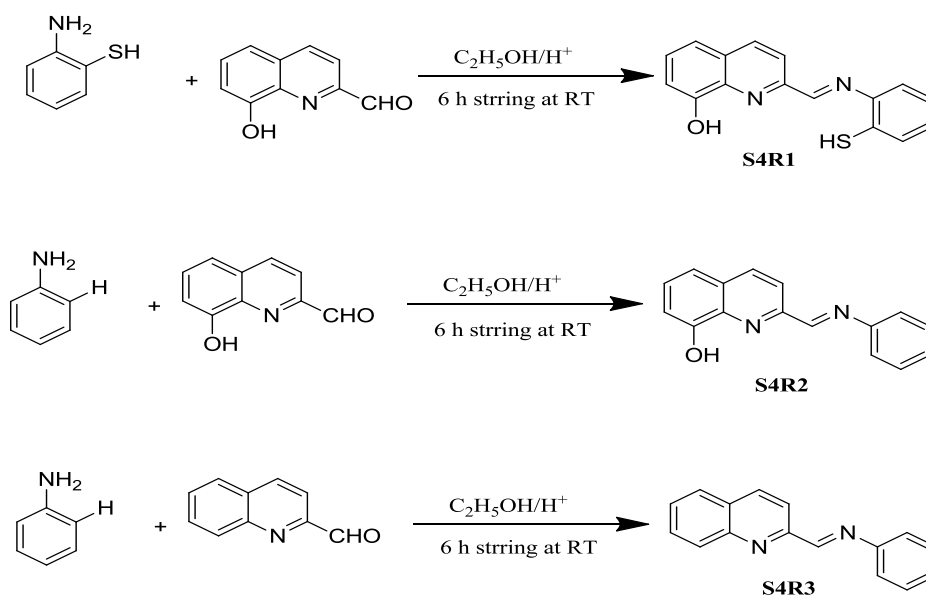
Scheme 5.1: Synthesis of receptors **S4R1, S4R2** and **S4R3**

2[(2- Mercapto-Phenylimino) methyl] - quinolin-8-ol, (S4R1): The receptor **S4R1** was synthesized by dropwise addition of an ethanolic solution (5ml) of 8-

Hydroxyquinoline 2-carboxaldehyde 2.89 mmol (0.5g) to an ethanolic solution (5ml) of 2-amino thiophenol 2.89 mmol (0.36g) with constant stirring for 6 h at room temperature (RT ≈25°C). The pale yellow color liquid compound was obtained and excess solvent was evaporated under vacuum. The crude sample was recrystallized from ethanol to get the desired pure compound. **Yield**: 91%, **Melting Point:** 262-264°C; **FT–IR (KBr, cm^{-1}):** 3424 (O–H str.), 3058 (Ar. H str.), 1619 (-C=N- str.), 1553, 1473, 1322 (Ar. C=C str), 823, 741 (Ar. C-H def.); **^{1}H–NMR (400 MHz, DMSO-d6, δ$_{ppm}$):** 7.23 (s, aromatic 2H), 7.38 (s, aromatic 3H), 7.8 (s, aromatic 3H), 8.2 (s, aromatic 2H), 10.15 (s, S–H) and 10.81 (s, O-H); **^{13}C-NMR (100 MHz, DMSO-d6, δ$_{ppm}$):** 163.00, 153.12, 147.67, 142.26, 138.25, 136.90, **MS (ESI, m/z):** calculated 280.10, found (M+1) 281.00.

2-Phenyliminomethyl - quinolin-8-ol (S4R2):

The receptor **S4R2** was synthesized by dropwise addition of an ethanolic solution (5ml) of 8-Hydroxyquinoline 2-carboxaldehyde 2.89 mmol (0.5g) to the ethanolic solution (5ml) of Aniline 2.89 mmol (0.269g) with constant stirring for 6 h at room temperature (RT ≈25°C). The pale yellow color liquid compound was obtained and excess solvent was evaporated under vacuum. The crude sample was recrystallized from ethanol to get the desired pure compound. **Yield**: 89%, **Melting point:** 210-212°C; **FT–IR (KBr, cm^{-1}):** 3354 (-OH str.), 3059 (C-H Ar. str.), 1628 (-C=N- str.), 1411 (Ar. C-H str.), 1244 (C–O Str.) 826 (Ar. C–H def); **^{1}H-NMR (400 MHz, DMSO-d6, δ$_{ppm}$):** 10.90 (s, 1H (O–H)), 8.64 (m, aromatic 2H), 8.01 (m, aromatic 2H), 7.8 (m, aromatic 3H), 7.6 (m, aromatic 2H), 7.4 (s, aromatic 1H HC=N), 7.1 (m, aromatic 1H); **^{13}C-NMR (100 MHz, DMSO-d6, δ$_{ppm}$):** 163.00, 153.12, 147.67, 142.26, 138.25, 136.90, 129.87; **MS (ESI, m/z):** calculated 247.10, found (M+1) 248.10.

(E)- *N*- (quinolin-2-yl methylene) aniline (S4R3):

The receptor **S4R3** was synthesized by dropwise addition of an ethanolic solution (5ml) of quinoline 2-carboxaldehyde 1.73 mmol (0.3g) to an ethanolic solution (5ml) of Aniline 0.173 mmol (0.161g) with stirring for 6 h at room temperature (RT ≈25°C). The pale yellow color liquid compound was obtained and excess solvent was evaporated under vacuum. The crude sample was recrystallized

from ethanol to get the desired pure compound. **Yield**: 93%, **Melting point:** 187-190°C; **FT–IR (KBr, cm^{-1}):** 3055 (-C-H Ar. str.), 1610(-C=N- str.), 1542, 1445 (Ar. C=C-str.), 1180 (C=C def.), 753 (Ar. C-H def.); **^{1}H-NMR (400 MHz, DMSO-d6, δ$_{ppm}$):** 8.16 (m, aromatic 2H), 8.3 (m, aromatic2H), 8.7 (m, aromatic 2H), 7.2 (m, aromatic 6H). **^{13}C-NMR (100 MHz, DMSO-d6, δ$_{ppm}$):**160.77, 123.12, 120.12, 116.34; **MS (ESI, m/z):** Calculated 232.20, found (M+1) 233.00.

CHARACTERIZATION SPECTRA OF RECEPTORS S4R1–S4R3
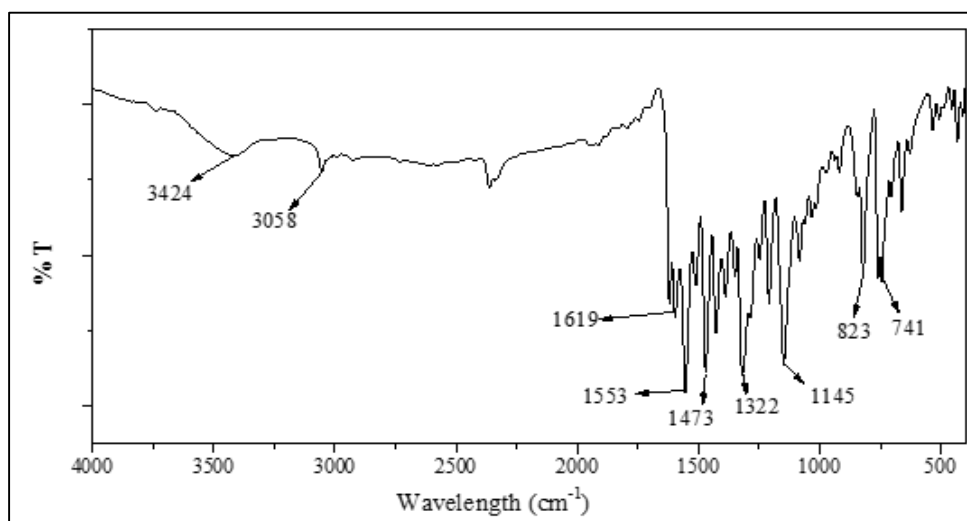
Fig. 5.1: FT-IR Spectrum of receptor S4R1
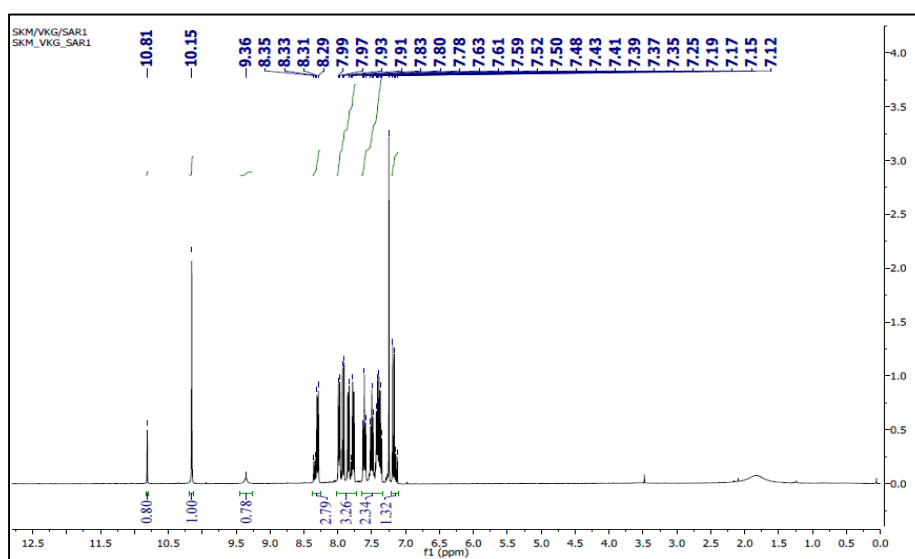
Fig. 5.2: ^{1}H NMR spectrum of receptor S4R1

80
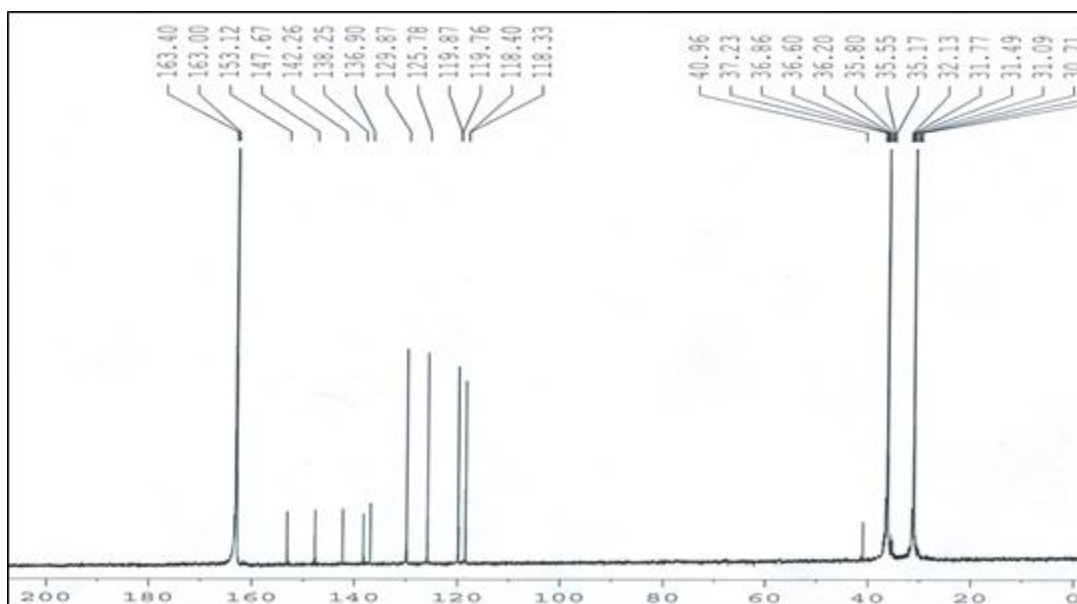
Fig. 5.3: ^{13}C NMR spectrum of receptor S4R1
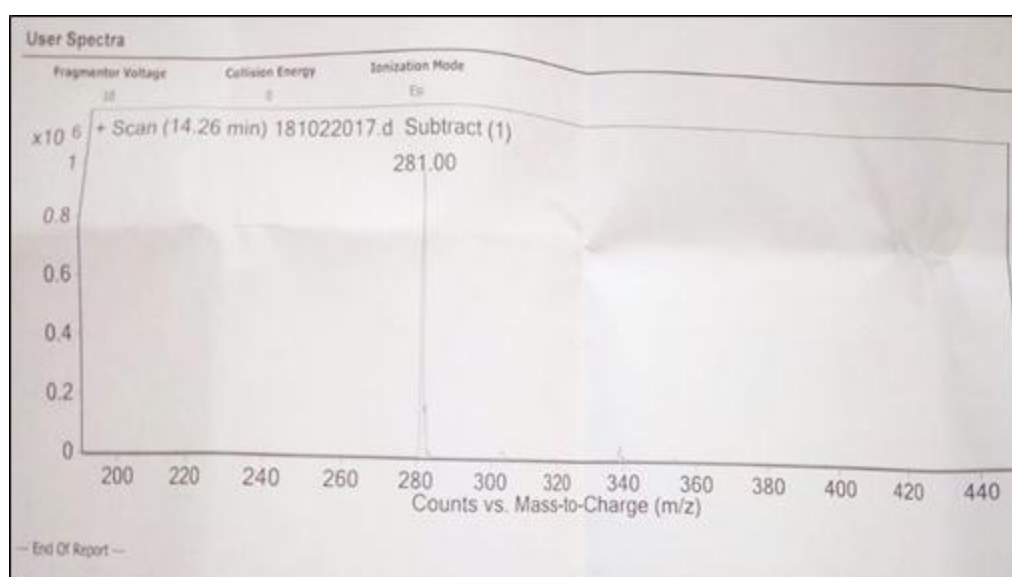
Fig. 5.4: ESI-MS spectrum of receptor S4R1
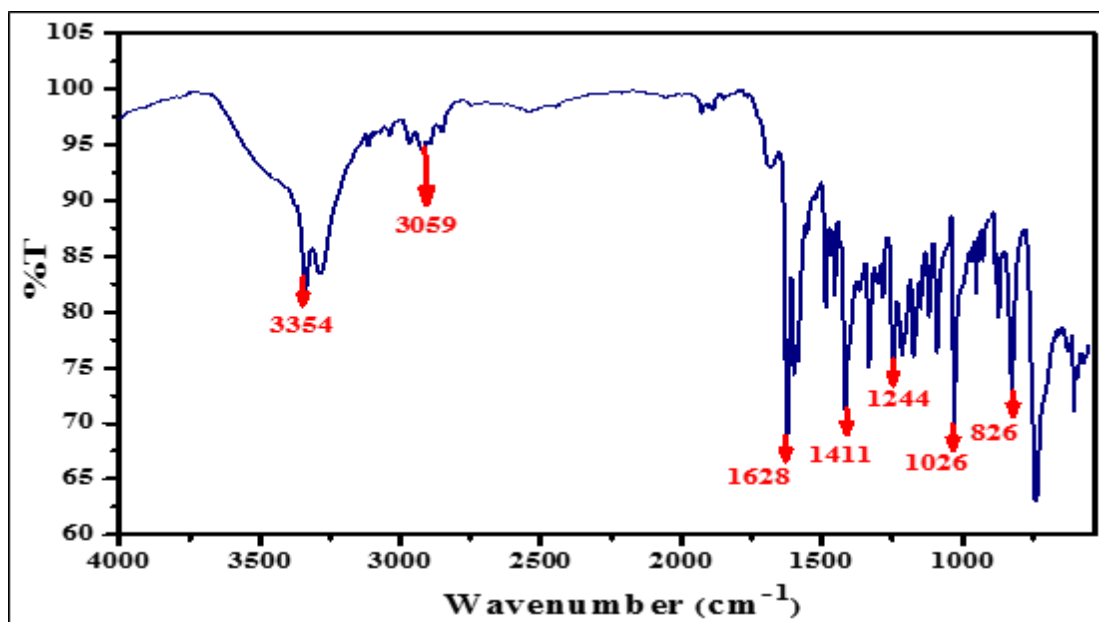
Fig. 5.5: FT-IR Spectrum of receptor S4R2
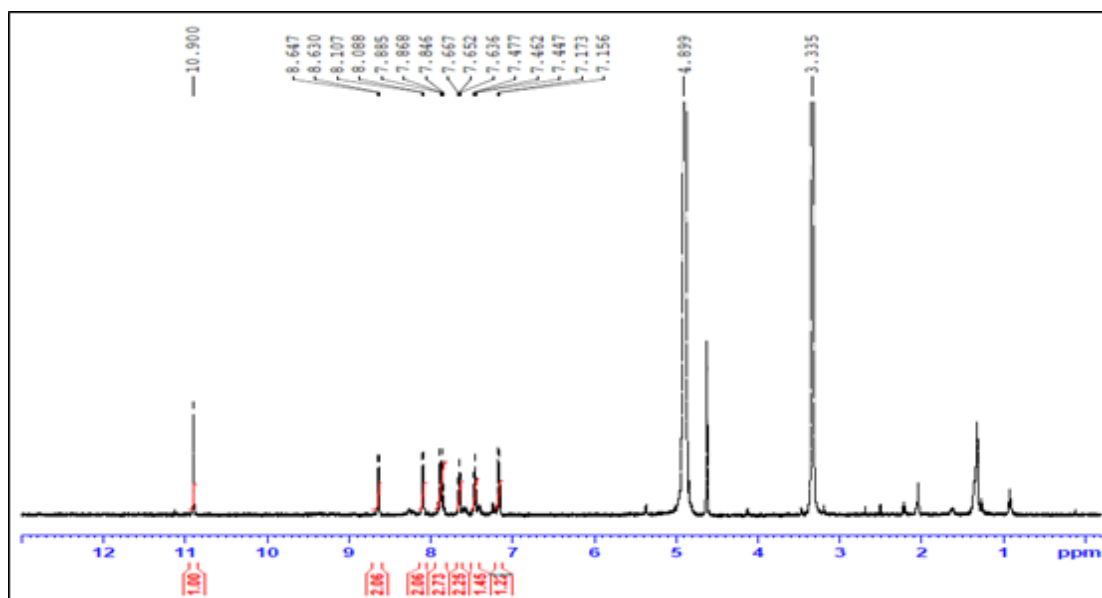
Fig. 5.6: ^{1}H NMR of spectrum receptor S4R2
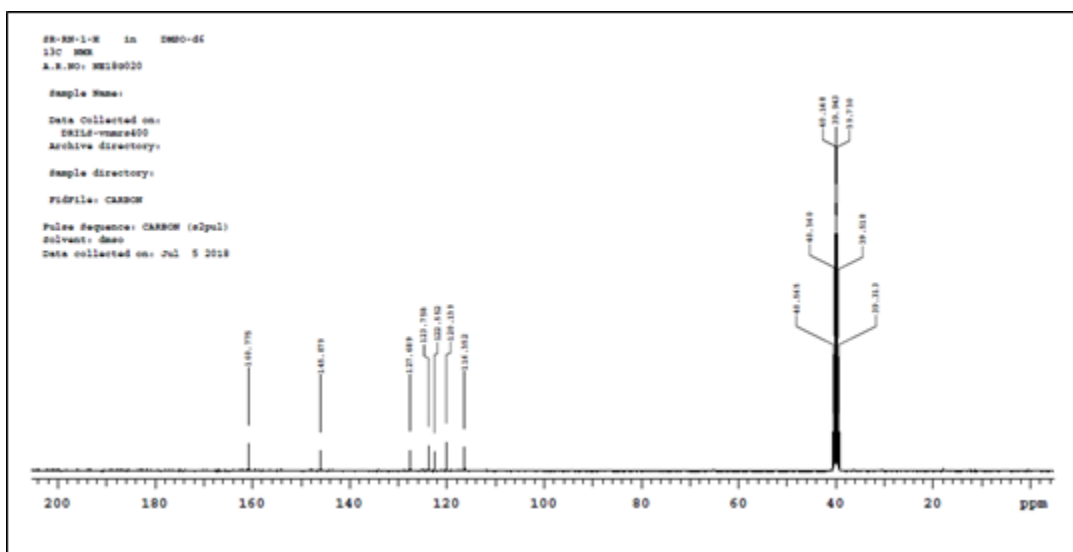
Fig. 5.7: ^{13}C NMR of spectrum receptor S4R2
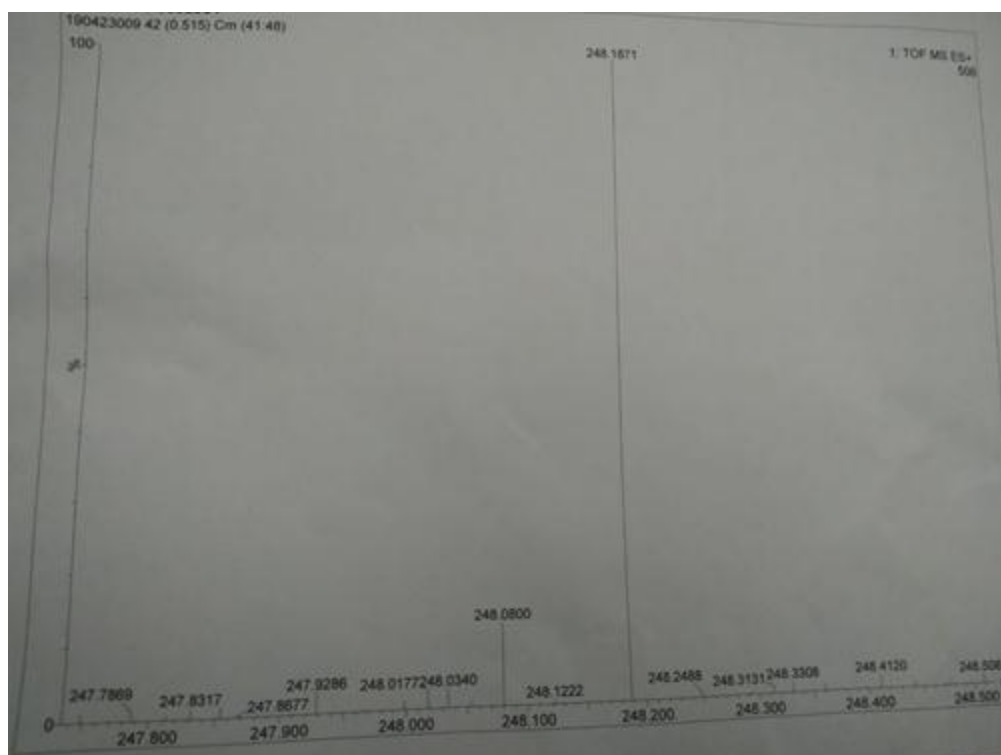
Fig. 5.8: ESI-mass spectrum of receptor S4R2
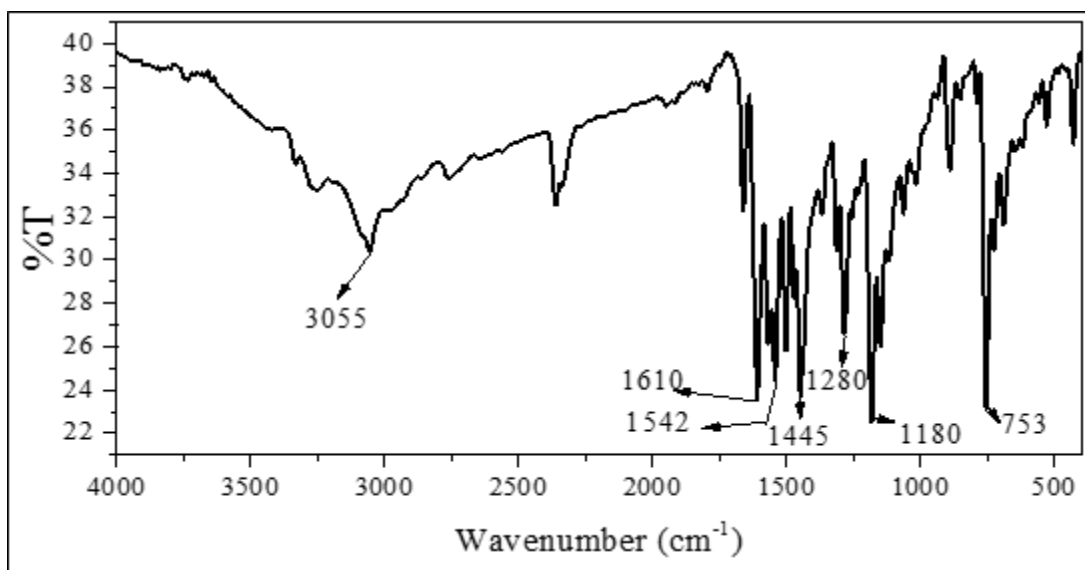
Fig. 5.9: FT-IR Spectrum of receptor S4R3
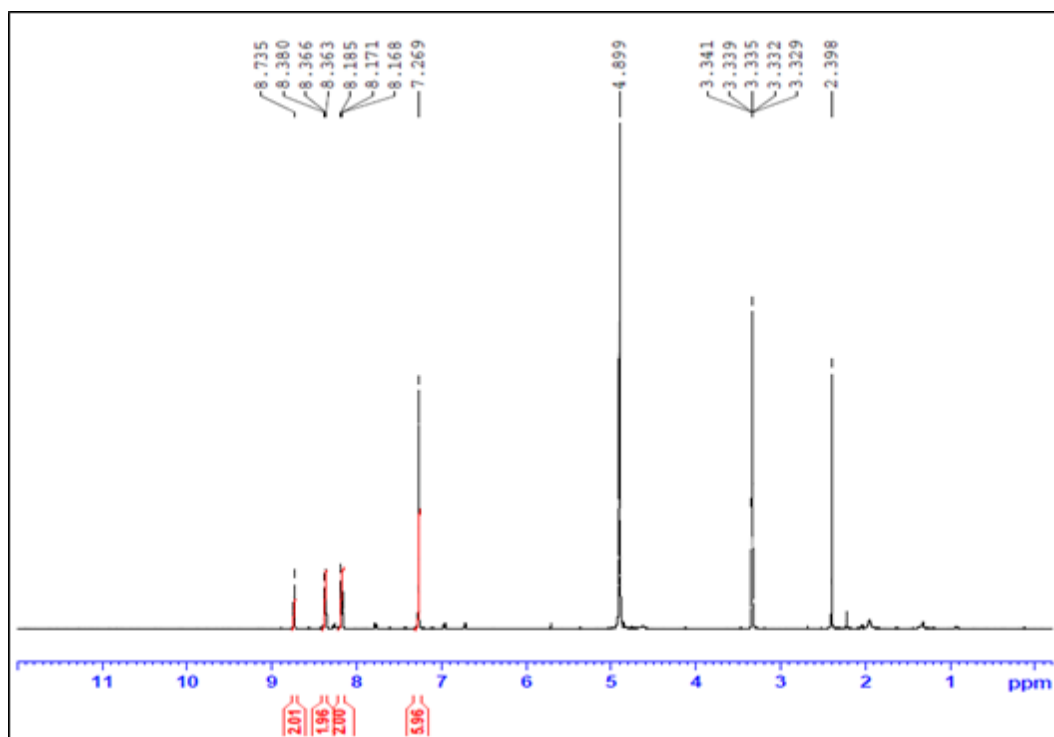
Fig. 5.10: ^{1}H NMR spectrum of receptor S4R3
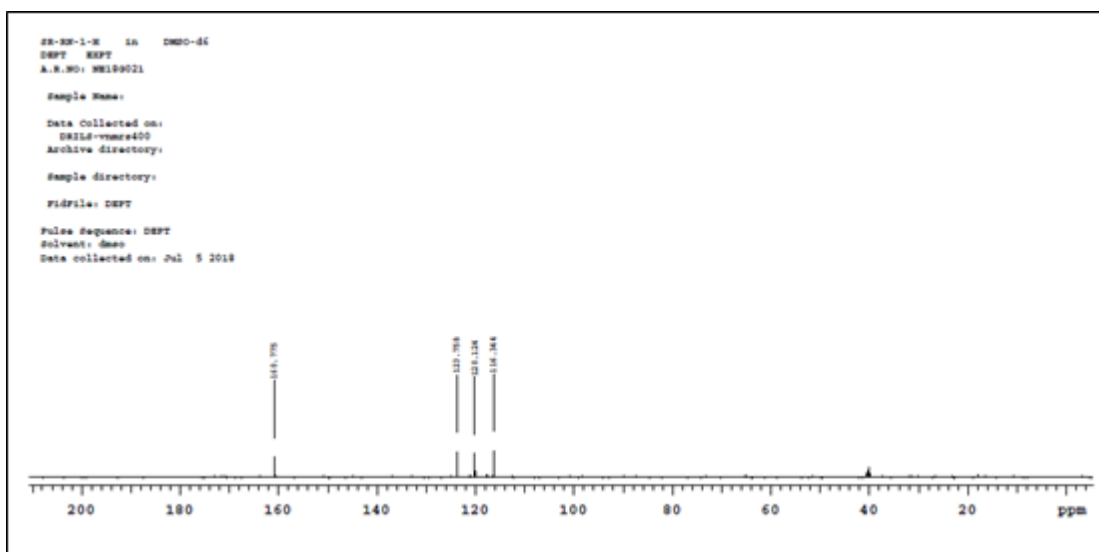
Fig. 5.11: ^{13}C NMR spectrum of receptor S4R3
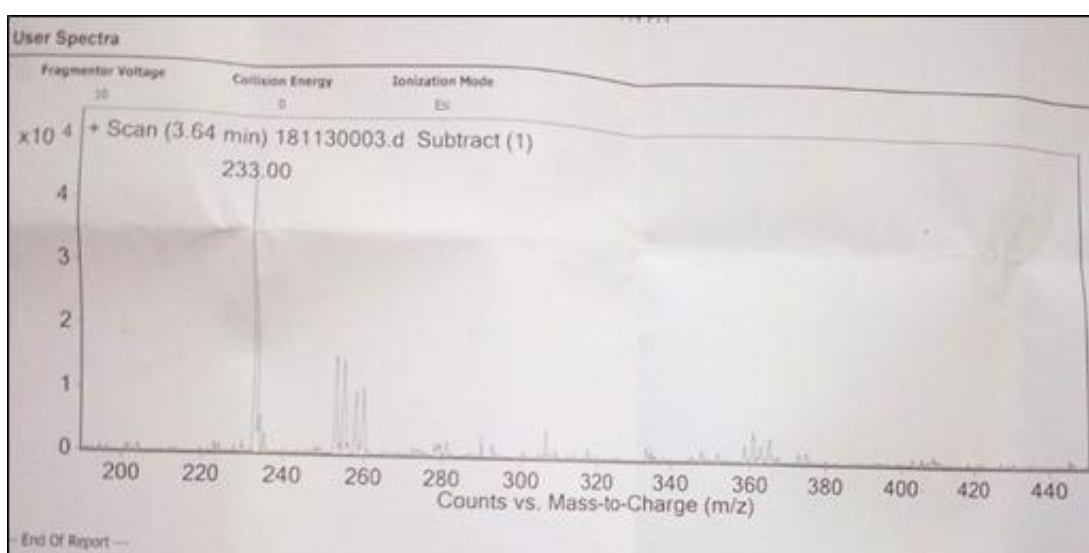
Fig. 5.12: ESI-mass spectrum of receptor S4R3

5.3 RESULTS AND DISCUSSION

5.3.1. UV–Vis Studies

Individual colorimetric studies were conducted for the synthesized receptors S4R1–S4R3, (2.5×10^{-5} M in DMSO solvent) for the detection of different cations such as Ni^{2+}, Hg^{2+}, Pb^{2+}, Cu^{2+}, Co^{2+}, Cr^{3+}, Cd^{2+} and Fe^{2+} (1.0×10^{-3} M in an aqueous solution). An important feature of the receptor S4R1 is its high selectivity toward the analyte (Cd^{2+}) over other competitive species. In the colorimetric study, the S4R1 displayed significant color change from pale yellow to pale orange color in the

85

presence of Cd^{2+} ions (**Fig. 5.13**). In a similar way the receptor S4R2 and S4R3 were investigated for colorimetric detection of cations and they did not show any color change in the presence 2.0 equiv. of Cd^{2+} and other tested cations (**Fig. 5.13**). To examine the feasibility of receptor S4R1 as a chemosensor for Cd^{2+}, we first investigated its chromogenic character in the absence and presence of Cd^{2+} ions. In the UV−Vis titration, the receptor S4R1 showed characteristic absorption peaks at 415 and 510 nm respectively. Upon addition of Cd^{2+} ions, the absorption peak at 415 nm decreased and the peaks at 510 nm are gradually increasing (**Fig. 5.14**). With the addition of other competitive ions, the receptor S4R1 did not display any significant changes in the absorption spectra (**Fig. 5.14 & 5.15**). It indicates high selectivity of receptor S4R1 towards Cd^{2+} ions.

Fig. 5.13. The colorimetric changes of receptor S4R1–S4R3 upon addition of 2.0 equiv. of various cations in an aqueous solution

86
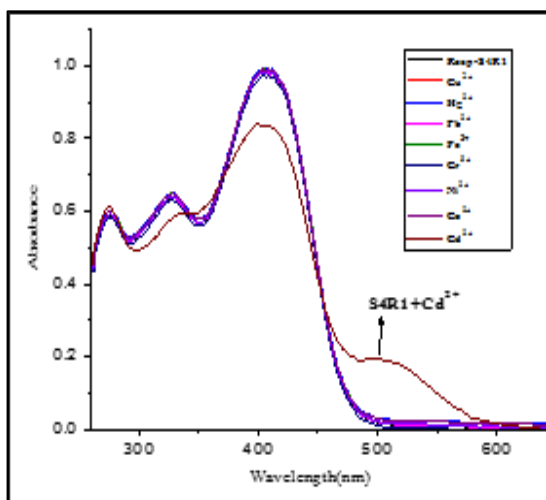
Fig. 5.14: UV-Vis spectral change of receptor **S4R1** (2.5×10⁻⁵ M in DMSO solvent) in the presence of 2.0 equiv. various metal ions. Insert showing the absorbance of receptor **S4R1** and S4R1+Cd²⁺ ions
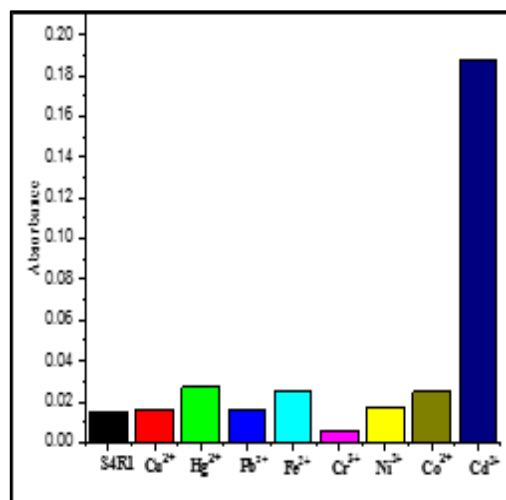
Fig. 5.15: A bar chart representation of absorption change of **S4R1** in the presence of 2.0 equiv. of various metal ions at wavelength 510 nm

UV-Vis titration experiment was performed to explore the sensing properties of receptor **S4R1** towards Cd^{2+} and the titration graph is represented in **Fig. 5.16.** The incremental addition from 0 to 2.0 equiv. of Cd^{2+} ions to receptor **S4R1,** the absorption intensity band at 415 nm corresponds to -SH group in the receptor **S4R1** gradually decreases and the other band at 510 nm gradually increases. This observation is due to the formation of the receptor–metal ion complex, the electron-rich thiophilic group functioned as a donor group and Cd^{2+} accepts electrons. To further elucidate the possible binding mode of the sensor S4R1 with Cd^{2+}, ESI-MS analysis was carried out by adding Cd^{2+} into the solution of S4R1. The free receptor displayed a mass peak at m/z 281 (M+1), whereas in the presence of Cd^{2+} ions it displayed a prominent mass peak at m/z 454.20 (M+1) corresponds to [**S4R1-Cd²⁺+NO₃⁻**]**, (Fig. 5.17).** Based on the UV–Vis and mass analysis the proposed binding interaction was given in **Fig. 5.18.**

87
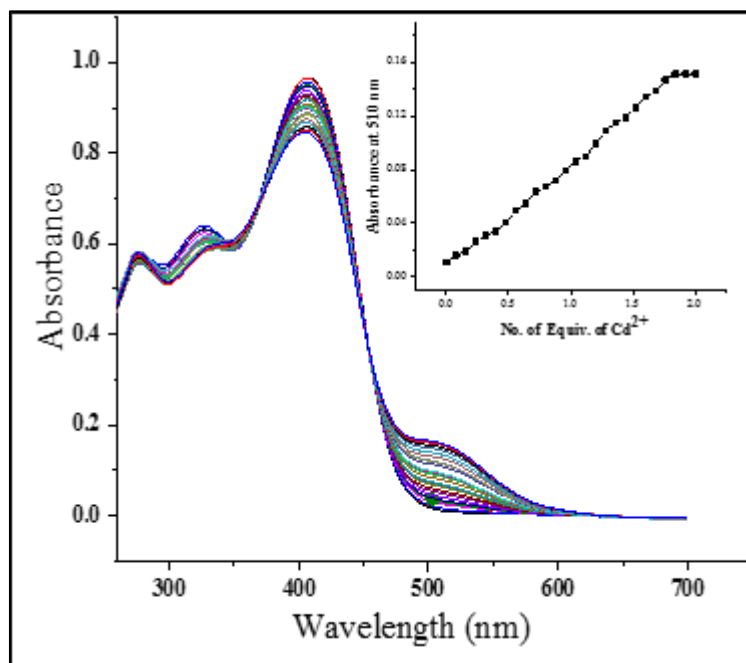
Fig. 5.16: UV–Vis spectra of **S4R1** (2.5×10^{-5} M, DMSO) with increasing concentration of Cd^{2+} ions (0 – 2 equiv.) in an aqueous medium. Inset graph shows binding isotherm at a selective wavelength (510 nm)
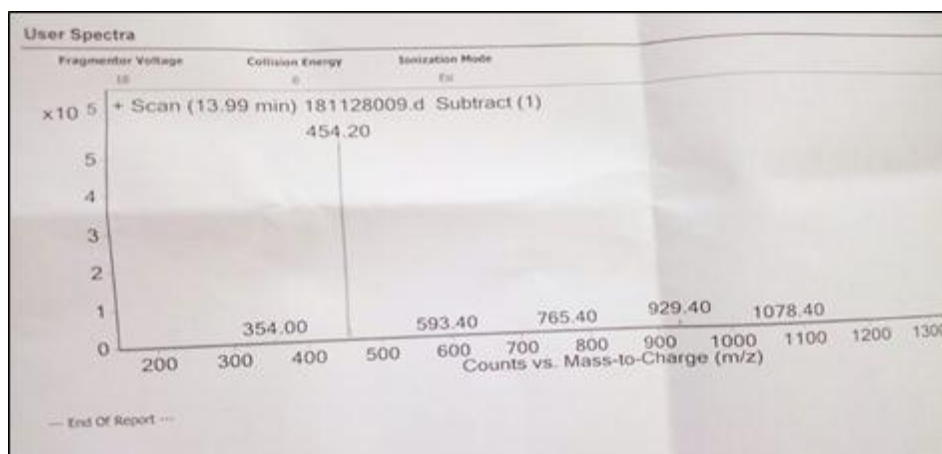
Fig 5.17: ESI-mass spectrum of complex **[S4R1-Cd²⁺+NO₃⁻].**
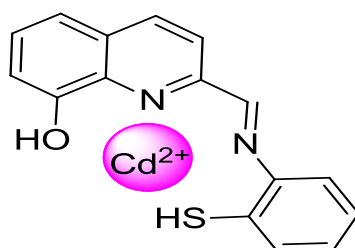
Fig. 5.18: Proposed binding mechanism of Cd^{2+} ions with receptor S4R1

88

The binding stoichiometry between receptor **S4R1** and Cd^{2+} ions was determined by the Benesi-Hildebrand (B–H) method using UV-Vis spectrometric titration data wavelength at 510 nm. The linearity of the graph confirms the formation of stable 1:1 complexation of receptor **S4R1** with Cd^{2+} ion as shown in **Fig. 5.19**. The association constant (K) was calculated using the following equation.

$$\frac{1}{(A - A_o)} = \frac{1}{\{K \, (A_{max} - A_o)[M_X^+]^n\}} + \frac{1}{[A_{max} - A_o]}$$

Where, A_0, A, A_{max} are the absorption considered in the absence of Cd^{2+}, at an intermediate, and at a concentration of saturation, K is binding constant, $[M_x^+]$ is the concentration of Cd^{2+} ions and n is the stoichiometric ratio. The found association constant (K) was to be 4.3×10^4 M^{-1}.
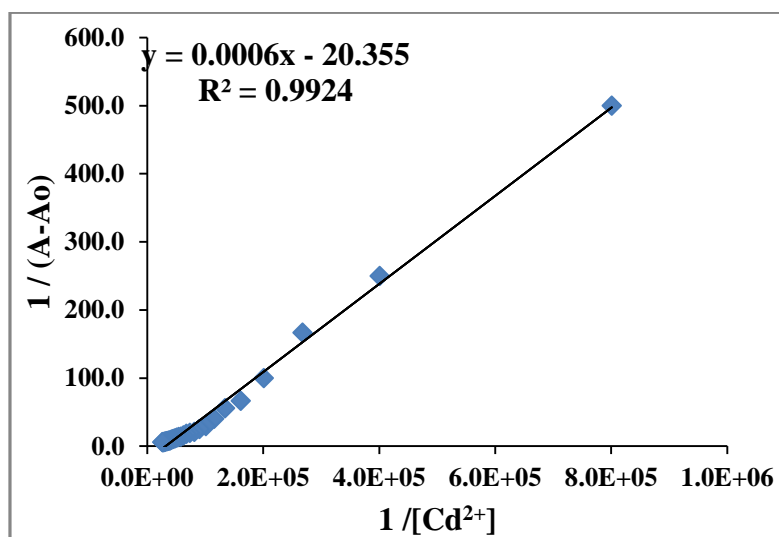
Fig. 5.19: Benesi–Hildebrand plot of receptor **S4R1** assuming 1:1 binding stoichiometry with Cd^{2+} ions, the wavelength at 510 nm

The Detection limit (DL) for Cd^{2+} ion was determined using the calibration plot drawn between Cd^{2+} metal ion concentration (range from $0.0–3.5 \times 10^{-5}$ M) and absorbance of receptor-metal complex (**S4R1-Cd^{2+}) (Fig. 5.20)**. The DL was calculated based on the standard deviation of the response and the slope using the following equation mentioned by ICH quality guideline Q2R1.

$$DL = \frac{C \times \sigma}{m}$$

Where, σ = standard deviation of blank measurement, m = slope of the calibration curve, C = constant (for 3.0) (ICH Q2R1 guideline), The calculated DL value was found to be 0.28 ppm.
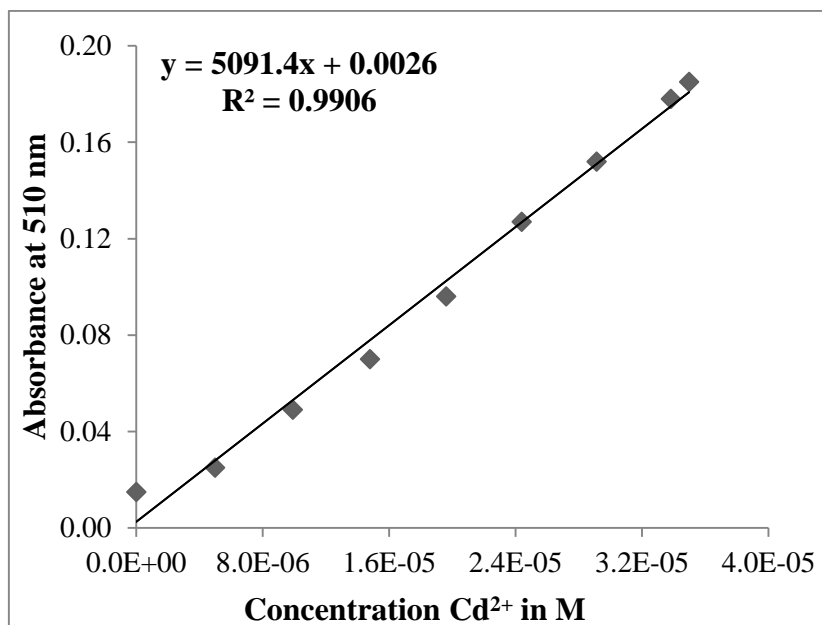
Fig. 5.20: Calibration plot of absorbance of complex (S4R1-Cd^{2+}) versus concentration of metal ions S4R1-Cd^{2+} vs. Cd^{2+}

5.3.2. Theoretical study

The S4R1 sensitively sense Cd^{2+} through ligand to metal charge transfer complex formation. In order to further understand the behavior of S4R1 with Cd^{2+} ions were investigated using Density Functional Theory (DFT) calculations. **Fig. 5.21** shows the optimized structures of S4R1 and S4R1 with Cd^{2+}. The structural optimization and all the computational calculations were carried out using Gaussian09 quantum chemistry package [Schlegel et.al 2009], DFT supported B3LYP/ 6-31G (d, p) model chemistry was applied predominantly for Schiff base ligands under gas phase condition. But its metal complexes were modeled using effective core potential-based LANL2DZ basis set to optimize the geometry of the complex. The entire metal atom present in the complex was treated under LANL2DZ where as other lighter atoms were treated under 6-31G (d, p) basis set. From the energy level diagram (**Fig. 5.22**), it can be seen that addition of the metal ions leads to the stabilization of the HOMO and LUMO of the sensor. From the calculated results, energy levels of

HOMO and LUMO of S4R1 decreased after addition of metal ion when compared with that the free S4R1 (**Table 5.1**).
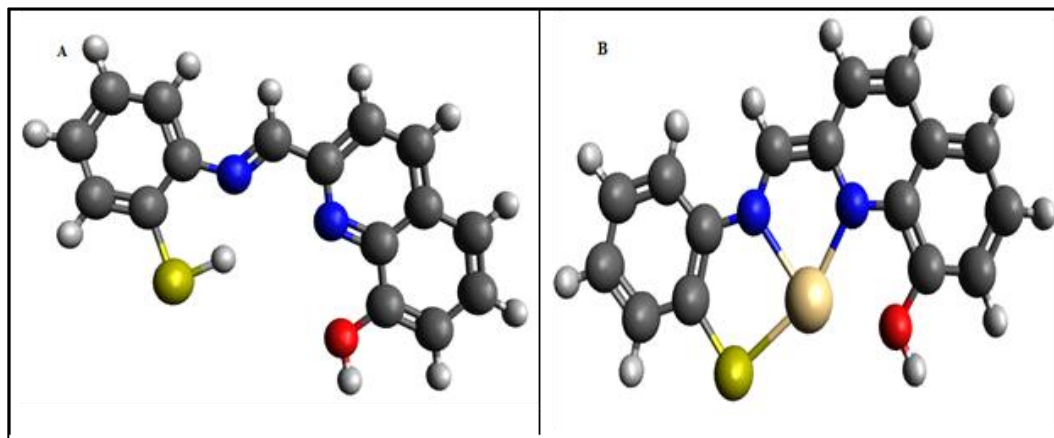
Fig. 5.21: Optimized structure of **(a) S4R1 (b) S4R1+ Cd^{2+}**
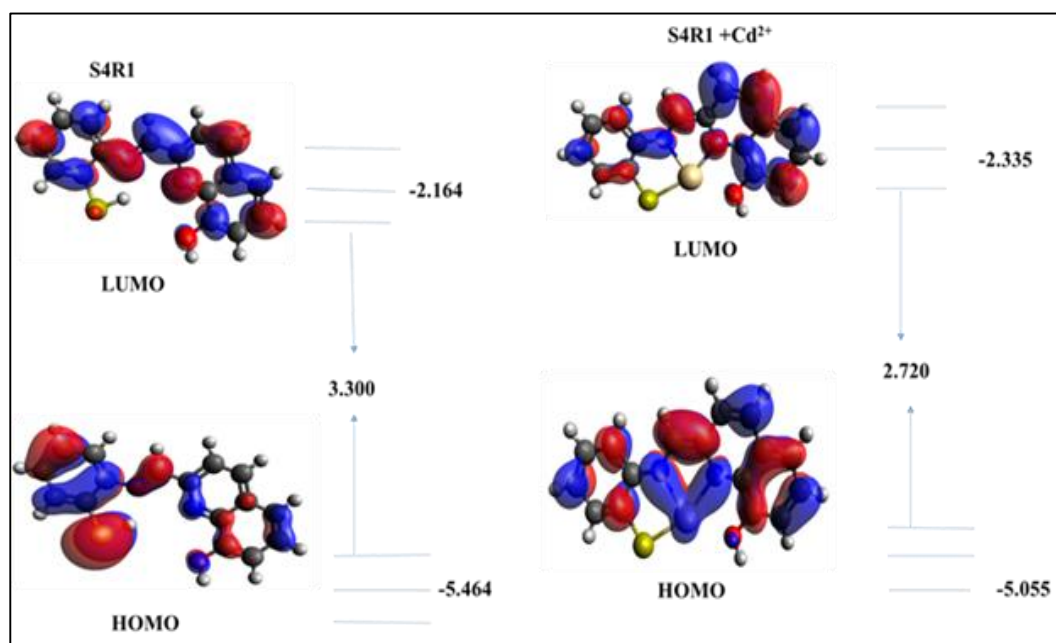
Fig. 5.22: Energy levels of various HOMO and LUMO of S4R1 in the absence and presence of Cd^{2+}

Table 5.1. Energies of HOMO and LUMO of the receptors and complexes

Ligand and metal complexes	HOMO (eV)	LUMO (eV)	ΔE(eV)
S4R1	-5.464	-2.164	3.300
S4R1-H^{+}+Cd(II)	-5.055	-2.335	2.720

5.4 CONCLUSIONS

In this chapter, we demonstrate the utility of receptor **S4R1** to detect the Cd^{2+} ions sensitively. The receptor **S4R1** has suitable binding sites like –SH, pyridine nitrogen and imenic nitrogen groups when compared to the receptors **S4R2** and **S4R3**. The –SH group plays a significant role in binding with Cd^{2+} ions. the behavior of S4R1 with Cd^{2+} ions were investigated using Density Functional Theory (DFT) calculations Receptor **S4R1** showed a 1:1 binding ratio with the binding constant of 6.3×10^3 M^{-1} for Cd^{2+} ions. The receptor **S4R1** showed good linear range from 0.0–6.0×10^{-6} M and displayed a low detection limit of the 0.41 ppm of Cd^{2+} ions.

CHAPTER-6

SUMMARY AND CONCLUSIONS

This chapter briefly explains the summary and conclusions drawn from the present research work.

6.1. SUMMARY OF THE PRESENT WORK

Among the detection of wide range of cations, the recognition of heavy metal ions has gained significant attention because of its high toxicity and environmental hazard. Still, beyond its acceptable limits is highly health concern as it can be a cause of various diseases. Owing to this, the detection of the heavy metal in the environment is became significant. Based on the literature reports, it has been aimed at to design and synthesis of new chemosensors that can detect the heavy metal ions colorimetrically over other comparative analytes in the organic media and also in aqueous media. The overall research work is summarized below.

- Four new different series of colorimetric chemosensors based on Schiff's base reaction using various backbones such as benzothiazole, thiocarbohydrazide, thiophene carboxaldehyde, and 8-hydroxy quinoline have been designed and synthesized for the detection of heavy metal ions.

- All the synthesized chemosensors (i.e. S1R1–S1R3, S2R1–S2R3, S3R1–S3R3 and S4R1–S4R3) have been characterized using different standard spectroscopic techniques like FT–IR, ^{1}H–NMR, ^{13}C–NMR, and LC–mass (ESI–MS). Three-dimensional structures of selected chemosensors (i.e. S2R1–S2R2 and S3R3), have been determined using Single Crystal X-Ray diffraction (SCXRD) studies.

- The qualitative and quantitative analysis of Hg^{2+}, Cu^{2+} and Cd^{2+} metal ions has been carried out using UV–Vis spectroscopic studies. The binding constant (k) for the chemosensors-metal ion complex has been calculated using the Benesi–Hildebrand equation.

- For all the four series of chemosensors, the detection/qualification limits have been calculated from the UV-Vis titration data.

- The binding mechanisms have been proposed based on UV–Vis titration, and then some have been supported by FT–IR and ^{1}H–NMR. Further, some series of

chemosensors (i.e. S3R1–S3R2 and S4R1) were supported by the theoretical density functional theory (DFT) studies.

- The selectivity and sensitivity of all chemosensors in the presence of various interfering analytes have been demonstrated by colorimetric and UV–Vis spectroscopic studies.

- The detection limit, binding constant and linear range of developed chemosensors was summarized in **table 6.1**.

Table 6.1: Detection limit, binding constant and linear range of developed chemosensors for the Hg^{2+}, Cu^{2+} and Cd^{2+} metal ions.

Chemosensor	Metal ion	Binding constant (k) (M^{-1})	Linear range (µM)	Detection limit (ppm)
S1R1	Hg^{2+}	6.8×10^3	0.25 – 6.0	0.03
S2R1	Hg^{2+}	1.0×10^3	5.0 – 38.9	0.55
S2R2	Cu^{2+}	6.2×10^3	5.0 – 29.9	0.21
S2R3	Cd^{2+}	6.2×10^3	5.0 – 29.9	0.36
S3R1	Hg^{2+}	1.6×10^4	0.0 – 31.5	0.28
S3R2	Hg^{2+}	1.0×10^3	0.0 – 36.1	0.45
S4R1	Cd^{2+}	4.3×10^4	0.0 – 35.0	0.28

6.2. CONCLUSIONS

Based on the obtained experimental results, the following important conclusions have been derived.

- Four different series of colorimetric chemosensors have been designed, synthesized, and characterized using standard spectroscopic techniques like FT–IR, ^{1}H-NMR, ^{13}C–NMR and LC–mass (ESI-MS). Few chemosensors structure were determined using Single Crystal X-Ray diffraction (SCXRD) studies.

- Chemosensors **S1R1-S1R3**, have developed using benzothiazole as a backbone for the selective detection of Hg^{2+} ions over other tested cations.

- The **S1R1** has shown response towards Hg^{2+} ions in an aqueous medium with 0.03 ppm detection limit.

- The chemosensors **S1R1**exhibited a good binding consent of 6.8×10^3 M^{-1} with a 1:1 binding stoichiometric ratio of S1R1 and Hg^{2+}.

- The chemosensors **S1R1** have shown good linear range from 0.25 to 6.0 μM for Hg^{2+} ions.

- The S1R2 and S1R3 did not show any activity for different tested cations and Hg^{2+} ions, due to the lack of suitable binding sits in their molecular structure like S1R1.

- The chemosensors S2R1, S2R2 and S2R3 showed high selectivity for Hg^{2+}, Cu^{2+} Cd^{2+} ions respectively, in the presence of other competitive tested metal ions.

- The UV−Vis, and colorimetric studies confirmed the selectivity of chemosensor S2R1 with the Hg^{2+}, S2R2 with the Cu^{2+} ions and S2R3 with the Cd^{2+} ions.

- The correlation study (absorption (A_0/A) versus ionic radii /electronegativity), reveals that, the high affinity of chemosensors **S2R1–S2R3** towards Hg^{2+}, Cu^{2+} and Cd^{2+} than other tested cations.

- The chemosensor **S2R1–S2R3** was accomplished for the detection of 0.55 ppm of Hg^{2+}, 0.21 ppm of Cu^{2+} and 0.36 ppm of Cd^{2+} by UV-Vis method in the water medium.

- Among the 3rd series chemosensors (i.e., S3R1-S3R3), the **S3R1, S3R2** showed the naked eye detection of Hg^{2+} ions in an aqueous medium.

- The **S3R3** did not show any activity towards Hg^{2+} ions and other tested cations due to lack of hydroxy group and suitable heteroatom in the thiophene ring-like **S3R1** and **S3R2**.

- The chemosensors S3R1–S3R2 has a low detection limit of 0.28 and 0.45 ppm for Hg^{2+} ions.

- The experimental results of S3R1 and S3R2 were well coordinated with that of calculated theoretical DFT results.

- Among the 4th series of 8-hydroxy quinoline based colorimetric chemosensors (**S4R1-S4R3**) the S4R1 displayed high selective for Cd^{2+} ions in the presence of other competitive metals.

- The chemosensors S4R2 and S4R3 did not show any activity for Cd^{2+} and other competitive metals, due to the lack of suitable binding site (i.e. –SH group) like S4R1 in their molecular structure.

- The good association constant value of 4.3×10^4 M^{-1} was found for the chemosensors **S4R1** and **Cd^{2+}** ions.

- The chemosensor **S4R1** has a low detection limit for Cd^{2+} ions (0.28 ppm).

- A good linear range of 0.0 – 35.0 μM was found for the Cd^{2+} ions. It indicates that the quantitative and qualitative applications in the field of colorimetric chemosensors.

- The experimental results of S4R1were well coordinated with that of calculated theoretical DFT results.

6.3. FUTURE WORK

6.3.1. Heavy metal ions detection and application

The development of colorimetric chemosensors for the detection of cations is one of the promising areas in the field of supramolecular chemistry. The majority of the sensors have been developed to the detection of cations such as Cu^{2+}, Ni^{2+}, Zn^{2+}, Fe^{2+}, Fe^{3+}, and Co^{2+}. However, there are very few chemosensors that have been designed for the selective detection of heavy metal ions in an aqueous media. The selective detection of Hg^{2+}, Pb^{2+}, Cd^{2+}, and Cr^{3+} ions at ppm detection limit is a difficult task due to their chemical and physical properties. Past decade, various researchers developed colorimetric and fluoresce sensors for the detection of heavy metal ions. The majority of these chemosensors has only quantitative applications and very few reports are available with the qualitative applications.

Hence, looking at the difficulty of heavy metal detection, we are planning to synthesize some simple suitable functionalized molecules with the hope that these chemosensors will act as potent heavy metal ion detectors. Further, the synthesized sensors will be applying for the quantitative and qualitative applications in an aqueous media. Further, the naked eye detection would utilize to develop simple and low-cost detection methods by using smartphone and test strips applications. This method would be enabled to field monitoring of toxic heavy metal ions.

REFERENCES

Agnihotri, P., Suresh, E., Paul, P., and Ghosh, P. K. (2006). Synthesis, Crystal Structures, Cation- Binding Properties and the Influence of Intramolecular C–H··· O Interactions on the Complexation Behaviour of a Family of Cone p- tert- Butylcalix [4] arene- crown- 5 Compounds. *Eur.J. Inorg. Chem.*, (17), 3369-3381.

Azadbakht, R., Almasi, T., Keypour, H., and Rezaeivala, M. (2013). "A new asymmetric Schiff base system as fluorescent chemosensor for Al^{3+} ion." *Inorg. Chem. Commun.*, 33, 63–67.

Beer, P. D., & Gale, P. A. (2001). Anion recognition and sensing: the state of the art and future perspectives. *Angewandte Chemie International Edition*, *40*(3), 486-516.

Böhmer, V. (1995). Calixarenes, macrocycles with (almost) unlimited possibilities. *Angew. Chem. Int. Ed.*, *34*(7), 713-745.

Boricha, V. P., Patra, S., Chouhan, Y. S., Sanavada, P., Suresh, E., & Paul, P. (2009). Synthesis, Characterisation, Electrochemistry and Ion- Binding Studies of Ruthenium (II) and Rhenium (I) Bipyridine/Crown Ether Receptor Molecules. *Eur.J. Inorg. Chem.*, (9), 1256-1267.

Chakraborty, A., Gunupuru, R., Maity, D., Patra, S., Suresh, E., & Paul, P. (2010). Synthesis and anion-sensing property of a family of Ru (II)-based receptors containing functionalized polypyridine as binding site. *Inorg. Chem. Comm.*, *13*(12), 1522-1526.

Chang, L. L., Gao, Q., Liu, S., Hu, C. C., Zhou, W. J., and Zheng, M. M. (2018). "Selective and differential detection of Hg^{2+} and Cu^{2+} with use of a single rhodamine hydrazone-type probe in the absence and presence of UV irradiation." *Dye. Pigment.*, 153, 117–124.

Choi, J. K., Kim, S. H., Yoon, J., Lee, K. H., Bartsch, R. A., & Kim, J. S. (2006). A PCT-based, pyrene-armed calix [4] crown fluoroionophore. *J .Org. Chem.*, *71*(21), 8011-8015.

Choi, Y. W., You, G. R., Lee, M. M., Kim, J., Jung, K.-D., and Kim, C. (2014). "Highly selective recognition of mercury ions through the naked-eye." *Inorg. Chem. Commun.*, 46, 43–46.

Dickson, S. J., Paterson, M. J., Willans, C. E., Anderson, K. M., & Steed, J. W. (2008). Anion binding and luminescent sensing using cationic ruthenium (II) aminopyridine complexes. *Chem. Eur .J. 14*(24), 7296-7305.

Elemental Impurities—Limits, (Pharm. Forum, 2013), 40(2), USP Chapter 232.Edition, Fourth. (2011). Guidelines for Drinking-water Quality. WHO chronicle, 38, 104-8.

Ermakova, E., Michalak, J., Meyer, M., Arslanov, V., Tsivadze, A., Guilard, R., & Bessmertnykh-Lemeune, A. (2013). Colorimetric Hg2+ sensing in water: from molecules toward low-cost solid devices. *Organic letters*, *15*(3), 662-665.

Ghidini, E., Ugozzoli, F., Ungaro, R., Harkema, S., Abu El-Fadl, A., & Reinhoudt, D. N. (1990). Complexation of alkali metal cations by conformationally rigid, stereoisomeric calix [4] arene crown ethers: a quantitative evaluation of preorganization. *J. Am. Chem. Soc.*, *112*(19), 6979-6985.

Ghosh, A. K., Jana, A. D., Ghoshal, D., Mostafa, G., & Chaudhuri, N. R. (2006). Toward the recognition of enolates/dicarboxylates: Syntheses and X-ray crystal structures of supramolecular architectures of Zn (II)/Cd (II) using 2, 2'-biimidazole. *Crystal growth & design*, *6*(3), 701-707.

Gokel, G. W., Leevy, W. M., & Weber, M. E. (2004). Crown ethers: sensors for ions and molecular scaffolds for materials and biological models. *Chemical reviews*, *104*(5), 2723-2750.

Gong, H. Y., Zhang, X. H., Wang, D. X., Ma, H. W., Zheng, Q. Y., & Wang, M. X. (2006). Methylazacalixpyridines: Remarkable Bridging Nitrogen- Tuned Conformations and Cavities with Unique Recognition Properties. *Chem. Eur .J., 12*(36), 9262-9275.

Goswami, S., Aich, K., Das, S., Das, A. K., Manna, A., and Halder, S. (2013). "A highly selective and sensitive probe for colorimetric and fluorogenic detection of Cd^{2+}

in aqueous media." *Analyst*, 138(6), 1903.

Guideline, I. H. T. (2005). *Validation of analytical procedures: text and methodology*. Q2 (R1), 1.

Gunupuru, R., Maity, D., Bhadu, G. R., Chakraborty, A., Srivastava, D. N., & Paul, P. (2014). Colorimetric detection of Cu2+ and Pb2+ ions using calix [4] arene functionalized gold nanoparticles. *J. Chem. Sci.*, *126*(3), 627-635.

Jason L. Sonnenberg, Kim F. Wong, Gregory A. Voth, and H. Bernhard Schlegel "Distributed Gaussian Valence Bond Surface Derived from Ab Initio Calculations" *J. Chem. Theory Comput.* 2009, 5, 4, 949–961

Jiang, X. H., Wang, B. D., Yang, Z. Y., Liu, Y. C., Li, T. R., and Liu, Z. C. (2011). "8-Hydroxyquinoline-5-carbaldehyde Schiff-base as a highly selective and sensitive Al^{3+} sensor in weak acid aqueous medium." *Inorg. Chem. Commun.*, 14(8), 1224–1227.

Jiao, Y., Zhou, L., He, H., Yin, J., and Duan, C. (2017). "A new fluorescent chemosensor for recognition of Hg^{2+} ions based on a coumarin derivative." *Talanta*, 162(September 2016), 403–407.

Jin, R.; Wu, G.; Li, Z.; Mirkin, C. A.; G. Schatz, C.; *J. Am. Chem.Soc*. 2003**,** *125*, 1643.

Kim, S. K., Kim, S. H., Kim, H. J., Lee, S. H., Lee, S. W., Ko, J., ... & Kim, J. S. (2005). Indium (III)-induced fluorescent excimer formation and extinction in calix [4] arene-fluoroionophores. *Inorg. Chem.*, *44*(22), 7866-7875.

Kim, H. N., Ren, W. X., Kim, J. S., & Yoon, J. (2012). Fluorescent and colorimetric sensors for detection of lead, cadmium, and mercury ions.*Chemical Society Reviews*, *41*(8), 3210-3244.

 Kumar, V. V., & Anthony, S. P. (2014). Silver nanoparticles based selective colorimetric sensor for Cd $^{2+}$, Hg $^{2+}$ and Pb^{2+} ions: tuning sensitivity and selectivity using co-stabilizing agents. *Sensors and Actuators B: Chemical*,*191*, 31-36.

Labbé, R. F., Vreman, H. J., & Stevenson, D. K. (1999). Zinc protoporphyrin: a metabolite with a mission. *Clinical chemistry*, *45*(12), 2060-2072.

Lauwerys, R. R., Bernard, A. M., Roels, H. A., & Buchet, J. P. (1994). Cadmium: exposure markers as predictors of nephrotoxic effects. *Clinical Chemistry*, *40*(7), 1391-1394.

Lee, J. S., Ulmann, P. A., Han, M. S., & Mirkin, C. A. (2008). A DNA-gold nanoparticle-based colorimetric competition assay for the detection of cysteine. *Nano letters*, *8*(2), 529-533.

Li, J., Lin, H., Cai, Z. and Lin, H. (2009). "A high selective anion colorimetric sensor based on salicylaldehyde for fluoride in aqueous media." *Spectrochem. Acta A. Mol. and Biomol. Spectrosco.* 72, 1062–1065.

Liu, C. W., Hsieh, Y. T., Huang, C. C., Lin, Z. H., & Chang, H. T. (2008). Detection of mercury (II) based on Hg^{2+}–DNA complexes inducing the aggregation of gold nanoparticles. *Chem. Comm.*, (19), 2242-2244.

Marbella, L., Serli-Mitasev, B., & Basu, P. (2009). Development of a fluorescent Pb^{2+} sensor. *Angewandte Chemie International Edition*, *48*(22), 3996-3998.

McFarland, C. N., Bendell-Young, L. I., Guglielmo, C., & Williams, T. D. (2002). Kidney, liver and bone cadmium content in the Western Sandpiper in relation to migration. *Journal of Environmental Monitoring*, *4*(5), 791-795.

Pall Thordarson (2010) "determining association constants from titration experiments in supramolecular chemistry" *chem. soc. rev.*, 2011, **40**, 1305-1323.

Pandya, A., Joshi, K. V., Modi, N. R., & Menon, S. K. (2012). Rapid colorimetric detection of sulfide using calix [4] arene modified gold nanoparticles as a probe. *Sensors and Actuators B: Chemical*, *168*, 54-61.

Patel, G., Kumar, A., Pal, U., & Menon, S. (2009). Potassium ion recognition by facile dithiocarbamate assembly of benzo-15-crown-5–gold nanoparticles. *Chem. Commun.*, (14), 1849-1851.

Pearson, R. G. (1963). Hard and soft acids and bases. *J. Am. Chem. Soc.*, 85(22), 3533-3539.

Que, E. L., Domaille, D. W., & Chang, C. J. (2008). Metals in neurobiology: probing their chemistry and biology with molecular imaging. *Chemical Reviews*, *108*(5), 1517-1549.

Renuga, D., Udhayakumari, D., Suganya, S., & Velmathi, S. (2012). "Novel thiophene based colorimetric and fluorescent receptor for selective recognition of fluoride ions". *Tetrahedron Letters*, *53*(38), 5068-5070.

Takahashi, K., Gunji, A., Guillaumont, D., Pichierri, F., & Nakamura, S. (2000). Through- Space Exciton Coupling and Multimodal Na+/K+ Sensing Properties of Calix [4] arenecrowns with the Thienylene Analogue of para- Terphenoquinone as Chromophore. *Angew.Chem., 39*(16), 2925-2928.

Udhayakumari, D., Suganya, S., Velmathi, S., and MubarakAli, D. (2014). "Naked eye sensing of toxic metal ions in aqueous medium using thiophene-based ligands and its application in living cells." *J. Mol. Recognit.*, 27(3), 151–159.

Wei, T.-B., Li, W.-T., Li, Q., Su, J.-X., Qu, W.-J., Lin, Q., Yao, H., and Zhang, Y.-M. (2016). "A turn-on fluorescent chemosensor selectively detects cyanide in pure water and food sample." *Tetrahedron Letters*, 57(25), 2767–2771.

Wickner, W., and Kornberg, A. (1973). "DNA Polymerase III Star Requires ATP to Start Synthesis on a Primed DNA." *PNAS*, 70(12), 3679–3683.

Wolfe-Simon, F., Blum, J. S., Kulp, T. R., Gordon, G. W., Hoeft, S. E., Pett-Ridge, J., Stolz, J. F., Webb, S. M., Weber, P. K., Davies, P. C. W., Anbar, A. D., and Oremland, R. S. (2011). "A Bacterium That Can Grow by Using Arsenic Instead of Phosphorus." *Science*, 332(6034), 1163–1166.

Xiong, C., Qin, Y., and Hu, B. (2010). "On-line separation/preconcentration of V(IV)/V(V) in environmental water samples with CTAB-modified alkyl silica microcolumn and their determination by inductively coupled plasma-optical emission spectrometry." *J. Hazard. Mater.*, 178(1–3), 164–170.

Xiong, J. J., Huang, P. C., Zhang, C. Y., and Wu, F. Y. (2016). "Colorimetric detection of Cu^{2+} in aqueous solution and on the test kit by 4-aminoantipyrine derivatives." *Sensors Actuators, B Chem.*, 226, 30–36.

Yan, X., Wang, F., Zheng, B., and Huang, F. (2012). "Stimuli-responsive supramolecular polymeric materials." *Chem. Soc. Rev.*, 41(18), 6042–6065.

Yu, G., Yan, X., Han, C., and Huang, F. (2013). "Characterization of supramolecular gels." *Chemical Society Reviews*, 42(16), 6697.

Yu, M., Yuan, R., Shi, C., Zhou, W., Wei, L., and Li, Z. (2013). "1,8-Naphthyridine and 8-hydroxyquinoline modified Rhodamine B derivatives: 'turn-on' fluorescent and colorimetric sensors for Al^{3+} and Cu^{2+}." *Dye. Pigment.*, 99(3), 887–894.

Zen, J.-M., Jou, J.-J., and Senthil Kumar, A. (1999). "A sensitive voltammetric method for the determination of parathion insecticide." *Analytica Chimica Acta*, 396(1), 39–44.

Zhang, L. N., Liu, A. L., Liu, Y. X., Shen, J. X., Du, C. X., and Hou, H. W. (2015). "A luminescent europium metal-organic framework with free phenanthroline sites for highly selective and sensitive sensing of Cu^{2+} in aqueous solution." *Inorg. Chem. Commun.*, 56, 137–140.

Zhang, S., Wu, X., Niu, Q., Guo, Z., Li, T., and Liu, H. (2017). "Highly Selective and Sensitive Colorimetric and Fluorescent Chemosensor for Rapid Detection of Ag^+, Cu^{2+} and Hg^{2+} Based on a Simple Schiff Base." *J. Fluoresc.*, 27(2), 729–737.

Zhou, Y., Xiao, Y., and Qian, X. (2008). "A highly selective Cd^{2+} sensor of naphthyridine: fluorescent enhancement and red-shift by the synergistic action of forming binuclear complex." *Tetrahedron Lett.*, 49(21), 3380–3384.

Zuber, G., Quada, J. C., and Hecht, S. M. (1998). "Sequence Selective Cleavage of a DNA Octanucleotide by Chlorinated Bithiazoles and Bleomycins." *J. Am. Chem. Soc.*, 120(36), 9368–9369.

LIST OF PUBLICATIONS

Papers published/ communicated in international journals

i.   **Bharath Kumar Momidi**, Venkatadri Tekuri, Darshak R. Trivedi, "Selective detection of mercury ions using benzothiazole based colorimetric chemosensor." Inorganic chemistry communications, **2016**, 74, 1-5.

ii. **Bharath Kumar Momidi**, Venkatadri Tekuri, Darshak R. Trivedi, "Multi-signaling thiocarbohydrazide based colorimetric sensors for the selective recognition of heavy metal ions in an aqueous medium." Spectrochimica Acta part a: molecular and Biomolecular spectroscopy, **2017**, 175-182.

iii. **Bharath Kumar Momidi**, Darshak R. Trivedi, "Dual ion sensing properties of new heterocyclic ligands: molecular logic gate application**," communicated.**

iv. **Bharath Kumar Momidi**, Darshak R. Trivedi, "Selective detection of cadmium ions using quinoline-based colorimetric chemosensor," **communicated.**

Papers presented in international conferences

i.   **Bharath Kumar Momidi,** Dr. Darshak R. Trivedi, "New colorimetric chemosensors for colorimetric detection of metal ions using pyridine based Schiff bases in aqueous medium," International conference on contemporary advances of sciences and technology& 6th annual conference of Indian JSPS Alumni association, BHU Varanasi, August 07-09, 2015.

CURRICULUM VITAE

BHARATH KUMAR MOMIDI

Department of Chemistry, National Institute of Technology Karnataka, Surathkal, Mangalore-575025, Karnataka, INDIA | **Mobile:** +917411870323 | **Email:** bharatnitk5@gmail.com

---

EDUCATION

- ➢ Ph.D. Chemistry (from 17th July 2014 to till date) - National Institute of Technology Karnataka (NITK) Surathkal, India.
- ➢ Master of Science (Organic Chemistry) – Secured 63.25 %- April 2010 - Sri Venkateswara University, Tirupathi, India.
- ➢ Bachelor of Science (Chemistry, Botany and Bio-Technology)-Secured 65 % - April 2008- Sri Venkateswara University, Tirupathi, India.

EXPERIENCE

- ➢ Assistant professor at Department of Chemistry, Sree Vidyanikethan College Tirupathi from 16th June 2017 to 2nd June 2019.
- ➢ Junior research fellow (JRF), Department of Chemistry, National Institute of Technology Karnataka from 12th May 2014 to 12th June 2017 (DST-SERB Project).
- ➢ Project fellow-II at CSMCRI (CSIR) Bhavnagar, Gujarat| from 22 November 2013 to 17 April 2014

PUBLICATIONS/ Papers presented in international conferences

- **Momidi, B. K.,** Tekuri, V., & Trivedi, D. R. (2017). Multi-signaling thiocarbohydrazide based colorimetric sensors for the selective recognition of heavy metal ions in an aqueous medium. *Spectrochimica Acta Part A: Molecular and Biomolecular Spectroscopy*, *180*, **175-182.**

- **Momidi, B. K.,** Tekuri, V., & Trivedi, D. R. (2016). Selective detection of mercury ions using benzothiazole based colorimetric chemosensor. *Inorganic Chemistry Communications*, *74*, 1-5.

- **Bharath Kumar Momidi**, Dr. Darshak R. Trivedi "A simple amine colorimetric chemosensors for selective and sensitive mercury ion detection in an aqueous medium" paper presented in "international conference on sciences and technology Future challenges and Solutions & 7th annual conference of Indian JSPS Alumni association" August 08-09, 2015, Mysore University.

REFERENCES

[1]. Dr. Darshak R. Trivedi,

Associate Professor,

Department of Chemistry,

National Institute of Technology Karnataka, Surathkal

Mangalore, Karnataka-575 025, India.

Ph: +91 9481271272.

Email: darshak_rtrivedi@yahoo.co.in

[2]. Dr. Adka Nityananda Shetty,

Professor,

Department of Chemistry,

National Institute of Technology Karnataka, Surathkal

Mangalore, Karnataka-575 025, India.

Ph: +91 9448779922.

Email: nityanand@nitk.ac.in